REACTOR MATERIALS

A Quarterly Technical Progress Review

4 - MAR 23
Copy ✓ 1962

Prepared for DIVISION OF TECHNICAL INFORMATION, USAEC, by
R. W. DAYTON, E. M. SIMONS, and ASSOCIATES, BATTELLE MEMORIAL INSTITUTE

February 1962

● VOLUME 5

● NUMBER 1

TECHNICAL PROGRESS REVIEWS

To meet the needs of industry for concise summaries of current atomic developments, the Atomic Energy Commission is publishing this series, Technical Progress Reviews. Issued quarterly, each of the reviews digests and evaluates the latest findings in a specific area of nuclear technology and science.

The four journals published in this series are:

Nuclear Safety, William Cottrell and associates, Oak Ridge National Laboratory

Power Reactor Technology, W. H. Zinn and J. R. Dietrich, General Nuclear Engineering Corporation

Reactor Materials, R. W. Dayton, E. M. Simons, and associates, Battelle Memorial Institute

Reactor Fuel Processing, Stephen Lawroski and associates, Chemical Engineering Division, Argonne National Laboratory

Each journal may be purchased ($2.00 per year for subscription and individual issues $0.55) from the Superintendent of Documents, U. S. Government Printing Office, Washington 25, D. C. See back cover for remittance instructions and foreign postage requirements.

The views expressed in this publication do not necessarily represent those of the United States Atomic Energy Commission, its divisions or offices, or of any Commission advisory committee or contractor.

Availability of Reports Cited in This Review

Unclassified AEC reports are available for inspection at AEC depository libraries and are sold by the Office of Technical Services, Department of Commerce, Washington 25, D. C. Some of the reports cited are not available owing to their preliminary nature; however, the information contained in them will eventually be made available in formal progress or topical reports.

Unclassified reports issued by other Government agencies or private organizations should be requested from the originator.

Unclassified British and Canadian reports may be inspected at AEC depository libraries. British reports are sold by the British Information Service, 45 Rockefeller Plaza, New York, N. Y.; Canadian reports (AECL series) are sold by the Scientific Document Distribution Office, Atomic Energy of Canada, Ltd., Chalk River, Ontario, Canada.

Classified U. S. and foreign reports identified in this journal as Classified may be purchased by properly cleared Access Permit Holders from the Division of Technical Information Extension, U. S. Atomic Energy Commission, P. O. Box 1001, Oak Ridge, Tenn. Such reports may be inspected at classified AEC depository libraries.

REACTOR MATERIALS

Prepared for DIVISION OF TECHNICAL INFORMATION, USAEC,
by R. W. DAYTON, E. M. SIMONS, and ASSOCIATES,
BATTELLE MEMORIAL INSTITUTE

● FEB. 1962

● VOLUME 5

● NUMBER 1

Foreword

Reactor Materials is one of a series of four quarterly technical progress reviews broadly covering the field of nuclear science and technology. Under the auspices of the USAEC Division of Technical Information, *Reactor Materials* is prepared by Battelle personnel from world-wide literature. It covers properties, behavior, and fabrication processes of materials applicable to nuclear reactor components and associated equipment.

The reader will recognize that the scope of this Review is too broad to permit detailed coverage of every topic. Rather, the authors and editors attempt to combine the highlights of significant new developments into an informative summary of current research for both management and the technical specialist. As a rule, enough of the results are presented to define the research and summarize the findings. For readers desiring more information on any particular topic, a complete set of references is provided at the end of each section.

Each quarter, a number of bibliographies, monographs, and books appear on subjects within the scope of *Reactor Materials*. Although the main purpose of this Review is to call attention to findings that are new and significant, such publications are noted in the text because they often represent excellent compilations of available information on important materials topics.

R. W. DAYTON
E. M. SIMONS
R. W. ENDEBROCK
Battelle Memorial Institute

Contents

Foreword

I FUEL AND FERTILE MATERIALS . . . 1

Unalloyed Uranium 1
Alpha-Phase Uranium Alloys 2
Gamma-Phase Uranium Alloys 4
Epsilon-Phase Uranium Alloys 5
Dilute Uranium Alloys 5
Plutonium Metal and Alloys 6
Plutonium Compounds 7
Thorium 8
Dispersion Fuels 9
Coated-Particle Fuel Materials 10
Refractory Fuel and Fertile Materials . . 14
Fundamental Studies of Irradiation Effects on Fuel Materials 20
References 21

II MODERATOR MATERIALS 25

Graphite 25
Beryllium Metal and Alloys 26
Beryllium Compounds 30
Solid Hydrides 31
References 32

III NUCLEAR POISONS 35

Metallic Poison Materials 35
Dispersion Control and Poison Materials . . 35
References 36

IV CLADDING AND STRUCTURAL MATERIALS 38

Corrosion 38
Metal-Water Reactions 43
Radiation Effects in Nonfuel Materials . . 44
Selected Mechanical Properties of Cladding and Structural Materials . . . 52
Selected Metallurgical Aspects of Cladding and Structural Materials . . . 56
Diffusion Studies 58
References 59

V SPECIAL FABRICATION TECHNIQUES 63

Melting and Casting 63
Fabrication and Heat-Treatment 64
Cladding 65
Explosive Forming 70
Welding and Brazing 71
Nondestructive Testing 72
References 74

VI GENERAL MATERIALS INFORMATION 77

Issued quarterly by the U. S. Atomic Energy Commission. Use of funds for printing this publication approved by the Director of the Bureau of the Budget on November 1, 1960.

Section I

Reactor Materials

Fuel and Fertile Materials

Unalloyed Uranium

Recent X-ray measurements[1] on high-purity polycrystalline uranium, using refined techniques, yielded the following cell dimensions for alpha uranium: $a_0 = 2.854$ A, $b_0 = 5.869$ A, and $c_0 = 4.955$ A, all ± 0.002 A. The new value for the atomic position parameter was $y = 0.1025 \pm 0.003$. Interatomic distances of the 12 nearest neighbors were two atoms at 2.754 and 2.854 A and four atoms at 3.263 and 3.342 A. The bond lengths were only slightly affected by the changes in y. The main effects of the new parameter are to alter the component of the bond along the b direction by 0.015 A and to change appreciably the calculated relative diffraction intensities.

The Japanese[2] have reported on their study of cold-drawn uranium rods which had been beta treated. They concluded that preferred orientations were found in rods having as little as 2 per cent reduction, and the dimensional instability was apparent in thermal cycling. The (0 1 0) poles are arranged near the rod axis as a component of preferred orientations, regardless of the degree of working.

The Canadians have issued a report[3] summarizing their experiences with uranium fuel rods in the NRX reactor at Chalk River, including the following observations:

1. The most stable rods irradiated in NRX have been alpha rolled and beta heat-treated.

2. Since these rods were prone to diametral growth with subsequent reduced coolant flow and to transverse fractures of the uranium core, recent work has been toward obtaining rods that will elongate at a small uniform rate. This has been done by cold drawing beta heat-treated rods.

3. As-rolled rods have been much more variable in their behavior. Rolling temperature, type of rolling mill, and reduction in area per pass were the most important variables in controlling the rate of irradiation elongation. However, process control was not sufficiently good to guarantee the production of as-rolled rods which would have the desired dimensional stability.

4. Although source of metal and chemical composition probably influence the irradiation performance, the effects were of lesser magnitude and were obscured by factors listed above.

5. The most prevalent cause for removal of rods before their scheduled irradiation has been reduced coolant flow, as evidenced by excessive pressure drop of the coolant.

6. The rupturing of aluminum cladding has been attributed to the longitudinal splitting of the uranium core on irradiation. This has been a function of flux and length of irradiation, and thin sheaths have been more prone to rupture than thick sheaths.

Work at Hanford[4] on the mechanical properties of irradiated uranium heat-treated above the alpha phase is summarized in Table I-1. The abnormally low yield strengths for all the annealed specimens listed are the result of cracks that effectively reduce the cross-sectional area. In nearly all cases, cracks were observed on the surface of the specimens after annealing. The severity of the cracking increased with burnup and annealing temperature, occurring as crack networks in extreme cases. This is reflected also by the density measurements, which show significant decreases after cycle annealing. Some specimens demonstrate considerable ductility after a single anneal even though cracks are present. Again the resulting ductility is dependent on annealing temperature and burnup. Apparently the annealed material attains through recovery the ability to arrest crack propagation. However, the cyclic-annealed

specimens, although held at the upper temperatures for comparable times, remain brittle in tension. (M. S. Farkas)

Table I-1 PROPERTIES OF IRRADIATED URANIUM HEAT-TREATED ABOVE THE ALPHA PHASE[4]

	As irradiated	Single anneal		Cycled anneal from 400°C to indicated temp.		No. of cycles
		700°C	800°C	700°C	800°C	
0.065 at.% burnup:						
Yield strength, 1000 psi	79.0	18.7	17.3	22.4	30.5	
Tensile strength, 1000 psi	88.0	49.1	36.1	33.5	43.7	
Total elongation, %	0.5	21.1	12.4	2.5	1.0	
Density, g/cm^3	18.8	18.9	18.9	18.8	18.6	3
Cracks visible*	No	No	Yes	Yes	Yes	
0.1 at.% burnup:						
Yield strength, 1000 psi	73.4	17.5	29.1	21.3		
Tensile strength, 1000 psi	77.4	22.4	32.2	35.6		
Total elongation, %	0.5	0.9	4.6	1.0		
Density, g/cm^3	18.9	18.7	18.7	18.4		3
Cracks visible*	No	No	Yes	Yes		

*By the unaided eye.

Alpha-Phase Uranium Alloys

The phase relations and properties of uranium–3, 5, 8, and 10 wt.% fissium alloys were studied at Argonne.[5] The fissium aggregate in the alloys consisted of the elements zirconium, niobium, molybdenum, ruthenium, rhodium, and palladium. The phase relations existing in the uranium-fissium system were shown to parallel closely those dominant in the uranium-molybdenum-ruthenium ternary system, a vertical section of which is presented in Fig. I-1. The uranium gamma phase is stabilized down to 552°C, but the beta phase is entirely suppressed at high fissium contents. Some crystallographic data are given, and the minor phases that occur in the alloys are identified. In the cast and gamma-quenched alloys, the retention of gamma uranium produced low hardness and low density. The thermal-expansion behavior of the alloys is shown to be dependent on composition and prior thermal history. Thermal-conductivity data for uranium and the uranium-fissium alloys are presented in Fig. I-2.

The Nuclear Development Corporation[6,7] is investigating the U-UO_2 system as a dispersion-hardening system analogous to sintered aluminum powder. The study has been concerned primarily with developing methods for producing fine uranium powders having oxide skins of controlled thickness, with fabricating specimens from these powders, and with comparing these specimens with pure uranium and the uranium–10 wt.% molybdenum alloy. Results indicated a definite superiority of the dispersion-hardened compositions (uranium and up to 27 vol.% UO_2) over pure wrought uranium in thermal-cycling behavior as well as in transverse bend strength at elevated temperatures. The results were sen-

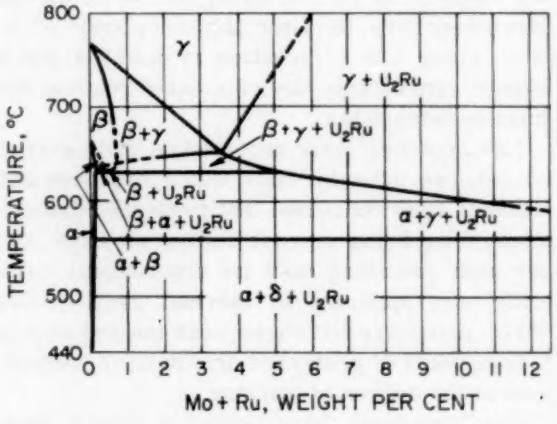

Fig. I-1 Vertical section through the uranium-rich corner of the uranium-molybdenum-ruthenium ternary system[5] at the molybdenum-to-ruthenium ratio of 1.0 : 0.8.

sitive to the amount of oxide that was introduced during the tumbling operation and from oxidation of decomposed hydride powder. The amount of oxide was not controllable and could be determined only by chemical analysis and density determinations on the final extruded sample. Furthermore, the decomposition of the hydride prior to oxidation produced undesirable sintering or agglomeration of the metallic uranium powder. This resulted in a large and varying particle size of the uranium powder prior to oxidation.

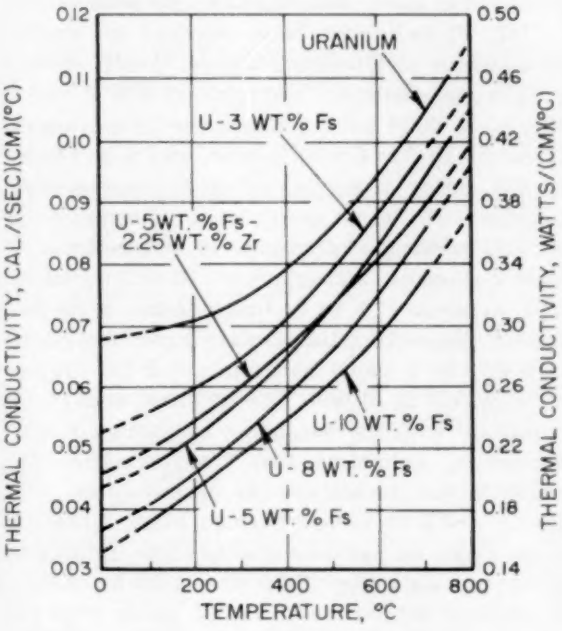

Fig. I-2 Thermal conductivity versus temperature for uranium and uranium-fissium alloys.[5]

The hot tensile and creep properties of uranium-molybdenum base alloys have been investigated by Atomics International.[8] Table I-2 shows tensile properties obtained, and Fig. I-3 is a plot of the secondary creep data at 580°C versus the initial stress. These data indicate uranium–low molybdenum alloys are strengthened at high temperatures by minor additions of aluminum and/or silicon. The increased strength is believed to be the result of a precipitation-hardening mechanism.

Investigators at Du Pont[9] have reported on the metallography of uranium–2 wt.% zirconium alloy before and after irradiation. Optical and electron metallographic techniques and electron diffraction were employed to characterize (1) the response of unirradiated uranium–2 wt.% zirconium alloy to various heat-treatments and (2) the effects of irradiation on the microstructure.

A variety of matrix grain sizes and second-phase distributions were produced by heat-treatment before irradiation. The matrix grain size varied from small needles to large equiaxed grains. The γ_1 phase was retained by quenching from 720°C ($\beta + \gamma_1$ region), but the γ_2 phase could not be retained by quenching from either 680°C ($\beta + \gamma_2$ region) or 650°C ($\alpha + \gamma_2$ region).

Table I-2 TENSILE PROPERTIES OF URANIUM ALLOYS[8]

Composition (balance uranium), wt.%	Ultimate tensile strength, 1000 psi			Yield strength, 1000 psi			Elongation in 2 in., %			Modulus of elasticity, 10^4 psi		
	482°C	550°C	600°C	482°C	550°C	600°C	482°C	550°C	600°C	482°C	550°C	600°C
1.5 Mo	59.0	44.4	27.5			13.3	9	12	13			5.3
1.5 Mo–0.5 Si	75.8	48.6	27.4	52.3	24.8	11.6	1.5	5	17			3.6
1.5 Mo–0.1 Al	68.2	52.6	34.8*	51.4	38.6	20.6*	6.5	7.5	11*	11.9	12.5	5.7*
1.5 Mo–0.1 Al–0.3 Si	79.3	61.5	37.0	63.7	41.8	19.7	4.0	4.0	12	14.8	12	4.3
3.5 Mo	110.4	52.3	23.0	66.9	18.3	4.6	6	15.5	68	10.9	4.3	1
3.5 Mo–0.5 Si	88.2	61.3	29.8	70.9	29.3	13.2	0.5	2.0	11	11.5	8.7	2.8
3.5 Mo–0.1 Al	127.5	77.7	33.3	71.3	37.0	15.0	4	6	24	11.0	7.0	2.9
3.5 Mo–0.1 Al–0.3 Si	127.5	83.4	46.6*	87.8	44.2	22.4*	2	2.5	9.5*			4.4*
3.5 Mo–0.05 Be	109.5	56.4	N.D.†	63.8	19.5	N.D.	4.5	10	N.D.	12.8	6.6	N.D.
3.5 Mo–0.1 Sn	120.2	58.2	N.D.	71.9	20.7	N.D.	3.5	7	N.D.	11.5	6.9	N.D.
10 Mo	67.0	64.3	59.9	64.9	59.3	44.6	1.5	2.5	8	8.5	7.9	7.9
10 Mo–0.5 Si	59.0	54.0	54.0			42.2	0	0	1.5	8.9	7.3	8.4
10 Mo–0.1 Al	60.5	52.8	59.9			52.4	1	1.5	2.5	9.4	8.3	8.7
5.0 Mo	108.9	58.8	33.3	58.0	24.9	14.0	2.5	10	16	9.5	3.8	3.7

*Results of one test only.
†N.D. = not determined.

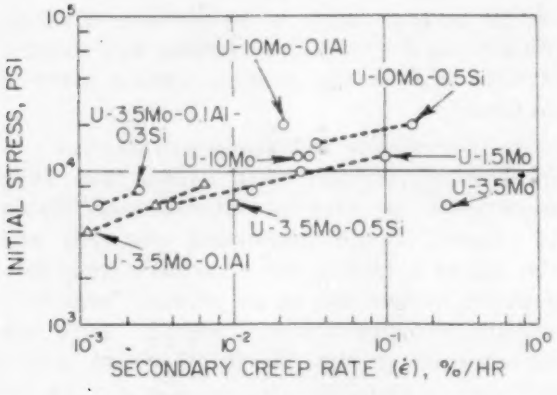

Fig. I-3 Initial stress versus creep rate for uranium-molybdenum alloys[8] at 580°C.

Irradiation of a lamellar structure of the delta phase in an alpha matrix caused distortion and partial dissolution of the delta lamellae and resulted in formation of gas bubbles. Although the lamellae were broken into small particles, the particles remained in bands, resembling the original pattern. At 0.1 at.% burnup, the gas bubbles formed near particles of the delta phase, but after 0.3 at.% burnup, the bubbles were more randomly distributed. (M. S. Farkas)

Gamma-Phase Uranium Alloys

Three uranium–10 wt.% molybdenum alloy slugs were irradiated by Atomics International[8] to burnups of 7250, 9560, and 9970 Mwd/metric ton of uranium at time-averaged central temperatures of 900, 1180, and 1230°F, respectively. These slugs experienced 0.27, 12.7, and 18.2 per cent diameter increases, respectively. The results, in conjunction with previous irradiation data, suggest that the uranium–10 wt.% molybdenum alloy is satisfactory for use at 1100°F but not at 1200°F for burnups to 10,000 Mwd/metric ton of uranium.

The uranium–10 wt.% molybdenum alloy fuel-development program for the Enrico Fermi reactor has been summarized in an excellent report[10] by Atomic Power Development Associates (APDA). Included is the background leading to selection of the fuel, irradiation test results under a variety of conditions, engineering-property test results, fabrication conditions, and fuel-cycle costs.

Atomics International reports[8,11] that alloys of uranium containing up to 12 wt.% molybdenum have been consistently produced in the form of 50-mil, 3- by 12-in. plates by vacuum-induction casting. The process is capable of yielding 100-mil, 3- by 36-in. plates of alloys containing up to 10 wt.% molybdenum, with indications that plates 5 ft long can be produced. Porosity, which has been a major problem, is reported to have been substantially reduced.

Oak Ridge[12] has been engaged in studies of uranium-molybdenum alloys. Creep studies of gamma-quenched material at 550°C and a stress of 5000 psi yielded creep rates ranging from 4×10^{-5} to 6×10^{-3} %/hr, which increased in the order uranium–13 wt.% molybdenum, uranium–15 wt.% molybdenum, uranium–10 wt.% molybdenum, uranium–10 wt.% niobium–4 wt.% zirconium, and uranium–10 wt.% niobium. The uranium–10 wt.% molybdenum alloy exhibited characteristic primary creep for 50 hr, followed by a rapid linear increase for the remaining 900 hr of test. The increase apparently coincided with the beginning of gamma transformation, indicating that transformation decreases the resistance to plastic flow. The uranium–13 wt.% molybdenum alloy, however, behaved as an age-hardenable alloy, exhibiting unmeasurable creep rates after 1500 hr of test. Increasing the stress to 10,000 psi in 1000-psi increments led to an apparent contraction of the specimen, believed to be associated with transformation to the higher density alpha plus U_2Mo phases.

Transformation studies at 500°C indicated that equivalent amounts of alpha uranium were produced in 900°C quenched alloys of 10, 13, and 15 wt.% molybdenum after 48, 500, and 1000 hr, respectively, with cold work prior to transformation increasing the amounts of alpha uranium by a factor of 10. The results are based on a hydrogen-absorption technique, assuming that the gamma and U_2Mo phases do not absorb hydrogen, whereas alpha uranium does. This assumption may be questionable since there is evidence that these phases can absorb hydrogen, particularly in the cold-worked condition.

Atomics International[8] has been studying the transformation kinetics of uranium–14 and 16 wt.% molybdenum alloys. A phase tentatively identified as alpha uranium on the basis of metallography appears in both alloys prior to gamma transformation to U_2Mo. This phase, which nucleates and grows along crystallo-

graphic directions of the gamma grains, is seen after 0.2 to 0.3 hr at 550°C in the 14 wt.% molybdenum alloy and after 0.1 hr in the 16 wt.% alloy. Once the shear type transformation to U_2Mo begins, this phase appears to redissolve.

(A. A. Bauer)

Epsilon-Phase Uranium Alloys

The electrical resistivity, specific heat, and thermal expansivity of U_3Si have been measured by Atomics International.[8] Results are shown in Figs. I-4 to I-6 along with data for other silicide compositions. The specific heat of U_3Si was found to follow the relation

$$C_p = 0.0412 + 3.16 \times 10^{-6}T$$

between 50 and 430°C. The Dulong-Petit specific-heat approximation is 0.0359 cal/(g)(°C).

(A. A. Bauer)

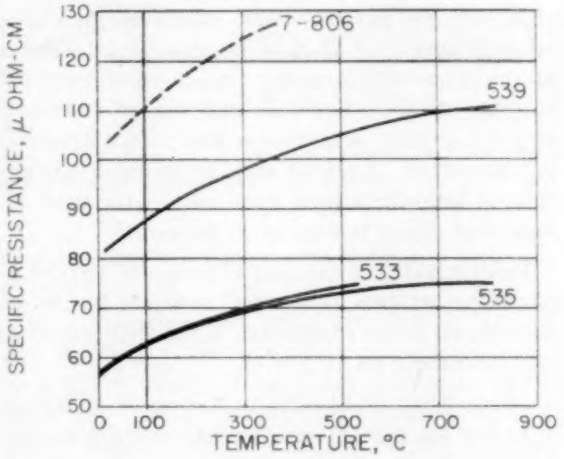

Fig. I-4 Electrical resistivity of uranium silicide.[8] Sample 533, 3.9% silicon. Sample 535, 3.9% silicon. Sample 539, 6.1% silicon. Sample 7-806, 7.3% silicon.

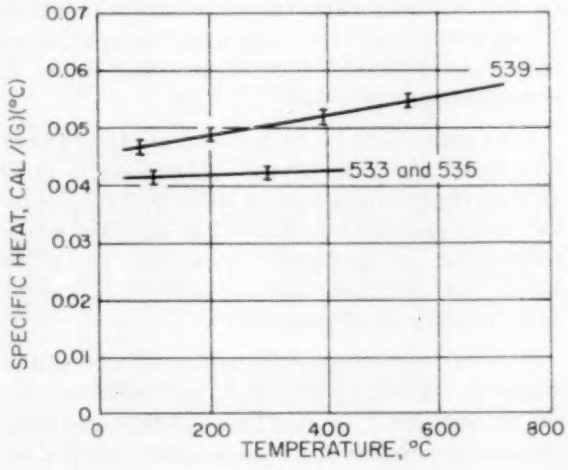

Fig. I-5 Specific heat of uranium silicide.[8] Sample 533, 3.9% silicon, 85 data points. Sample 535, 3.9% silicon, 33 data points. Sample 539, 6.1% silicon, 70 data points.

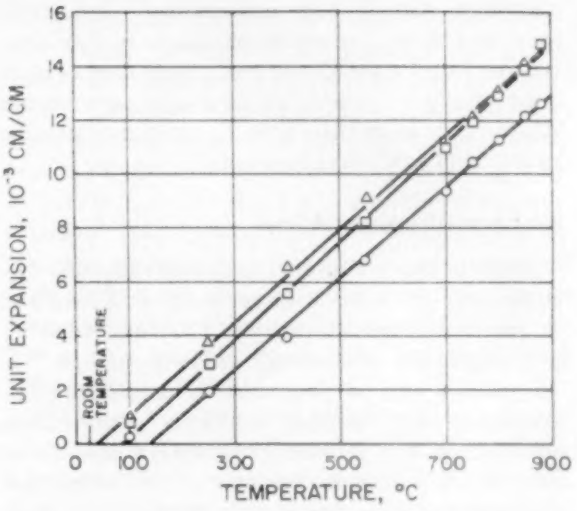

Fig. I-6 Thermal expansion of uranium silicides.[8] ○, 3.9 wt.% Si(U_3Si), $\epsilon = 17.1 \times 10^{-6}$ cm/(cm)(°C). □, 6.15 wt.% Si, $\epsilon = 18.2 \times 10^{-6}$ cm/(cm)(°C). △, 7.3 wt.% Si(U_3Si_2), $\epsilon = 17.3 \times 10^{-6}$ cm/(cm)(°C). Each point represents average readings from two runs.

Dilute Uranium Alloys

Aluminum-Uranium Alloys

In a novel method[13] of producing aluminum-uranium alloy fuel elements, workers at Nuclear Metals cut a pattern of $\frac{1}{8}$- by $\frac{1}{2}$-in. slots in rolled sheets of aluminum–16 wt.% uranium. These slots are then filled with similarly shaped plugs of aluminum–0.8 wt.% magnesium alloy. The plugs are then dimpled on one side, producing projections on the other. When a series of such plates is placed together, the dimpled inserts provide for separation of the fuel plates and produce a suitable coolant channel. Bowen and Dillon[14] have tested aluminum-uranium binary alloys and aluminum-silicon-uranium ternary alloys in deionized water at 350°C in an attempt to predict the behavior of aluminum-

plutonium alloys. They report that alloys with less than 6 wt.% uranium exhibited higher corrosion rates than alloys containing 6 wt.% uranium. However, the aluminum-silicon-uranium alloys with less than 6 wt.% uranium exhibited reasonably low corrosion rates.

Niobium-Uranium Alloys

Battelle has completed the preirradiation development of niobium-base uranium alloys and is currently irradiating, at 1000 and 1800°F, two capsules containing various alloys.[15–17] The alloys can be prepared by a consumable-electrode skull-melting technique. Fabrication difficulties are present with alloys containing over 25 wt.% uranium because of the coring type microsegregation that occurs during solidification.

At 2000°F the niobium–4.38, 14.3, and 20 wt.% uranium alloys exhibited 0.2 per cent offset yield strengths of 16,880, 22,370, and 28,600 psi, respectively. At this temperature these alloys are among the strongest niobium-base alloys. At 2000°F there were only small differences in the stress required to establish various creep rates in the three alloys. About 4000 psi was required to establish a rate of 0.001 per cent per hour; about 5500 psi for a rate of 0.01 per cent per hour; and about 10,000 psi for 0.1 per cent per hour.

Alloys containing 10, 20, and 30 wt.% uranium were heated in sodium for 2400 hr at 1600 and 1800°F with only small weight gains (between 0.02 and 0.13 mg/cm^2 at 1600°F and between 0.1 and 0.23 mg/cm^2 at 1800°F). Decreasing the uranium content reduced the weight gain. As would be expected, the addition of uranium lowered both the thermal and electrical conductivities of niobium. However, the thermal-expansion characteristics were essentially unaffected. A study of the gamma immiscibility gap in the niobium-uranium system indicates that oxygen contents ranging from 100 to 1000 ppm did not affect the composition limits.

Miscellaneous Alloys

Partridge and Clayton[18] have successfully prepared zinc-base binary alloys containing from 2 to 11 wt.% uranium by induction melting. Although the application of this particular alloy is very limited, the technique of preparation might be applicable to other systems. Basically, the zinc is melted at about 420°C and the uranium is charged as a part of the stirring apparatus. The system is then pressurized to 680 mm with argon, the temperature is raised to 850°C, and the stirrer is rotated at about 40 rpm for 10 min. (R. F. Dickerson)

Plutonium Metal and Alloys

Hanford[19] has reevaluated the kinetics of the beta-to-alpha transformation using higher purity plutonium. Data indicate that the rates of transformation were significantly greater than those observed in earlier work. However, impurity content appeared to have no effect on the shape of the time-temperature-transformation (TTT) curves. Studies were also carried out on effects of cooling rate on hardness and microstructure of plutonium, physical and mechanical properties of beta-stabilized plutonium-zirconium alloys, and creep testing of plutonium.

Preliminary investigations of the gold-plutonium system at Mound[20] indicate the existence of an AuPu compound. A eutectic exists at approximately 14 at.% gold.

Tests were completed at Argonne[21] to determine the load-carrying capacity of a plutonium–1.25 wt.% aluminum alloy in the temperature range of 400 to 640°C. Heat-treatments of 145 hr at 450°C or 3 hr at 550°C were found to improve the load-carrying ability of the alloy at temperatures up to 550°C. Above 550°C the amount of deformation increases by a factor of 7, regardless of heat-treatment. No specimens collapsed suddenly without warning, even at temperatures up to 640°C.

Aluminum–5 to 20 wt.% plutonium alloys were irradiated at Chalk River[22] to burnups up to 20 at.% at temperatures up to about 600°C. Metallographic examination showed no eutectic spheroidization in specimens irradiated at 350 to 400°C but complete spheroidization in specimens irradiated at about 600°C.

A tentative niobium-plutonium-silicon phase diagram, shown in Fig. I-7, has been worked out at Battelle.[23] On the basis of this diagram, it appears possible to prepare alloys consisting of plutonium silicides in niobium matrices.

Heat testing niobium–10 wt.% plutonium–10 and 30 wt.% zirconium alloys at 1000°C revealed a tendency for the plutonium-zirconium

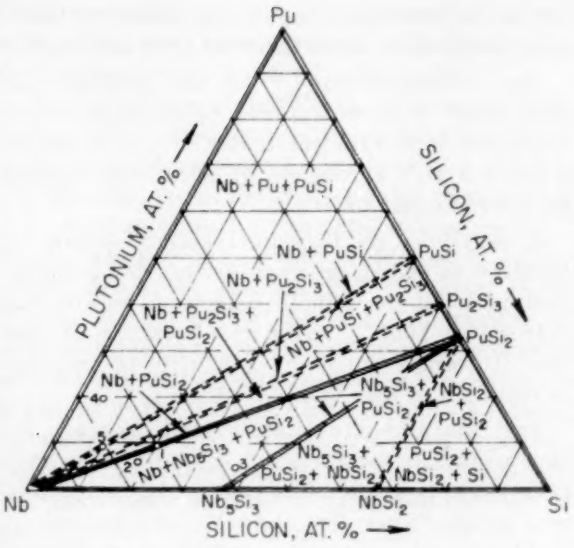

Fig. I-7 Probable phase relations in the niobium-plutonium-silicon system based on cast alloys.[23]

alloy phases to coalesce to form discrete particles.

Cast uranium–10 wt.% niobium–5, 10, 15, and 20 wt.% plutonium alloys were found to increase in diamond pyramid hardness (DPH) from 296 to 438 with increasing plutonium content.[24] Similar alloys with quaternary additions of zirconium exhibited varying degrees of hardness but were generally softer than the ternary alloys.[17] (V. W. Storhok)

Plutonium Compounds

The thermal-expansion coefficient of PuO_2 in the range 20 to 1000°C has been reported by Parsons Nuclear Research Center[25] as shown in Table I-3.

Mound Laboratory continues the investigation of plutonium-bearing glasses in a cooperative effort with Rensselaer Polytechnic Institute and Owens-Corning Fiberglas Corporation.[20,26,27] Most compositions are below 15 wt.% PuO_2, the apparent limit of solubility at 1600°C. The tensile strength of a 20 wt.% PuO_2–glass fiber is 87,000 psi as prepared and drops to 61,000 psi after one month in ambient air. Sodium silicate glasses containing 15 wt.% PuO_2 lost 2.95 per cent of the PuO_2 on leaching 2 hr in 6*N* HCl at 100°C. PuO_2 and beryllium are reported to be mutually soluble in these silicate glasses. A weak neutron source was prepared with 0.44 g of PuO_2 (plutonium-to-beryllium atom ratio of 1 : 10) dissolved homogeneously in 5.9 g of a silicate glass. The source yielded 1762 neutrons/sec.

Table I-3 THERMAL COEFFICIENT OF EXPANSION[25] FOR PuO_2

Temp., °C	α, 10^{-6}/°C
20–300	8.2
20–600	9.9
20–800	10.5
20–1000	11.4

Plutonium carbide was melted and an attempt made by workers at Argonne[21] to cast it into 0.144-in.-diameter graphite molds, but the fluidity was too low for filling. There was a surface reaction between the PuC and graphite, presumably forming Pu_2C_3. In addition, Argonne has prepared PuC-UC solid solutions by powder reactions of PuO_2-UO_2 with petroleum pitch. Pressing and sintering at 1750°C resulted in compacts of 80 per cent of the theoretical density.

Nuclear Materials and Equipment Corporation (NUMEC)[28,29] has begun operation of a continuous oxalate precipitation process for the production of PuO_2. The properties of the end product vary considerably with prior history of the feed solution. Workers report maximum sintered densities for PuO_2 and high PuO_2-UO_2 pellets after 1 to 2 hr at 1200 to 1400°C in a 94 per cent nitrogen–6 per cent hydrogen atmosphere. High UO_2-PuO_2 compositions require sintering at 1600°C.

The sinterability of PuO_2 was found by the British to be enhanced by ball milling. Harwell workers were able to obtain a maximum density of 11.2 g/cm^3 after 3 hr at 1500°C, when the oxygen partial pressure[30a] was 10^{-13} atm. A cathodic etching procedure using argon ions has been developed[30b] to etch PuO_2. The British have also prepared (U-Pu)C by sintering cold-pressed uranium–10 wt.% plutonium with hypostoichiometric amounts of carbon. A density of 9.6 to 10.0 g/cm^3 was obtained[30c] after sintering at 1150 to 1200°C.

Attempts were made by Hanford people[31] to analyze the beta PuC_{1-x} phase, but they were unable to observe its existence. They also attempted to prepare plutonium silicide by powder reactions of PuO_2 with SiC in an oxidized tantalum crucible at 1400°C in vacuum. No product identification has been made. Arc melting of

plutonium with silicon produced a material that was identified as Pu_2Si_3. An investigation of PuO_2 additives to ZrO_2 shows that PuO_2 markedly improves the thermal-shock properties of the ZrO_2 by the formation of a face-centered cubic solid solution at all compositions above 1200°C.

Battelle[32] reports that PuO_2 can be reduced to hexagonal Pu_2O_3 by heating in dry hydrogen at 1700°C. (W. M. Pardue)

Thorium

A bibliography[33] of 856 reports, books, patents, conferences, and journal items relating to the production and properties of thorium has been issued by Gmelin Institute. Atomics International has compiled 109 references[34] dealing with the effects of radiation on thorium.

Further studies (by Brown and Norreys) of the constitution of the thorium-silicon system have been published.[35] The compounds Th_3Si_2, ThSi, Th_3Si_5, Th_6Si_{11}, and $ThSi_2$ were identified. A eutectic exists between thorium and Th_3Si_2 at about 10 at.% silicon and 1400°C. A second eutectic exists at about 1350°C and 82 at.% silicon. ThSi melts above 1900°C. The remaining compounds probably decompose peritectically below the melting point of ThSi. Some of these compounds have more than one allotropic form.

Two investigations[36,37] of the solubility of zirconium in face-centered cubic (alpha) thorium are in agreement that thorium dissolves about 9.5 at.% zirconium at 900°C and about 5 at.% zirconium at 650°C.

A study[38] of the thorium-tantalum system by McMasters and Larsen has established that this system is of the simple eutectic type with the eutectic at 1565°C and 4 wt.% tantalum. At the eutectic temperature the solubility of thorium in tantalum is less than 0.2 wt.%.

The thorium-ytterbium system appears to have unusually low terminal solubilities for two rare-earth type elements having atomic diameters within 15 per cent of each other. According to Evans and Raynor,[39] no intermediate phases exist in the thorium-ytterbium system, thorium dissolves a maximum of 0.4 at.% ytterbium, and ytterbium dissolves a maximum of 0.25 at.% thorium.

On the basis of hot-hardness tests, Oak Ridge reports[12] that indium is the most potent strengthener of thorium at temperatures above 500°C. It is observed, for example, that at 600°C a thorium–4 wt.% indium alloy has a hardness of about 90 DPH as compared with 60

Table I-4 TENSILE-TEST DATA FOR IRRADIATED AND UNIRRADIATED THORIUM[4]

Specimen	Specimen origin*	Irradiation data: 10^{20} nvt	Irradiation data: Burnup, at.%	Irradiation data: 10^{18} fissions/cm^3	Strength, 1000 psi: 0.2% offset yield	Strength, 1000 psi: Tensile	Total elongation, %	Modulus of elasticity, 10^6 psi
B-1	Battelle				15.7	25.1	47	11.3
B-2	Battelle				15.4	24.2	37	12.1
H-1	Hanford				15.9	24.9	36.5	10.2
H-2	Hanford				20.7	28.6	39	8.2
EZ	Battelle	3.4	0.011	3.2	37.2	37.3	44.2	7.2
GZ	Battelle	3.5	0.012	3.5	37.6	37.8	34.6	8.7
DZ	Hanford	3.4	0.011	3.2	40.3	40.3	3.6†	9.7
FZ	Hanford	3.5	0.012	3.5	39.8	39.8	31.7	9.1
EW	Battelle	5.7	0.035	11.0	42.1	42.7	8.4	8.3
GW	Battelle	5.8	0.035	11.0	43.9	44.4	21.0†	8.9
DW	Hanford	5.7	0.035	11.0	43.9	43.8	15.6	8.6
FW	Hanford	5.8	0.035	11.0	53.1	52.9	7.4†	9.1
28	Battelle	9.9	0.12	35	49.8	50.8	17.8	12.2
27	Hanford	11.6	0.16	47	53.9	56.5	13.2	10.7
30	Battelle	31.2	0.95	300	69.1	74.9	2.4	11.2
26	Battelle	34.7	1.15	340		48.8‡	0.8†	8.1
25	Hanford	44.6	1.65	480		55.9‡	0.7†	9.6
29	Hanford	49.9	1.90	560	69.1	75.6	3.2	8.6

*Grain size at 100×: Hanford, 150 grains per square inch; Battelle, 50 grains per square inch.
†Sample broke outside of gauge length.
‡Breaking strength.

DPH for a thorium–10 wt.% zirconium alloy. Difficulties have been encountered in fabricating the thorium–4 wt.% indium alloy, however.

Bement has reported[4,40] the results of a long series of low-temperature irradiations of unalloyed thorium. One series of specimens was irradiated at about 150°C to fission burnups of U^{233} ranging from 0.01 to 0.04 at.% of the thorium. Another series was irradiated at about 300°C to fission burnups of U^{233} ranging from 0.1 to 2 at.% of the thorium. The results of tensile tests on unirradiated control specimens and on the irradiated specimens are summarized in Table I-4 and Figs. I-8 and I-9. These data show that unirradiated, unalloyed, annealed thorium yields plastically at about 15,000 psi and then work hardens to an ultimate stress of about 25,000 psi. The same material after a very slight neutron irradiation yields at a stress well above the former ultimate strength of 25,000 psi; then, as shown in Fig. I-8, it "work softens" to failure at a much lower stress than that at which plastic yielding first commenced. Figure I-9 shows that the yield point increases and the total elongation of thorium decreases progressively with increasing dosage.

(W. Chubb)

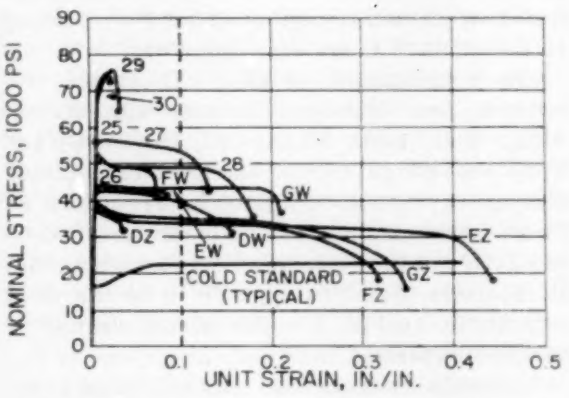

Fig. I-8 Stress-strain curves for irradiated thorium.[4] See Table I-4 for specimen exposures.

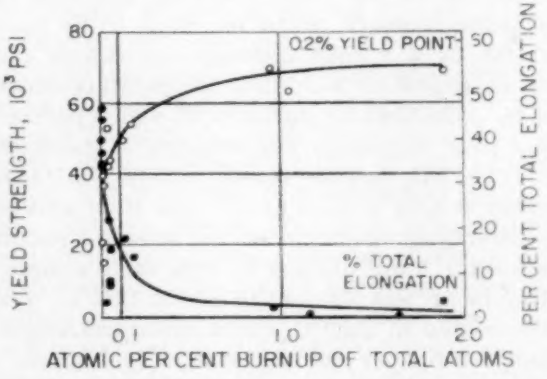

Fig. I-9 Variation of yield strength and per cent elongation of thorium with burnup.[4]

Dispersion Fuels

Los Alamos investigations[41] have demonstrated that molybdenum powder containing 20 vol.% UO_2, compacted by powder rolling or by cold pressing, may be densified by impacting at elevated temperatures. By impacting at 1700°C (3092°F) under a pressure of 61 tsi and then sintering at 1700°C for 14 hr, initial densities of powder-rolled material may be increased from 85.5 per cent to 96.2 per cent of theoretical density, whereas initial densities of cold-pressed material may be increased from 79.9 per cent to 95.3 per cent of theoretical density. Effective hot impacting requires temperatures above 1500°C (2732°F); below this temperature, densification is marginal regardless of impacting pressure.

The linear thermal expansion of a stainless steel–35 wt.% UO_2 dispersion, measured at Oak Ridge[12] over the temperature range 25 to 800°C, was about 9 per cent less than that of pure stainless steel. It is also reported by Oak Ridge that UO_2 and UC dispersions in a uranium–molybdenum alloy matrix can be roll clad with molybdenum quite successfully at temperatures of 1150°C. Cladding with zirconium–3 wt.% aluminum was attempted at 910°C, but a brittle interface was formed with the uranium-alloy matrix.

An irradiation study of dispersions of fully enriched 30 wt.% MCW spherical UO_2 and 30 wt.% ORNL hydrothermal UO_2 in type 318 stainless steel was performed at Battelle[42] to compare the irradiation stability of the two dispersions. Eight specimens were irradiated in the Materials Testing Reactor (MTR) in two capsules equipped with thermocouples. Temperature measurements and isotopic-burnup analyses indicated that the specimens were irradiated at centerline temperatures ranging from about 800 to 1600°F with burnups ranging from 11.8 to 15.1 at.% of the U^{235}.

The postirradiation examination of the specimens from these capsules included fission-gas analyses, dimensional and density determina-

tions, isotopic-burnup analyses, quantitative metallographic examinations, and a study of swelling in the individual fuel particles. Only minor changes in the dimensions and appearance of both types of dispersions were observed as a result of irradiations. Measurements of UO_2 particle sizes revealed that gross swelling had not occurred in either type of UO_2 dispersion during irradiation.

Four capsules containing specimens prepared in the SM-2 Core Materials Development Program have been irradiated and examined.[43] Each capsule contained five to eight flat-plate dispersion specimens roll clad with type 347 stainless steel. Six additional capsules, containing 36 specimens, are still under irradiation in the Engineering Test Reactor (ETR). Variables being studied include use of (1) fuel concentrations of 26 and 40 wt.% UO_2 and 34 wt.% UN; (2) hydrothermal UO_2, spherical UO_2, and UN fuels; (3) B_4C, NbB_2, and ZrB_2 dispersion poisons and no poison loading; (4) a half-loading of reference ZrB_2 dispersion poison; (5) a B^{10} stainless-steel picture frame; and (6) sintering or green pressing alone for core preparation.

The specimens in the first four capsules underwent burnups of 20 to 40 at.% of the U^{235} at surface temperatures near 700°F. It was found that the burnable poisons, both dispersed in the fuel and alloyed in the cladding, performed satisfactorily. No specimens containing a nominal 40 wt.% UO_2 or equivalent UN concentration were included in the first four capsules, but at the 26 wt.% loading, both the hydrothermal and spherical UO_2 performed well. Encouraging results were obtained for the nonsintered core.

(D. L. Keller)

Coated-Particle Fuel Materials

Preparation and Fabrication

Oxide-Base Fuel. Coatings studies, particularly at higher temperature levels, for Al_2O_3, BeO, MgO, and pyrolytic carbon films are being continued at Battelle.[17] Two lots of Al_2O_3-coated 127-μ UO_2 particles were prepared at 1400°C in a mullite reactor. The first lot was coated with 27 μ of Al_2O_3 by direct steam hydrolysis of $AlCl_3$, and the second lot consisted of 33 μ of Al_2O_3 prepared by indirect hydrolysis, using a mixture of H_2 and CO_2 together with the $AlCl_3$. Both coatings appeared to be essentially transparent, fully dense, and the crushing strengths were approximately 50 per cent of the crushing strength of typical coatings prepared at 1000°C. However, the hardness was about equal to the hardness of the 1000°C coating and that of sapphire. Neither coating prepared at 1400°C had surface protrusions. Both coatings were contaminated with silicon, from 1000 to 6000 ppm, which may affect their properties considerably. In the sectioned and as-polished condition, both 1400°C coatings appeared to consist of columnar grains, with grain boundaries extending from the substrate to the coating surface. Most of the particles in the first lot, containing the higher level of silicon impurity, failed when heated to 1400°C for 48 hr in an oxygen atmosphere but were essentially unaffected by heating at 1400°C for 48 hr in a hydrogen atmosphere. The second lot was unaffected by oxidation testing at 1400°C. Coating studies at 1225°C are also under way.

The compatibility of CO_2, CO, steam, air, nitrogen, and hydrogen coolants with carbon, Al_2O_3, BeO, MgO, Nb_2O_5, SiC, UO_2, ZrC, and ZrO_2 was compared[44] on the basis of available free-energy data up to a temperature of 1500°K. Under conditions prescribed in the study, Al_2O_3 and ZrO_2 are the ceramics most compatible with all coolants. Nitrogen appears to be the most compatible coolant for the widest variety of ceramic materials.

Additional studies[17] on Al_2O_3 coatings deposited at 1000°C continue to suggest that failure under oxidizing conditions at elevated temperatures is due to the difference in thermal expansion of the Al_2O_3 and UO_2. The rate of oxidation appears to be too rapid to be controlled by a volume diffusion mechanism and too dependent on a critical temperature range to be controlled by diffusion through a permanent pore structure. For example, a specimen of 127-μ UO_2 powder coated with 53 μ of Al_2O_3 heated at 1300°C for 1 hr in 1 atm of O_2 showed no detectable weight change but showed a weight gain after 5 min at 1350°C. This same sample, after being held for only 15 min at 1350°C, was then cooled to 1300°C, and a continuous weight change of 0.1 per cent per hour was observed.

Samples of particles of 127-μ UO_2 coated with 53 μ of Al_2O_3 and then overcoated with 120 μ of pyrolytic carbon were heated in vacuum to

1800°C for periods[32] of 2 and 4 hr. Despite the fact that, under ordinary circumstances, appreciable reaction would be expected, the relatively thick carbon coatings evidently prevent the escape of carbon monoxide and thereby limit any appreciable degree of reaction, since no metallographic evidence of reaction was found.

Other samples of these pyrolytic carbon/Al_2O_3 coated UO_2 particles were chemically fabricated[24] into fuel specimens by infiltrating a packed bed of these particles with carbon by thermal decomposition of methane at temperatures of about 1150°C. A residual porosity of less than 10 per cent was obtained at a loading of 1.4 vol.% UO_2. The fueled pellets had crushing strengths of 9300 psi, as compared with 6600 psi for unfueled ATJ graphite pellets.

The more conventional fabrication methods have been improved for solvent mixing specimen quantities of coated-particle fuels and matrix materials. The presently preferred procedure is to mix the quantities of fuel particles, graphite filler, pitch, and benzene solvent by a magnetic mixer until sufficient evaporation of the solvent occurs so that the mix consistency approaches that essential for molding. A pellet is then lightly pressed, the solvent is removed under vacuum, and the pellet is finally formed under pressure-baking conditions. Coated oxide fuels dispersed in graphite by these procedures have generally exhibited xenon-release ratios of less than a few parts per million at 1150°C after neutron activation.[17,24,32]

A recent patent[45] has been issued on the coating of Al_2O_3, BeO, or MgO particles electrolytically with a fissionable oxide by use of an intermediate metallic coating.

Carbide-Base Fuel. Studies are continuing at General Atomic on the use of pyrolytic carbon-coated uranium-thorium dicarbide particles in the High-Temperature Gas-Cooled Reactor (HTGR). The importance of coating thickness was clearly demonstrated in thermal-cycle tests, when coatings less than 20 μ thick ruptured in a 2000°C thermal-cycle test, but carbon coatings greater than 20 μ thick behaved satisfactorily.[46] Rather striking effects on fuel migration in these coated particles under the influence of a temperature gradient were found at temperatures of about 1800°C. Graphite compacts containing coated particles were subjected to a temperature drop of 150°C from center line to compact surface. Under these conditions,

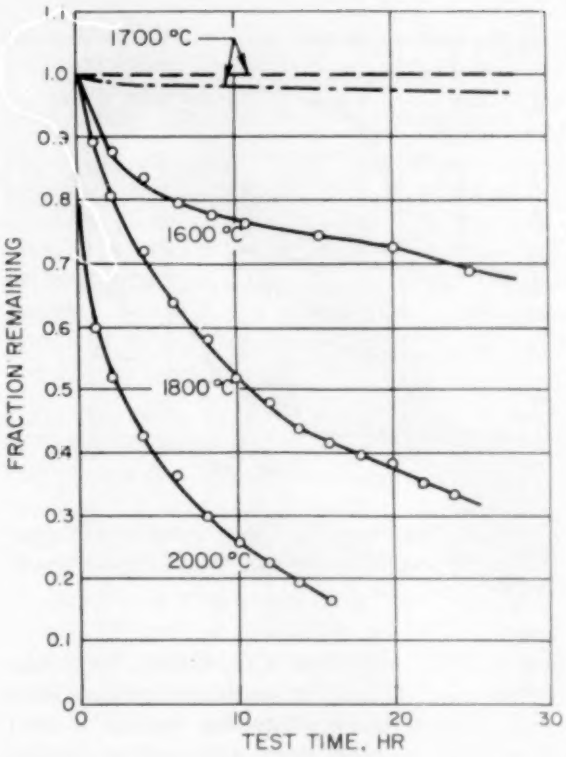

Fig. I-10 Release of Xe^{133} from compacts with coated and uncoated fuel particles at indicated test temperatures.[48] – ——–, compact with coated fuel particles (25-μ coating from C_2H_2 at 1400°C). —— ——, coated fuel particles (60-μ coating from CH_4 at 1400°C). ○, compact with uncoated fuel particles.

coatings on carbide particles failed in 150 to 250 hr as a result of carbide attack on the high-temperature side of the particles. Although the temperature drop across the particles was only 2°C, the gradient of course was still relatively large, since the particle dimensions are very small.[47]

A xenon-release curve for one of the first compacts prepared with 30-μ pyrolytic carbon coatings on 105-μ $(Th:U)C_2$ particles with a 3:1 Th:U ratio is shown in Fig. I-10. Recent tests with pyrolytic carbon-coated $(Th:U)C_2$ particles which were not in a compact have shown no detectable release during 48 hr at 1700°C, as may be seen[48] in the upper curve of Fig. I-10.

The British have activated carbon-coated uranium powders in the BEPO reactor and studied the fission-gas release out of pile. The results obtained were not impressive. However, it is now appreciated that the method of coating is very important.[49] National Carbon Company[50]

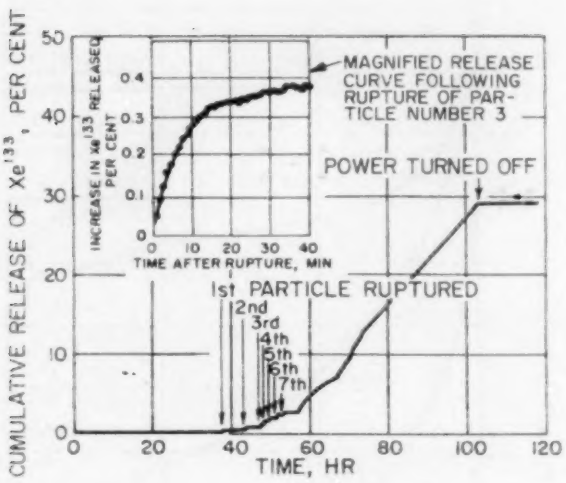

Fig. I-11 Release of Xe^{133} from irradiated UC_2 particles with pyrolytic coatings during heat-treating[51] at 2050°C.

has also revealed that it is studying the preparation and coating of carbide fuel particles. National Carbon verified the earlier work at Oak Ridge on the rapid diffusion of uranium through pyrolytic carbon coatings at temperatures of about 1900°C with material purchased from Minnesota Mining and Manufacturing Company.

Oak Ridge[51] has evaluated material prepared by Minnesota Mining and Manufacturing Company and High Temperature Materials by alpha counting and neutron activation. The particles consisted of about 100 μ of pyrolytic carbon on 300-μ uranium dicarbide cores. The initial surface activity was between 0.8 and 9.0 ppm, and the coatings generally resisted thermal cycling to 1450°C. Results after neutron activation for 160 hr at a flux of 8×10^{11} are shown in Fig. I-11. Evidence for stepwise rupture of the coatings after 37 hr at 2050°C can be seen. It is also reported that Ba^{140} and La^{140} leakage is a more serious problem than that of Xe^{133}.

Three methods are being studied at Battelle[24] to measure the density of carbon coatings. These include

1. Calculation of the coating density from xylene pycnometer measurements of the coated-particle density, core-particle density, and chemical analysis
2. Measurement by flotation of the density of coating fragments obtained by controlled cracking of the coated particles and leaching of the core material
3. Measurement on the coating fragments prepared as described above by the use of the xylene pycnometer

The densities of the coatings have ranged between 1.55 and 1.90 g/cm³ and are a function of temperature and rate of deposition.

Carbon coatings on a number of lots of uranium dicarbide particles have been prepared.[24] Generally speaking, heat-treatment at 1300°C after neutron activation revealed that all samples have xenon-release ratios of less than a few parts per million so long as the coating temperature is somewhat less than 1600°C. Methods of preparing matrix specimens containing carbon-coated carbide fuel are essentially the same as those employed for oxide-coated oxide fuel.

Irradiation and Evaluation

Oxide-Base Fuel. Battelle has reported[24] additional information on the damage to Al_2O_3-

Table I-5 KRYPTON AND XENON RELEASE DATA FOR CARBON-COATED URANIUM-THORIUM DICARBIDE PARTICLES IN A GRAPHITE MATRIX AT ELEVATED TEMPERATURES[48]

Sample series	Date removed from GETR	Irradiation time,* Mwd	Fuel-compact temp., °C	Steady-state release, %						
				Xe^{138} (17 min)	Kr^{87} (78 min)	Kr^{88} (2.8 hr)	Kr^{85m} (4.4 hr)	Xe^{135} (9.1 hr)	Xe^{133} (5.3 days)	Kr^{85} (10.3 years)
8	11/22/60	191	1524		0.11	0.19	0.35	0.028	0.14	1.0
10	12/8/60	494	1702		0.39	0.65	0.94	0.0049	0.78	7.2
13	1/13/61	794	1760		0.37	0.49	0.76	0.047	0.53	
15	1/19/61	974	1799		0.79	0.62	0.92	0.072	0.79	
18	1/26/61	1141	1904	0.68	0.56	0.58	0.80	0.073	1.17	25
21	2/2/61	1351	1751		0.11	0.19	0.36	0.016	0.27	5.4
24	3/24/61	1525			0.27	0.31	0.70	0.027	0.18	

*1400 Mwd is equivalent to ~9 per cent U^{235} burnup, or 26,000 Mwd/ton, or 280 kw-hr/cm³.

coated UO_2 particles which were irradiated in the SP-5 sweep experiment. In this experiment a $1\frac{1}{2}$-in.-diameter graphite sphere fueled with about 10 wt.% of fully enriched particles consisting of 42 μ of Al_2O_3 on 127-μ UO_2 particles was employed. The coatings were actually deposited in six steps, and one of the inner layers consisted of a thin porous Al_2O_3 deposit, perhaps 60 per cent of the theoretical density, as contrasted to the near theoretical density for the other thicker layers. The irradiation temperature was about 600°C and the uranium burnup approximately 6 per cent. The *R/B* values (rate of release to rate of birth of an isotope) were initially in the 10^{-7} to 10^{-8} range but slowly rose to the 10^{-4} to 10^{-1} level near the end of the irradiation. This increase in release of activity was evidently a result of coating failure during irradiation. At the end of the experiment, approximately 3.5 per cent of the coatings had failed based on metallographic examination, and about 8 per cent based on acid leaching experiments. The latter figure is believed to be more reliable. Other static irradiation experiments are currently under way with various types of Al_2O_3 and pyrolytic carbon coatings on 127-μ UO_2 particles at temperature levels of 90 and 1100°C to burnups of about 2.5 and 5.0 per cent.

Table I-6 FISSION-GAS-RELEASE DATA FOR INITIAL SAMPLE OF CARBON-COATED URANIUM DICARBIDE PARTICLES IN A GRAPHITE MATRIX AT A TEMPERATURE[32] OF 1070°C

Sample*	Time after start of irradiation, hr	*R/B* value†		
		Kr^{85m}	Kr^{87}	Kr^{88}
1A	1.0	2.2×10^{-8}	9.5×10^{-9}	6.1×10^{-8}
2A	3.0	2.6×10^{-8}	10.3×10^{-9}	5.8×10^{-8}
3A	14.0	3.5×10^{-8}	8.5×10^{-9}	7.0×10^{-8}
4A	27.5	2.5×10^{-8}	5.9×10^{-9}	4.3×10^{-8}

*"A" samples designate adsorption samples.
†Rate of release of a fission product divided by rate of birth.

Carbide-Base Fuel. Oak Ridge[51] is currently irradiating unsupported pyrolytic carbon-coated UC_2 particles in static experiments in the Low-Intensity Test Reactor (LITR). A burnup of about 10 at.% is to be obtained in four months, and a capsule temperature of about 1100°C will be maintained. Sweep experiments with graphite-matrix specimens containing pyrolytic carbon-coated UC_2 particles are planned for the near future. Materials from Minnesota Mining and Manufacturing, National Carbon, and High Temperature Materials are being considered as candidate fuels.

Compacts containing thorium-uranium dicarbide particles coated at Battelle with pyrolytic carbon showed continuing fission-product holdup times of several hundred hours after a burnup of 5.4×10^{19} fissions/cm^3 at 1500 to 1900°C in studies being carried out by General Atomic.[48] Typical data for one of these compacts are shown in Table I-5. Neutron-activation

Table I-7 FISSION-GAS-RELEASE DATA FOR SECOND SAMPLE OF CARBON-COATED URANIUM DICARBIDE PARTICLES IN A GRAPHITE MATRIX AT A TEMPERATURE[17] OF 1070°C

Sample*	Time after start of irradiation, hr	*R/B* value†					
		Kr^{85m}	Kr^{89}	Kr^{91}	Xe^{133}	Xe^{137}	Xe^{140}
1A	2	4.6×10^{-10}					
2A	4	4.3×10^{-9}					
3A	24	2.2×10^{-8}					
4A	42	3.0×10^{-9}					
5A	68	8.2×10^{-9}					
6A	90	3.1×10^{-8}					
7A	114	3.1×10^{-8}					
8A	136	2.5×10^{-8}					
9A	171	2.2×10^{-4}			3.2×10^{-3}		
10A	190	3.6×10^{-6}			1.1×10^{-3}		
11DT	190		6.9×10^{-4}	2.7×10^{-5}		3.4×10^{-4}	2.1×10^{-5}
12A	195	4.7×10^{-5}			2.5×10^{-4}		
13A	210	3.5×10^{-6}			3.2×10^{-5}		
14A	379	4.3×10^{-3}			3.8×10^{-3}		

*"A" samples designate adsorption samples; "DT" samples designate daughter-trap samples.
†Rate of release of a fission product divided by rate of birth.

data are presumably not available, but it is suspected that the coated particles initially had relatively high release ratios (perhaps a few thousand parts per million), since the coating was done in a one-step operation.

Initial results in a sweep experiment carried out on carbon-coated uranium dicarbide particles were very promising, as indicated by the data in Table I-6. The 200-μ UC_2 particles were coated with 55 μ of pyrolytic carbon at a temperature of 1400°C using a carbon-deposition rate of about 7 μ/hr and acetylene as the reactant hydrocarbon. The particles were then dispersed in a graphite matrix and irradiated at a temperature of 1070°C. However, a leak in the capsule necessitated termination of the experiment[32] after only 28 hr. A repeat of this experiment was carried out later,[17] and the data in Table I-7 were reported. Unfortunately this experiment also met with difficulty, the release ratios rising abruptly from 10^{-8} to 10^{-5} levels after about 150 hr; simultaneously an abrupt increase in system pressure drop occurred. The experimental difficulties are believed to be associated with the problem of trace impurities in the helium sweep gas. Static experiments with samples of carbon-coated uranium dicarbide particles, one sample coated at low rates and the other at high rates of deposition, are also under irradiation at temperatures of 90 and 1100°C. Results of these experiments are not yet available. (J. H. Oxley)

Refractory Fuel and Fertile Materials

Properties and Behavior of Uranium Oxide Fuels

The Naval Reactors Branch, Division of Reactor Development, AEC, recently published a most valuable addition to the literature.[52] This book, *Uranium Dioxide: Properties and Nuclear Applications*, was written by workers from many laboratories who have participated in the development of UO_2 as a nuclear fuel material and was edited by J. Belle, of Bettis Atomic Power Laboratory, the organization which has carried on more such research than any other. This 726-page book is for sale by the Superintendent of Documents, U. S. Government Printing Office, Washington 25, D. C., for $2.50 with a paper cover.

A book on UO_2 has been urgently needed. Ever since the use of bulk UO_2 was pioneered by Naval Reactors and Bettis for use in the Shippingport power station, interest in this material has increased rapidly, and it has become the dominant fuel for civilian power reactors. Consequently, UO_2 has been studied in great detail by many laboratories, and an enormous amount of information has been built up. Unfortunately, the data have been so widely scattered in the technical literature and laboratory reports that it is a major undertaking for the expert just to keep abreast of it and a tremendous one for those beginning work in the field to study it all. The literature has been badly in need of summing up.

This need has been filled by the publication of this book. It provides the much-needed compilation and exhaustive review of the literature and does it in a concise manner. Use of UO_2 as a fuel material not only in bulk but also as a dispersion in a ceramic or metallic matrix is covered. Information is also given, where available, on solid solutions of UO_2 with other ceramic materials.

The book is generally very well written, and especially well in the case of some chapters or sections. This reviewer was particularly impressed by two chapters covering topics whose literature had been widely scattered and previously uncorrelated, namely, those dealing with phase relations and irradiation damage. Both of these chapters were outstandingly well done.

Some peculiarities proved annoying. For example, the section on thermal conduction contained no reference to radiation heat transfer, where one would expect to find it. Instead, it appeared in the section on irradiation effects and was located only by reference to the Index. Again, the section on fabrication contained no discussion of sintering—that appears in the chapter on solid-phase reactions. However, these occasional oddities are not so serious that they interfere appreciably with the over-all high quality of this book. Considering the multiplicity of authors (42 from 16 laboratories), the book is surprisingly uniform in style and quality. Anyone who has had experience with many-authored publications will be well aware of the enormous job of editing which must have been required to put the manuscript into its present form. The editor deserves a great deal of credit for having done his work well.

Knowledge in this field is increasing so rapidly that this book will become out of date sooner than most. It is hoped that plans for frequent revision have been made and that a second edition will be prepared by the same group before the present one is completely out of date. Meanwhile, the present edition fills an urgent need and does it so well that anyone with serious interest in power reactors should own a copy. (R. W. Dayton)

Thermal-conductivity measurements at Sylvania-Corning[53] show that their earlier findings that additions of CaO, Y_2O_3, and Nb_2O_5 improved the thermal conductivity of UO_2 can now be attributed to radiant-heating effects in the experimental apparatus. The recent results indicate that an addition of 3.85 mole % Y_2O_3 reduces the thermal conductivity of UO_2 by 22 per cent at 500°C and by 7 per cent at 800°C. In-pile measurements conducted at Chalk River showed that the average thermal conductivity at temperatures between 350 and 2700°C was lowered 5 to 10 per cent by the addition of 3.85 mole % Y_2O_3. At Battelle[32] the thermal conductivity of an unsintered powder consisting of crushed fused UO_2 vibrationally compacted to a density of about 87 per cent was determined, in both helium and argon, to have an almost constant value of 1.0 Btu/(hr)(ft)(°F) over the temperature range 150 to 900°C.

Compatibility tests have been performed between UO_2 and different prospective cladding materials.[11] Tungsten and UO_2 appear to be highly compatible, even above the melting point of UO_2. Molten UO_2 reacts rapidly with tantalum; however, below 2800°C they appear quite compatible. With molybdenum, there was no evidence of a reaction with UO_2 at temperatures up to 2275°C. Zircaloy-2, 304L stainless steel, Hastelloy F, Fansteel-80, and Fansteel-82 were all found to react to some extent with UO_2 at temperatures 100°C below their respective melting points.

Chalk River[54] reports that Xe^{133} diffusion from slightly irradiated single-crystal UO_2 powder during postirradiation heating follows the relation $D = 2.4 \exp(-120{,}000/RT)$ cm²/sec between 1000 and 1500°C. More recent results from Chalk River[22] suggest that the initial high release of Xe^{133} normally observed in postirradiation-heating experiments with UO_2 is connected with a loss of oxygen from the oxide, which enhances Xe^{133} release. Oxygen loss occurs when the amount of oxygen exceeds the concentration which would be in equilibrium with the partial pressure of oxygen in the surrounding atmosphere. Battelle investigators[55] have measured Xe^{133} diffusion from highly polished flat plates of single-crystal UO_2. Diffusion coefficients are expressed by the relation $D = 1.99 \times 10^{-13} \exp(-30{,}200/RT)$ cm²/sec from 1200 to 1400°C.

An Italian paper by Brisi[56] describes the UO_2-SrO and UO_2-BaO systems. The uranium-oxygen-niobium system and various alkali metal–uranium oxygen systems have been investigated by means of X-ray diffraction at 1100°C at General Atomic.[57]

Pellets of BeO containing 19 and 28 vol.% 125-μ UO_2 particles irradiated at surface temperatures of about 1500°F to exposures of 2×10^{20} and 7×10^{19} fissions/cm³, respectively, showed no significant changes except for minor decreases in abrasion resistance and crushing strength.[58] In another series of experiments,[59] cold-pressed and sintered UO_2-BeO pellets contained in metal tubes were irradiated at 1450 to 1725°F to burnups of 1.5 to 2.0 at.%. One type of specimen consisted of 59 wt.% fully enriched UO_2 in 86.4 per cent dense BeO clad with type 316 stainless steel; the other type, 56 wt.% fully enriched UO_2 in 98 per cent dense BeO with Hastelloy-X cladding. Irradiated pellets from both types of specimens exhibited only small decreases in density and no visible signs of deterioration.

Studies are in progress at Hanford[4] to find additives to control crystal growth in UO_2 in high-temperature fuel cores, which results in a high release of fission gas. Differences were observed between the crystal-growth characteristics at high temperatures of UO_2 and UO_2 containing 0.4 wt.% Nb_2O_5 and 0.7 wt.% TiO_2. Pure UO_2 crystals grew up to three times as fast at 2700°C as did UO_2 crystals containing the additives. The additives in the UO_2 also changed the crystal-growth pattern, resulting in the formation of crystals without definite shapes and faces.

Single-phase face-centered cubic structures of various UO_2-ZrO_2-CaO compositions with densities ranging from 90 to 94 per cent of the theoretical density have been prepared by Combustion Engineering[60,61] by sintering in hydrogen at 1750°C. Compositions up to 15 mole % UO_2 were found to be thermally stable after 28-day heat-treatments in argon at 1000°C. Heat-

treatments in air at 1500°C resulted in the formation of a limited single-phase cubic structure for UO_2 contents up to about 12 mole % and CaO contents of 16 to about 26 mole %. A face-centered cubic phase plus a $CaZrO_3$ phase extended above the single-phase cubic region in the high CaO region for UO_2 contents up to about 20 mole %. Higher UO_2 compositions heated in air were multiphase. Specimens of UO_2-CeO_2 containing 7 and 21 mole % UO_2, sintered in hydrogen to densities between 95 and 98 per cent of the theoretical density, were found to be highly unstable to thermal shock.

Recent work on the ZrO_2-UO_2 phase diagram is reported by Bettis.[62] Small amounts of neutron irradiation were found to induce multiphase mixtures in the ZrO_2-UO_2 binary system to combine into a single phase. Above 6×10^{20} fissions/cm^3, this single phase is cubic. In-pile thermal-conductivity measurements are continuing with accumulated exposures in UO_2, ZrO_2–34 wt.% UO_2, and ZrO_2–46 wt.% UO_2 fuel specimens having reached 13×10^{20}, 11×10^{20}, and 10×10^{20} fissions/cm^3, respectively. The effective thermal conductivity of the UO_2 has decreased from 0.033 watt/(cm)(°C) to about 0.025 watt/(cm)(°C), whereas there has been no change with the ZrO_2–34 wt.% UO_2. The average temperatures are about 525 and 550°C, respectively. In the case of the ZrO_2–46 wt.% UO_2, the thermal conductivity at an average temperature of 400°C has decreased from 0.021 to 0.019 watt/(cm)(°C). (R. H. Barnes)

Fabrication of UO_2-Containing Ceramics

United Nuclear Corporation (formerly Olin Mathieson, Nuclear Division) has made further observations on the role of oxidation-reduction cycling in removing densification-inhibiting fluorine impurities from UO_2 powder.[63] The presence of moisture in the furnace atmosphere during either oxidation or reduction appeared to be the major factor responsible for fluorine removal. It seems possible that the failure to correlate powder characteristics with sinterability may be partly the result of uncontrolled variations in fluorine content.

Mallinckrodt has undertaken a program[64] to characterize sinterable UO_2. Early data seem to support the contention of several workers that the oxygen-to-uranium ratio is not a controlling factor in sintering UO_2 but that more sinterable powders tend to oxidize more rapidly during storage.

The Canadians have reported some preliminary findings[65] on the evolution of gas from sintered pellets of UO_2 on heating. Although there was wide variation in results from replicates, the limited data suggest (1) no correlation between sintering atmosphere and composition of evolved gases and (2) higher gas evolution from ground specimens than from unground ones.

Since recent irradiation test data have indicated that lower density fuel is less inclined to swell on high burnup, Bettis is developing a process for fabricating porous fuel wafers of natural UO_2 for a Pressurized-Water Reactor (PWR) blanket. The wafers are to have a geometric density of 90 per cent of theoretical, in which "macropores" are enclosed in a high-density (>96 per cent) matrix.[62] Controlled porosity was attained by dry addition of 0.2 wt.% stearic acid and 1 wt.% methocel to UO_2 granules, followed by cold pressing and sintering.

(H. D. Sheets)

Properties of Refractory Fuels Other Than Uranium Oxides

A review of the technology on uranium carbides was presented[66] at the April 1961 symposium on reactor fuel materials. Although the potential application of this material as a high-temperature, high-burnup fuel appears very promising, its limitations have not been completely investigated. Various laboratories are continuing to evaluate the uranium carbides.

An analysis[67,68] of the ignition behavior of uranium monocarbide powder in oxygen is shown in Table I-8. Here, difference in particle size and material source is seen to modify the ignition temperature by as much as 60°C. Rate studies[69] on the oxidation of bulk UC show that it proceeds rapidly above 275°C in oxygen and above 350°C in air. A two-step process is indicated from the rate data. X-ray-diffraction analyses show that UC oxidizes first to UO_{2+x} or U_3O_7, which converts to U_3O_8 upon final oxidation. The oxidation products of the dicarbides UC_2 and ThC_2 in moist air were investigated.[70,71] Addition of thorium to UC_2 or of uranium to ThC_2 slows the reaction to some extent. Both UC_2 and ThC_2 are stable in nitrogen at ambient temperatures. The gases evolved during reaction of UC and UC_2 with water at 80 and 90°C

Table I-8 IGNITION BEHAVIOR OF URANIUM MONOCARBIDE POWDER IN OXYGEN[68]

Mesh size	Source A		Source B	
	Specific area, cm^2/g	Ignition temp., °C	Specific area, cm^2/g	Ignition temp., °C
−270 +325	314	255	157	280
−230 +270			131	290
−200 +230	233	275	112	305
−170 +200	187	275	93.5	315
−140 +170	157	290		
−80 +100	93	280		
−70 +80	78	295		
−50 +70	33	310		
−25 +30	23.5	315		
−20 +25	19.5	320		

were[72] hydrogen, methane, ethane, and propane. As the UC_2 content of the specimens increased, the methane content of the evolved gas decreased, with a corresponding increase in the amount of hydrogen evolved.

Because of the reactivity of the uranium carbides, cladding materials and alloy carbides are of great interest. The carbides of hafnium, zirconium, niobium, and tantalum react with UC and are reported[73] to increase the stability of the UC structure in the presence of carbon. UC_2 and U_2C_3 do not form solid solutions with these carbides. The UC solubility in ZrC, HfC, NbC, and TaC is 30, 14, 28, and 23 mole %, respectively, at 1700°C and increases at higher temperatures. The melting-point curve for UC-ZrC was reported[74] to fall smoothly from 3535°C for ZrC to 2640°C for UC. Lattice-parameter data on solid solutions show a linear change with composition: 4.6871 *kX* units for ZrC to 4.9495 *kX* units for UC. Melting-point data[75] for UC-NbC also gave a nearly straight, smooth line from 3485°C for NbC to 2550°C for UC.

In UC-cladding compatibility investigations,[76] niobium−0.75 wt.% zirconium and niobium−3 wt.% aluminum−3 wt.% vanadium alloys showed no interdiffusion zone between the alloy and UC after 100 hr at 1100°C.

The irradiation behavior of UC, UC_2, and U_2C_3 is being determined[17,77] at temperatures ranging from 500 to 1600°F. NaK-filled capsules containing these carbides were irradiated to burnups of 0.01 to 0.7 at.% and examined. Lattice strains and electrical resistivity reached maxima at 0.01 at.% burnup at 500°C. At 1100 to 1400°C, UC_2 completely disintegrated during a 0.5 at.% burnup experiment. However, compatibility studies indicate this deterioration could be a result of attack by NaK at the higher temperatures. The U_2C_3 specimens were partially broken, whereas UC showed no apparent change after the 0.7 at.% burnup. Density changes in UC specimens were found to be of the order of 1 per cent.

The properties of US and ThS are being evaluated[21] for reactor applications. The oxidation of US proceeds by the formation of a black surface coating at 250°C which protects the remaining material up to 460°C, at which temperature it ignites to form UOS and UO_2. Hardness measurements showed US and ThS to be approximately the same, whereas areas containing the oxysulfide were harder by a factor of 1.5 to 2. US and ThS form a complete solid-solution series at 2050°C. The modulus of rupture increases from 20,000 psi for US to 30,000 psi for ThS. (D. A. Vaughan)

The thermal conductivity, electrical resistivity, specific heat, and thermal expansivity of U_3Si_2 (7.3 wt.% Si) and mixtures of U_3Si and U_3Si_2 are reported by Atomics International.[8] Some of these data are shown in the previous epsilon-phase alloy section (Figs. I-4 to I-6) and in Fig. I-12. The specific heat for a

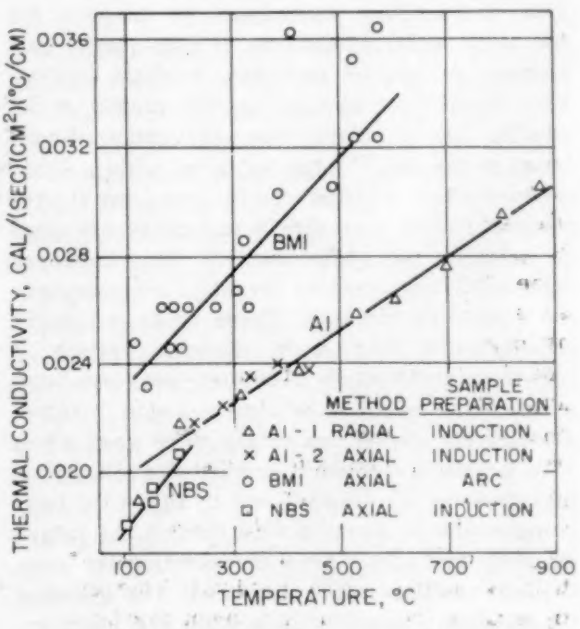

Fig. I-12 Thermal conductivity[8] of U_3Si_2.

uranium–5.9 wt.% silicon alloy was found to follow the relation

$$C_p = 0.0455 + 16.1 \times 10^{-6} T$$

between 50 and 715°C. The Dulong-Petit specific-heat relation was found to be 0.0416 cal/(g)(°C) for U_3Si_2. Dynamic-modulus measurements on U_3Si_2 yielded modulus values varying from 20×10^6 psi at 24°C, to 19×10^6 psi at 450°C, to 21.5×10^6 at 850°C.

U_3Si_2 compatibility with type 304 stainless steel was also studied. Silicon was found to diffuse from the U_3Si_2 into stainless steel to form a new phase. The reaction layer was observed to grow with an activation energy of 36.3 kcal/mole according to the following equation:

$$\frac{x^2}{t} = 22 \times 10^{-6} \exp\ (36.3/RT)$$

where x is given in centimeters and t in seconds. In sodium-bonded stainless steel–U_3Si_2 capsules, silicon was found to be the only mobile species, diffusing through the sodium to the stainless steel. (A. A. Bauer)

Fabrication of Ceramic Fuels Other Than Uranium Oxides

Further refinements are being made in skull type arc-melting techniques to provide for the large-scale production of high-quality cast shapes of uranium carbides. Battelle melters have found that excess carbon pickup in the casting due to gravity type segregation of uranium in the skull[78] adjacent to the bottom of the water-cooled crucible can be overcome if prealloyed rather than virgin materials are used to prepare the initial skull.[23] The improved type skull was used to investigate atmosphere as a process variable. Three types of furnace atmospheres were tried: dynamic vacuum, a one-third atmosphere of helium, and a one-third atmosphere of a 3:1 helium-to-argon mixture. Prealloyed charge materials were used along with uranium nibbles to compensate for carbon pickup from tip erosion and to adjust the final composition to about 5 wt.% carbon. As judged by metallography, good compositionally controlled castings were produced. The greatest tip erosion occurred in vacuum; the least occurred in the argon-helium mixture. The arc stability was improved by the argon addition to the helium. Melting in vacuum resulted in the largest molten pool and the soundest castings, but the quantity of the molten pool in all three atmospheres was sufficient to produce 1-in.-diameter by 8-in.-long castings.[23]

Oak Ridge workers contend[12] that stoichiometric UC (4.80 wt.% carbon) can be arc melted and cast into sound shapes without disturbing the stoichiometry if a carefully designed copper mold containing a graphite insert is used to prevent the formation of UC_2 by minimizing the exposure time of molten UC to the graphite. They selected high-purity uranium with less than 50 ppm carbon and spectrographic carbon as charge materials, used a tungsten-tipped electrode, and arc melted on a water-cooled copper hearth. Knowledge of the charged constituents, particularly carbon in the uranium, the weights of material both before and after arc melting, and metallographic examination were the criteria for stoichiometry. After remelting, four 100-g crack-free small-diameter cylinders with microstructures free of dicarbide needles within the grains were cast in the specially designed mold.

In the fabrication of UC by powder-metallurgy techniques, liquid-phase sintering is receiving some attention. Additions of 0.1 to 1.0 wt.% iron appear to improve sinterability and promote grain growth,[79] as does 0.1 to 0.5 wt.% nickel.[80] It is interesting to note that chemical analyses at the Carborundum Company show that the nickel addition remains after sintering for 4 hr at 1525°C and is not removed by an additional hour at 1850°C, although, during the additional heat-treatment, there is an increase in grain size, a decrease in the amount of grain-boundary phase, and an increase in UC_2. British workers have obtained higher densities by adding VF_2 to "reaction" sintered uranium-graphite mixtures.[81]

A somewhat different concept, liquid-phase sintering with a permanent cementing agent, was investigated by Oak Ridge workers. They added nickel, chromium, and the uranium intermetallics U_2Mo, U_3Si_2, and USi_2. They report that 18 wt.% U_3Si_2 gave 97.5 per cent density on sintering at 1550°C. Under certain conditions of fabrication, the U_3Si_2 binder assumed a continuous network that improved the corrosion resistance of the UC. Bodies cemented with 5, 10, and 15 wt.% USi_2 were consolidated to a density of 97 per cent of the theoretical density by

firing in vacuum for 2 hr at 1650°C. X-ray-diffraction analysis indicated that the bodies after firing were UC plus alpha USi_2.

The more unconventional powder-metallurgy processes for fabricating UC have included slip casting,[82] extrusion,[78] hot pressing at ultrahigh pressures,[78] high-energy-rate forming, and vibratory compaction. At Hanford,[83] UC that had been previously fused and crushed to −6-mesh size was compacted by high-energy impact (Dynapak) at 1200°C and 500,000 psi to a machinable solid having a density of 13.28 g/cm^3 (97.4 per cent of theoretical density). Using arc-melted UC stock with a particle-size distribution of 50 per cent +12 mesh, 12 per cent −12 +20 mesh, 17.5 per cent −20 +80 mesh, and 20 per cent −200 mesh, compacts with 84.6 per cent of theoretical density (12 in. long by 0.530 in. in diameter) have been produced at Atomics International[8] by vibratory compaction. Optimum results were obtained by pouring the powders while simultaneously vibrating at frequencies that were varied from 2500 to 200 cps and then increased again to 2500 cps over a 1-min cycle. Compaction was in 0.010-in.-wall stainless-steel tubing under an argon atmosphere.

Preliminary microstructural investigations led workers at Atomics International[78] to conclude that dense UC could not be pressed at any pressure if the temperature was much below 1000°C. By using UC_2 platelets in hyperstoichiometric UC as natural grids to reveal shape changes during pressing at ultrahigh pressures (10,000 to 46,000 atm), they found these additional mechanisms of densification:[8]

1. Fragmentation of individual grains along cleavage planes and subsequent slide along these planes
2. Slide of irregular boundaries accompanied by shearing of zones on both sides of the boundary
3. Distortion of the grain interior

The successful reduction of zone-refined hyperstoichiometric UC to stoichiometric by annealing in hydrogen at 1400°C or higher has been reported.[8] During zone refining, a 4.5 wt.% carbon starting material increased in carbon by 0.48 per cent and a 7.3 wt.% carbon starting material increased by 0.1 per cent after a single pass at the rate of 3 in./hr. Some measure of success was also obtained by annealing in uranium vapor at a partial pressure corresponding to stoichiometric UC near 1900 to 2000°C.

In a continuing study of the handling and storage problems associated with UC, the best results in cutting and grinding of UC have been obtained with Winthrow Chemical Company type ACW-803 cutting oil. Significant increases in storage life have been obtained by coating the UC with this oil and storing in an airtight container along with a regenerated silica-gel desiccant. The oil is removed prior to use with a low hygroscopic solvent hexane in a vapor degreasing unit.[8]

Sylvania-Corning is trying to bypass the conventional intermediates, uranium or UO_2, by utilizing the reaction $UF_4 + Si + C \rightarrow UC + SiF_4$ to produce[82] UC. Residual silicon contents as low as 0.01 per cent; fluoride, 0.011 per cent; oxygen, 0.04 per cent; and nitrogen, 0.011 per cent have been obtained. The carbon contents of individual experiments ranged from 4.5 to 5.5 wt.%. The blended and compacted powders are sintered for 1 hr at 1600°C in a graphite boat. The UC is produced in the form of friable pellets. Neither reaction kinetics nor the effects of the principal variables on product quality have been established.[83]

Atomics International claims to have produced a microstructurally homogeneous 90 wt.% UC, 10 wt.% ZrC casting by arc-melting the prealloyed uranium-zirconium alloy with carbon addition in a carbon hearth with a carbon electrode.[8]

Argonne is improving the quality of their US powder which is produced by reacting uranium powder with H_2S. Details of the process were previously presented.[78] The most recent batch of US produced analyzed 99.8 wt.% US and only 0.2 wt.% insoluble UO_2 residue. The improvement is attributed to multiple hydriding of the uranium turnings in the low-temperature sulfiding step.[21]

High-melting thorium-uranium compounds having low thermal-neutron cross sections, namely $(Th_9U)B_4$, $(Th_9U)Be_{13}$, $(Th_9U)C$, and $(Th_9U)C_2$, can be cast with some success. Three cylindrical castings, $\frac{3}{8}$ in. in diameter by $2\frac{1}{2}$ in. long, of each of the above compounds have been produced at Battelle.[3] All three $(Th_9U)C_2$ castings were sound. Two each of the others were shown by radiography to have some cracks.[17]

Cylindrical castings of Th_2Al, ThC, ThC_2, Th_3Si_2, ThSi, and these compounds with 10 at.%

uranium additions have also been made. Although arc-melted buttons of the beryllide ($ThBe_{13}$) and boride (ThB_4) were made, satisfactory arc-cast cylinders were not obtained. The castings produced were within 2 per cent of theoretical density.[32]

A method of producing ThO_2 pellets by tumbling compacted cubes to form spheres was previously reported.[82] Oak Ridge engineers are devising other methods for preparing and fabricating ThO_2 fuels. Large, rounded ThO_2 particles have been prepared by a sol-gel process, which consists of partial denitration of thorium nitrate with superheated steam and subsequent dispersion in water to form a ThO_2 sol. The sol, then evaporated at 70 to 80°C, forms a gel, which breaks up into large particles which can be converted to dense ThO_2 by calcination at 1150°C. The particles thus formed are irregular in shape but can be rounded by grinding. No success was achieved in preparing rounded pellets by forming the gel into spheres for calcining.[84] Japanese workers have apparently accomplished this by spraying a sol through a nozzle into certain organic solvents to get spherical hydroxides, which are then heated to convert them to oxides. A thorium hydroxide slurry containing a small amount of thorium nitrate became a yellow sol when heated for several hours. Several experiments were performed to find the optimum conditions and to determine the mechanism for forming the microspheres. Isopropyl alcohol was the best solvent, although a mixture of ethyl alcohol and isobutyl alcohol (2 : 3) was also effective. The preferable sol-to-solvent ratio was about 1 to 10. It was necessary that the sol concentration be greater than 1.5*M*, and the water content of the alcohol less than 10 per cent. By controlling the spray speed of the sol, spherical particles up to 50 or 60 μ in diameter were produced.[85]

(E. O. Speidel)

Fundamental Studies of Irradiation Effects on Fuel Materials

Metallic Fuels

Theories have also been developed by Blackburn[86] to derive the effects of irradiation growth and uniform continuous thermal cycling on the creep of uranium under applied uniaxial stress when the material remains elastic. Two alternative assumptions are made, one being uniform deformation, and the other being uniform internal stress in the uranium crystals.

Solutions were obtained in several cases, and an approximate method was obtained which applies over a large range if primary creep effects are neglected. Over this range, tables were deduced from which it may be seen how the internal stress at any temperature increases with the irradiation growth and the mean temperature deviation of the cycle, while remaining independent of its period. The way is shown in which the logarithm of the creep acceleration factor varies as the logarithm of the ratio of internal to applied stress decreases, decreasing linearly at first and then more slowly.

The creep rate under a uniaxial load has also been deduced for the case when the uranium has become plastic due to irradiation growth or to a constant rate of change of temperature and also, if the applied stress is small, when it is plastic due to thermal cycling and irradiation growth acting together. Satisfactory agreement between theory and experiment was found for both the elastic and plastic ranges.

Theories to deduce the effect of irradiation growth have been derived by Blackburn[87] for the creep of uranium under a uniaxial load when the stress is too low to cause plastic flow. The theory based on the assumption of uniform deformation is reported as probably slightly more reliable, but the alternative theory, the stress being the sum of the applied stress and the internal stress that would exist if each crystal were prevented from deforming in the absence of applied stress, leads to a simpler formula for the creep rate. For ratios of creep stress to asymptotic internal stress (W/I) less than $\frac{1}{3}$, the proportionate increase in creep rate was found to vary approximately as $(I/W)^{m-1}$, where $m = 2.52$, whereas I tends to a value which varies in proportion to the nth root of the rate of irradiation growth.

In a study at Atomics International,[88] it has been shown that swelling in uranium alloys during irradiation can be correlated with the creep strength about 100°C above the irradiation temperature. This suggests that a decrease in strength may be caused by the irradiation. The total fuel swelling for a given temperature and burnup is about the same in both the MTR and SRE above 500°C. Since the burnup rate is

much higher in the MTR, it is concluded that irradiation affects the swelling rate by increasing the mobility and/or the number of dislocations. Variations in thermal cycling and thermal stress in uranium slugs had relatively little effect on the swelling.

Anisotropic irradiation growth was negligible in uranium alloys between 350 and 500°C and in uranium above 500°C. Appreciable anisotropic growth was observed in alpha-rolled, beta-quenched uranium up to 500°C.

By means of Castaing probe microanalyzer, local concentrations of rare gases were measured in metallic samples into which the gases were introduced by an electron discharge.[89] After heating, the formation of gas bubbles in those regions where the gas concentration was sufficiently high could be verified by optical microscopy. (F. A. Rough)

Ceramic Fuels

Examinations have been made on the release of fission products from a graphite-moderator lattice.[90] The initial release from the fuel to the graphite is by recoil. Subsequent migration in the graphite follows solid-state diffusion behavior. The mechanism for transport above 1000°C appears to differ from the mechanism below 1000°C. For the elements barium, strontium, cerium, cesium, lanthanum, iodine, xenon, and tellurium, diffusion coefficients appear to increase with increasing atomic radius. Also, the diffusion of metal oxides ZrO_2, ZrO, BeO, Y_2O_3, and SrO in graphite increases as the fraction T/T_m, where T is the diffusion temperature and T_m is the melting temperature. A suggested mechanism of transport is the formation of a carbide of the diffusing species, with subsequent diffusion of the carbide.

Measurements[91] of the release of cesium and xenon from UO_2 have shown an apparent connection between in-pile UO_2 grain growth and excessive release of these two elements. In highly rated UO_2 sintered pellets

$$\int_{\theta_{surface}}^{\theta_{center\ line}} K(\theta)\, d\theta = 44 \text{ watts/cm}$$

where K = thermal conductivity and θ = temperature, the postirradiation structure consists of several distinct regions: a centerline void, encircled by an annular region of radial columnar grain wheels, in turn enclosed in a ring of smaller but more equiaxed grains, and finally a surface region that exhibits no change from the preirradiation structure. In the regions showing grain growth during irradiation, the cesium and xenon concentrations were lower than would be predicted from a simple volume diffusion model for xenon and cesium migration. In the surface region that was unchanged microstructurally during irradiation, the experimental determinations of xenon and cesium were in agreement with the theoretical predictions based on the diffusion model. The reason for the depletion in regions of grain growth has not been established, but the possibility has been suggested that moving grain boundaries collect and release cesium and xenon at a much higher rate than would occur by simple diffusion of the gases through the UO_2 lattice. It was concluded that fission-gas release from high-density, stoichiometric UO_2 where grain growth does not occur is only a small factor in capsule pressure buildup. (J. B. Melehan and F. A. Rough)

References

1. E. F. Sturcken and B. Post, A Precise Determination of the Atomic Position Parameter for α-Uranium, in *Advances in X-Ray Analysis*, Vol. 4, pp. 85–92, Plenum Press, New York, 1961.
2. Ko Soeno, Properties of Cold-Drawn Uranium Rods. I. On the Thermal Expansion Coefficients and the Thermal Cycling Growths of Recrystallized Rods, USAEC Translation AEC-tr-4380 [translated from *J. At. Energy Soc. Japan*, 2: 89–95 (1960)].
3. G. C. Garrow, Summary of the Fabrication and Behavior of Standard Uranium Rods in the NRX Reactor, 1947 to 1960, Canadian Report IOI-210 (AECL-1298), February 1961.
4. Hanford Atomic Products Operation, Quarterly Progress Report, Fuels Development Operation, October, November, December 1959, USAEC Report HW-64863, Jan. 15, 1960. (Classified)
5. S. T. Zegler and M. V. Nevitt, Structures and Properties of Uranium-Fissium Alloys, USAEC Report ANL-6116, Argonne National Laboratory, July 1961.
6. W. Arbiter, The Preparation and Properties of Dispersion-Hardened Uranium Powder Products, USAEC Report NDA-2119-1, Nuclear Development Corp. of America, Feb. 21, 1961.
7. W. Arbiter, An Investigation of Dispersion Hardening in the Uranium–Uranium Dioxide System—Research in Progress, USAEC Report TID-13339, Nuclear Development Corp. of America, May 18, 1960.

8. Atomics International, Annual Technical Progress Report, AEC Unclassified Programs, Fiscal Year 1961, USAEC Report NAA-SR-6370, Aug. 15, 1961.
9. C. L. Angerman and W. R. McDonell, Metallography of Uranium–2 Wt.% Zirconium Alloy Before and After Irradiation, USAEC Report DP-589, Savannah River Laboratory, July 1961.
10. W. G. Blessing et al., Summary of the APDA Fuel Development Programs, Report APDA-143, Atomic Power Development Associates, Inc., April 1961.
11. Atomics International. (Unpublished)
12. Oak Ridge National Laboratory, Metallurgy Division Annual Progress Report for Period Ending May 31, 1961, USAEC Report ORNL-3160, Aug. 17, 1961.
13. Nuclear Metals, Inc., Fundamental and Applied Research and Development in Metallurgy, Progress Report for March 1961, USAEC Report NMI-2095, May 19, 1961.
14. H. C. Bowen and R. L. Dillon, High-Temperature Aqueous Corrosion of Aluminum-Uranium and Aluminum-Silicon-Uranium Alloys, *Corrosion*, No. 7: 9–11 (July 1961).
15. J. A. DeMastry et al., Development of Niobium-Uranium Alloys for Elevated-Temperature Fuel Applications, USAEC Report BMI-1536, Battelle Memorial Institute, Aug. 9, 1961.
16. J. A. DeMastry et al., Niobium–20 Wt.% Uranium, High-Temperature Metallic Fuel of the Future, *Nuclear Sci. and Eng.*, 9: 299–304 (1961).
17. R. W. Dayton and C. R. Tipton, Jr., Progress Relating to Civilian Applications During August 1961, USAEC Report BMI-1541, Battelle Memorial Institute, Sept. 1, 1961. (Classified)
18. B. A. Partridge and R. F. Clayton, The Preparation of Uranium/Zinc Alloys on the 10-Kg Scale, British Report AERE-M-814, January 1961.
19. Hanford Atomic Products Operation, Quarterly Progress Report, Plutonium Metallurgy Operation, January, February, March 1960, USAEC Report HW-64339, Mar. 15, 1960. (Classified)
20. J. F. Eichelberger, Mound Laboratory Monthly Progress Report for April 1961, USAEC Report MLM-1114, Mound Laboratory, Apr. 30, 1961.
21. Argonne National Laboratory, Reactor Development Program Progress Report, July 1961, USAEC Report ANL-6399, Aug. 15, 1961.
22. Atomic Energy of Canada, Ltd., June 30, 1961. (Unpublished)
23. V. W. Storhok et al., Development of Dilute Plutonium Alloys, USAEC Report BMI-1532, Battelle Memorial Institute, July 27, 1961.
24. R. W. Dayton and C. R. Tipton, Jr., Progress Relating to Civilian Applications During July 1961, USAEC Report BMI-1534, Battelle Memorial Institute, Aug. 1, 1961. (Classified)
25. G. Arthur, Ceramics Properties, *Nuclear Eng.*, 6: 253–257 (June 1, 1961).
26. L. V. Jones et al., Progress Report on Plutonium-Bearing Glass, July 1960–March 1961, USAEC Report NYO-9834, Mound Laboratory, Owens-Corning Fiberglas Co., and Rensselaer Polytechnic Institute, July 1, 1961.
27. Rensselaer Polytechnic Institute and Owens-Corning Fiberglas Corp. (Unpublished)
28. K. H. Puechl, Development of Plutonium-Bearing Fuel Materials, Monthly Progress Letter for Month of August 1961, USAEC Report NUMEC-P-34, Nuclear Materials and Equipment Corp., Sept. 5, 1961.
29. Nuclear Materials and Equipment Corp., Development of Plutonium-Bearing Fuel Materials, Progress Report for Period April 1 Through June 30, 1961, USAEC Report NUMEC-P-70, July 20, 1961.
30*a*. Paper 25.10.61 Presented at the American Ceramic Society Conference, Toronto, Apr. 26, 1961.
30*b*. G. A. Keig and H. R. Haines, The Cathodic Etching of Plutonium Ceramics, British Report AERE-R-3866.
30*c*. M. Palfreyman and L. E. Russell, Paper Presented at the 4th Plansee Seminar, Reutte, Austria, June 1961, proceedings to be published.
31. F. W. Albaugh, Reactor and Fuels Research and Development Operation Monthly Report, August 1961, USAEC Report HW-70872A, Hanford Atomic Products Operation, Sept. 15, 1961. (Classified)
32. R. W. Dayton and C. R. Tipton, Jr., Progress Relating to Civilian Applications During June 1961, USAEC Report BMI-1524, Battelle Memorial Institute, July 1, 1961. (Classified)
33. Gmelin Institut für Anorganische Chemie, Thorium: Production and Properties of the Elements, Bibliographic Compilation (in German), German Report AED-BRD-C-08-1, Dec. 20, 1960.
34. M. Bloomfield, Thorium, a Bibliography, USAEC Report NAA-SR-Memo-6108, Atomics International, Feb. 7, 1961.
35. A. Brown and J. J. Norreys, The System Thorium-Silicon, *J. Inst. Metals*, 89: 238–240 (March 1961).
36. R. H. Johnson and R. W. K. Honeycombe, The Solid Solubility of Zirconium in Alpha Thorium, *J. Nuclear Materials*, 4(1): 59–65 (May/June 1961).
37. D. S. Evans and G. V. Raynor, The Solubility of Zirconium in Alpha Thorium, *J. Nuclear Materials*, 4(1): 66–69 (May/June 1961).
38. O. D. McMasters and W. L. Larsen, Phase Equilibria in the Thorium-Tantalum System, *J. Less-Common Metals*, 3: 312–320 (1961).
39. D. S. Evans and G. V. Raynor, The System Thorium-Ytterbium: Its Alloy Properties, *J. Less-Common Metals*, 3: 179–180 (April 1961).
40. A. L. Bement, Jr., Tensile Properties of Irradiated Thorium, USAEC Report HW-66693, Hanford Atomic Products Operation, Sept. 1, 1960.

41. D. J. Murphy et al., Elevated Temperature Impact Densification of Mo-UO_2 Powder Mixtures, USAEC Report LA-2563, Los Alamos Scientific Laboratory, July 11, 1961.

42. D. G. Freas et al., Radiation Stability of Spherical and Hydrothermal UO_2 Dispersed in Type 318 Stainless, USAEC Report BMI-1529, Battelle Memorial Institute, July 14, 1961.

43. S. J. Paprocki et al., Fabrication and Irradiation of SM-2 Core Materials, USAEC Report BMI-1528, Battelle Memorial Institute, July 12, 1961.

44. A. Levy and J. F. Foster, The Compatibility of Gas Coolants and Ceramic Materials in Coated-Particle Nuclear Fuels, USAEC Report BMI-1530, Battelle Memorial Institute, July 18, 1961.

45. O. Flint, Fuel Elements for Thermal-Fission Nuclear Reactors, U. S. Patent 2,967,811 (to USAEC), Jan. 10, 1961.

46. General Atomic Div., General Dynamics Corp., 40-Mw(e) Prototype High-Temperature Gas-Cooled Reactor Research and Development Program, Quarterly Progress Report for the Period Ending December 31, 1960, USAEC Report GA-1982.

47. General Atomic Div., General Dynamics Corp., 40-Mw(e) Prototype High-Temperature Gas-Cooled Reactor Research and Development Program, Quarterly Progress Report, January 1–March 31, 1961, USAEC Report GA-2204.

48. W. V. Goeddel, The Development and Evaluation of Graphite-Matrix Fuel Components for the HTGR, USAEC Report GA-2289, General Atomic Div., General Dynamics Corp., Aug. 8, 1961.

49. European Nuclear Energy Agency, OEEC High-Temperature Reactor Project Dragon, Second Annual Report, April 1, 1960–March 31, 1961, Report NP-10483.

50. National Carbon Co., Fuel-Cycle Development Program Monthly Newsletter, June 1961, USAEC Report ORO-474, Sept. 8, 1961.

51. Oak Ridge National Laboratory, Gas-Cooled Reactor Program, Quarterly Progress Report for Period Ending June 30, 1961, USAEC Report ORNL-3166, Aug. 28, 1961.

52. J. Belle (Ed.), *Uranium Dioxide: Properties and Nuclear Applications*, U. S. Government Printing Office, Washington 25, D. C., 1961.

53. R. M. Powers et al., The Effects of Solid Solution Additions on the Thermal Conductivity of UO_2, USAEC Report SCNC-317, Sylvania-Corning Nuclear Corp., November 1960.

54. W. H. Stevens et al., The Diffusion Behavior of Fission Xenon in Uranium Dioxide, in Nuclear Reactor Chemistry, First Conference, Gatlinburg, Tennessee, October 12–14, 1960, USAEC Report TID-7610, pp. 7–22.

55. R. H. Barnes et al., Xenon Diffusion in Single-Crystal and Sintered UO_2, USAEC Report BMI-1533, Battelle Memorial Institute, Aug. 1, 1961.

56. C. Brisi, Binary Compounds in the Systems Between Alkaline-Earth Oxides and Uranium and Thorium Oxide, *Ricerca sci.*, 30: 2376–2381 (December 1960).

57. C. F. Miller et al., Chemistry of Uranium-Oxygen Systems, Final Report, USAEC Report GA-1896, General Atomic Div., General Dynamics Corp., Jan. 13, 1961.

58. D. E. Johnson et al., Irradiation of BeO-UO_2 Ceramics, USAEC Report GA-2268, General Atomic Div., General Dynamics Corp. and Battelle Memorial Institute, June 28, 1961.

59. J. E. Gates, Irradiation Testing of Beryllium Oxide–Uranium Dioxide Bodies at Battelle, in Proceedings of the Beryllium Oxide Meeting Held at Oak Ridge National Laboratory, December 1 and 2, 1960, USAEC Report TID-7602(Pt. I), pp. 12–16.

60. Combustion Engineering, Inc., March 1961. (Unpublished)

61. G. Zuromsky and W. P. Chernock, The Development and Testing of Homogeneous Ceramic Fuels, Quarterly Report, March 1, 1961–May 31, 1961, USAEC Report CEND-140, Combustion Engineering, Inc., Nuclear Div., June 1961.

62. Westinghouse Electric Corp., Bettis Atomic Power Laboratory, Aug. 23, 1961. (Unpublished)

63. United Nuclear Corp., Nuclear Fuel Research Fuel-Cycle Development Program Quarterly Progress Report, April 1–June 30, 1961, USAEC Report NYO-2693, Aug. 10, 1961.

64. J. F. Carpenter and C. W. Kuhlman, Characterization of UO_2 Powders, First Quarterly Report, Oct. 10, 1960, to Jan. 10, 1961, USAEC Report ORO-395, Mallinckrodt Nuclear Corp., Mar. 22, 1961.

65. H. R. Longfield (Comp.), Atomic Energy of Canada, Ltd., April 1961. (Unpublished)

66. Proceedings of the Symposium on Uranium Carbides as Reactor Fuel Materials, Held at Germantown, Maryland, April 4, 1961, USAEC Report TID-7614.

67. M. Tetenbaum et al., Uranium and Uranium Carbide Ignition Studies, *Trans. Am. Nuclear Soc.*, 4(1): 89–90 (June 1961).

68. Argonne National Laboratory, Chemical Engineering Division Summary Report, January, February, March 1961, USAEC Report ANL-6333, June 1961.

69. E. W. Murbach, The Oxidation of "Reactive" Uranium Carbide, USAEC Report NAA-SR-6331, Atomics International, July 15, 1961.

70. G. B. Engle et al., Reaction-Rate Studies of Thorium-Uranium Dicarbides in Moist Air, USAEC Report GA-2068, General Atomic Div., General Dynamics Corp., Apr. 11, 1961.

71. G. B. Engle et al., Reaction-Rate Studies of Thorium-Uranium Dicarbides in Moist Air, USAEC Report GA-2195, General Atomic Div., General Dynamics Corp., Apr. 20, 1961.

72. M. J. Bradley and L. M. Ferris, Processing of Uranium Carbide Reactor Fuels. I. Reaction with Water and HCl, USAEC Report ORNL-3101, Oak Ridge National Laboratory, Aug. 15, 1961.
73. F. Benesovsky and E. Rudy, Information on the System Uranium-Zirconium (Hafnium, Niobium, Tantalum)-Carbon, *Planseeber. Pulvermet.*, 9: 65–76 (April 1961).
74. K. Whitehead and L. D. Brownlee, The Zirconium Carbide–Uranium Carbide System, British Report AERE-X/PR-2477, February 1956.
75. K. Whitehead and L. D. Brownlee, The Niobium Carbide–Uranium Carbide System, British Report AERE-X/M-178, May 1957.
76. J. J. Finley et al., Columbium Alloy Clad Uranium Carbide Fuel Elements, USAEC Report ORO-366, Union Carbide Metals Co., Sept. 1, 1960.
77. R. W. Dayton and C. R. Tipton, Jr., Progress Relating to Civilian Applications During September 1961, USAEC Report BMI-1546, Battelle Memorial Institute, Oct. 1, 1961. (Classified)
78. *Reactor Core Materials*, 4(4): (November 1961).
79. K. M. Taylor and C. H. McMurtry, Synthesis and Fabrication of Refractory Uranium Compounds, First Quarterly Report, March 1 Through May 31, 1961, USAEC Report ORO-448, Carborundum Co., June 29, 1961.
80. K. M. Taylor and C. H. McMurtry, Synthesis and Fabrication of Refractory Uranium Compounds, Monthly Progress Report No. 4, July 1 Through July 31, 1961, USAEC Report ORO-476, Carborundum Co., Aug. 8, 1961.
81. Proceedings of the Uranium Carbide Meeting Held at Oak Ridge National Laboratory, Oak Ridge, Tennessee, December 1–2, 1960, USAEC Report TID-7603.
82. *Reactor Core Materials*, 4(3): (August 1961).
83. Hanford Atomic Products Operation, Uranium Ceramic Fuels, U.S./U.K. Research Newsletter No. 11, April 1961.
84. Oak Ridge National Laboratory, Homogeneous Reactor Program Progress Report for Period from December 1, 1960, to May 31, 1961, USAEC Report ORNL-3167, Sept. 6, 1961.
85. Y. Yamazaki et al., The Preparation of Spherical Thorium Oxide Microspheres. I. On the Preparation of Spherical Thorium Hydroxide Particles (in Japanese), *J. At. Energy Soc. Japan*, 3: 360–364 (May 1961).
86. W. S. Blackburn, The Effect of Internal Stresses Due to Irradiation Growth and Thermal Cycling on the Creep of Uranium, in the Cases of Both Elastic and Plastic Behavior, *J. Nuclear Energy, Pt. A, Reactor Sci.*, 14: 107–116 (May 1961).
87. W. S. Blackburn, Effect of Irradiation Growth on the Creep of Uranium Under a Uniaxial Load, *Phil. Mag.*, 6: 503–508 (April 1961).
88. G. G. Bentle, Irradiation Swelling of Uranium and Uranium Alloys, USAEC Report NAA-SR-4893, Atomics International, Sept. 30, 1961.
89. V. Levy et al., Contribution to the Study of the Precipitation of Rare Gases in Metals, French Report CEA-1922 [from *Compt. rend.*, 252: 876–878 (Feb. 6, 1961)].
90. A. R. Saunders, A Study of Fission-Product Transport Mechanisms in High-Temperature Gas-Cooled Reactor Fuel Elements, USAEC Report ORNL-3145, Oak Ridge National Laboratory, July 13, 1961.
91. W. W. Morgan et al., A Preliminary Report on Radial Distribution of Fission-Product Xenon and Cesium in UO_2 Fuel Elements, Canadian Report CRDC-1027(AECL-1249), April 1961.

Section II

Reactor Materials

Moderator Materials

Graphite

Studies are reported in three areas of graphite-oxidation control. Samples of Si-SiC coated graphite were irradiated by Hanford[1] in a helium-CO_2 atmosphere at about 500°C to a dosage of approximately 8×10^{20} nvt ($E > 1$ Mev). There was no visible evidence of radiation damage to the SiC. Following irradiation, samples were heated to 1000°C in flowing air and weighed periodically to determine weight changes. In the cases where coating failure occurred, it apparently resulted from stresses in the coating originating from either radiation or thermally induced dimensional changes in the graphite. Thus the data indicate that Si-SiC coated graphite can be used successfully in a radiation environment if the base graphite is carefully selected.

The Si-SiC coated samples irradiated[2] to 3000 Mwd/adjacent ton at 500°C were cycled in air from 250 to 1200°C at a frequency of 7 cycles/hr. After 27 hr of test, there was an almost negligible weight gain.

Successful procedures have been developed by the British[3] for impregnating a commercial graphite with up to 4.8 wt.% silicon or up to 2.5 wt.% titanium, using $SiCl_4$ or $TiCl_4$ as the impregnant gas. This was not a mere surface impregnation but extended throughout the bulk pore structure of the graphite. Silicon impregnation reduced the permeability of the base graphite from 1×10^{-2} cm^2/sec to between 7×10^{-3} and 2×10^{-5} cm^2/sec. Titanium impregnation did not measurably reduce the permeability of the base graphite. Oxidation tests of the impregnated graphites had not been conducted.

Evaluation at Hanford[4] of the chlorine inhibition of graphite oxidation as a gas-cooled-reactor safeguard showed that it was effective in both the presence and absence of ionizing radiation. Chlorine reduced oxidation rates at a temperature of about 700°C by a factor of 5 when present in a chlorine-to-oxygen mole ratio of 0.1 in dry gas. It was less effective in the presence of moisture. A rate law derived on the premise of chlorine chemisorption on active carbon sites, essentially poisoning the surface, agreed with observed data.

Effects of thermal annealing on the structure of pyrolytic graphites deposited at temperatures between 1700 and 2300°C have been studied by General Electric.[5] As-deposited density varied between 1.36 and 2.20 g/cm^3, but average layer spacing was between 3.415 A and 3.43 A regardless of density and deposition temperature. Annealing data indicate that only small permanent changes occur upon heating pyrolytic graphite until a critical temperature is reached. At this temperature, 2500 to 2600°C in the case studied, shrinkage across the thickness of the deposit begins and there is an expansion in the plane of deposition. Three stages in annealing are associated with creep due to internal stress, ordering of parallel basal planes, and growth of facets on the puckered layers. Data from this study indicate that density and deposition temperature are not sufficient to indicate the temperature at which pyrolytic graphite transforms. Differences in initial microstructure associated with the amount of gas-phase nucleated carbon that is present affect the temperature ranges in which the second and third stages of annealing begin. A 20-min anneal at 3000°F appeared sufficient to complete transformation in most specimens.

Studies are in progress[6,7] to measure the effect of chemical additives on the dimensional behavior of graphite under irradiation. At a cold test hole exposure of 4241 Mwd/adjacent ton, a Texas coke-base graphite with 1 wt.% iron oxide addition had 43 per cent greater

transverse growth than an identical graphite without the additive. Other levels of iron oxide additions and other oxide additions will be studied. (M. C. Brockway)

Beryllium Metal and Alloys

The compaction of beryllium powder into solid bodies often involves the production of unusually large sizes. For example, powder valued at $60 per pound is converted into blocks weighing up to 5 tons. Several excellent publications[8–12] have appeared recently that review this process and stress the controls of particle size, degree of oxidation, and over-all purity required to obtain a satisfactory product.

A bibliography[13] of 109 United Kingdom Atomic Energy Authority (UKAEA) publications on beryllium and beryllia, plus 51 references to articles published by UKAEA personnel, has become available. Another bibliography[14] carries 670 references to articles on the toxicology of beryllium.

Purification

The attempt to produce pure beryllium by distillation that was carried out at Nuclear Metals yielded metal with a high degree of purity, although silicon was not removed efficiently.[15] However, the purest beryllium obtained by this process showed essentially zero ductility in both tensile and bend tests. Electron-microscope examination of specimens broken at 77°K revealed spherical particles of less than 2 μ diameter on each fracture surface. Fracture surfaces of single crystals which were refined at Franklin Institute and which exhibited considerable room-temperature ductility did not show these particles. The spherical precipitate particles were not redissolved by a vacuum treatment at 1000°C for 3 hr. The particles could not be identified.[15,16]

Meanwhile, as shown in Table II-1, Franklin Institute[17] reported results of tensile tests on their single crystals which appear to indicate that impurities in beryllium strongly influence the possible amount of basal-plane glide. Along this line, the British have prepared an exhaustive review[18] of the literature on plastic deformation and fracture of single crystals of beryllium and application of the theories evolved to deformation and fracture of a polycrystalline aggregate. However, the ultimate reasons for brittleness in beryllium could not be deduced with certainty.

Beryllium Fabrication

Hot Working. Although beryllium can undergo mild deformation in closed forging dies without the use of a supporting jacket, a positive method for keeping the beryllium in compression is necessary for drastic forging operations.[19] In some cases an expendable carbon-steel support ring can be used to alleviate the tensile stresses and make jacketing unnecessary. Unclad beryllium parts consisting of a center hub with a circumferential web were forged from blanks made from Berylco HP-20

Table II-1 RESULTS OF TENSILE TESTS ON BERYLLIUM SINGLE CRYSTALS[17]

Starting material	No. of zone melting passes	Orientation*	Heat-treatment prior to testing	Resolved shear stress at yielding, psi	Strain at fracture, % glide strain	Operating glide systems
Pechiney	Vacuum cast	$\chi_0 = 45°$ λ_0 unknown	Unknown	2000 ± 500	~5	Basal plane
Berylco vacuum-cast ingot	2	$\chi_0 = 47°$ $\lambda_0 = 51°$	800°C, 1 hr	2400	16	Basal plane
Berylco vacuum-cast ingot	5	$\chi_0 = 20°$ $\lambda_0 = 25°$	900°C, 1 hr	1350	64	Prism plane
Pechiney	8	$\chi_0 = 48°$ $\lambda_0 = 55°$	None	520	156	Basal plane

*χ_0 = angle between slip plane and tensile axis; λ_0 = angle between slip direction and tensile axis.

block. The blanks were preheated to 1400°F in closed dies with a solid lubricant. Mechanical properties of the forged beryllium are given[20] as:

	Ultimate tensile strength, psi	0.2% offset yield strength, psi	Elongation, %
Hot pressed	48,100	30,700	4.3
Forged	66,400	50,700	3.0
Forged	67,300	49,100	5.1

A British patent[21] claims that an adherent electrolytic coating of gold or silver makes drawing or extrusion of beryllium easier. For drawing, the coated beryllium is preheated to between 400 and 500°C and drawn at this temperature with die speeds of 0.2 to 40 in./min; for extrusion, the metal is preheated to between 500 and 700°C and a die speed of 1 to 5 ft/sec is maintained.

Machining. General Electric[22] recommends that blind holes be avoided when tapping beryllium because they shorten tool life and that fine threads should be used because they are easier to tap than coarse threads. Threaded inserts have been designed and fabricated that can be installed successfully in beryllium. If the edge distance is great enough, beryllium threads can develop strength up to the ultimate strength of the beryllium or even of the steel bolts.

Joining. Beryllium sheet 0.015 in. thick can be welded to itself ultrasonically, as demonstrated[15] by Aeroprojects, Inc. Brush Beryllium was unable to find a silver-base brazing alloy for beryllium superior to the commercial silver plus lithium used in production. A British patent[23] describes a method of brazing beryllium, using a brazing solder containing 55 to 70 wt.% silver, 20 to 30 wt.% copper, and 10 to 20 wt.% palladium. The method involves heating in high-purity hydrogen at reduced pressure for 5 min at 830 to 840°C, followed by heating at 910°C for 1 min, and rapid cooling to 700°C. Considerable grain growth might be expected after this treatment, even if excessive penetration of the beryllium did not occur.

By hot-roll planishing of the welding reinforcement along the direction of welding on beryllium sheet directly after stress relieving (30 min at 825°C), Brush workers[15] produced tensile specimens from 0.062-in. sheet with average strengths of 45,300 psi. Resistance butt welds have been made by Brush in cylindrical beryllium rods with the joint area enclosed in alumina tubes that are almost invisible on a micrograph at 250× magnification. These joints showed tensile strengths varying from 45.3 to 52.5 psi × 10^3.

Resistance-welding experiments at Rensselaer[15,16] revealed that, at the end of the welding portion of the weld sequence, the cooling rate exceeded 3300°C per second. Defect-free spot welds in 0.040-in.-thick beryllium sheet were obtained consistently by (1) adjusting the postheat cycle as shown below to decrease the cooling rate and (2) increasing the initial 450-lb welding force to 1500 lb at 77 cycles after the end of the main weld time.

	Time (60 cycles = 1 sec)	% of main welding current (9000 amp)
Preheat	200 cycles	75
Main weld heat	8 cycles	100
Postheat	110 cycles	95

Physical Metallurgy of Beryllium

Several British reports have been received that describe the metallography of beryllium. Point projection X-ray microscope pictures of several beryllium alloys were reported[24] to offer some advantage in detail over the more usual contact microradiography. The application of electron-probe X-ray microanalysis to the identification of constituents and the use of an etchant to reveal hitherto unreported details were described in another report.[25] Studies by optical metallography, electron-probe analysis, and divergent-beam X-ray microscopy of a zone-refined beryllium single crystal revealed that impurities expand the lattice.[26] It was also noted that the impurities increased in steps, not continuously, along the zone-refined crystal. The same group of authors used an aqueous copper sulfate etchant to obtain microstructures of cast and hot-extruded beryllium that strongly suggest a precipitation reaction,[27] starting at the grain boundaries, on aging at 500 to 600°C.

Examination of the fracture surfaces of beryllium cast from Pechiney flake has shown dendrites lying on grain-boundary surfaces. The dendrites were either titanium rich or calcium rich but were not mixed. On the basis of this observation, a modification of the beryllium-titanium-calcium diagram was proposed.[28]

Russian authors[29] reported the identification of a new phase, delta, in the beryllium-boron system. This phase, Be_5B, crystallizes in the tetragonal system with $a = 3.362 \pm 0.002$ *kX*, $c = 7.036 \pm 0.005$ *kX*, and $c/a = 2.093$. The electrical resistivity of the delta phase (0.015 ohm-cm) is similar to that of the alpha phase, Be_2B (0.014 ohm-cm). The delta phase is stable up to 1500°C but is highly reactive.

Another group of Russian authors[30] determined the distribution of beryllium between the phases of nickel-beryllium, nickel-beryllium-tungsten, and nickel-beryllium-molybdenum. They carried out electrolysis at room temperature with a current density of 0.06 amp/cm^2 in an electrolyte containing ammonium citrate and ammonia.

Analysis of the asterisms of Laue spots and a study of extinction figures of a single crystal in divergent clusters[31] showed the following four slip systems for beryllium:

1. $\langle 11\bar{2}0 \rangle$ (0001) from 0 to 1000°C
   $(10\bar{1}0)$ from 0 to 1000°C
   $(10\bar{1}1)$ from 0 to 1000°C
   $(10\bar{1}4)$ at high temperature
2. $\langle 10\bar{1}0 \rangle$ (0001) at high temperature
3. $\langle 10\bar{1}3 \rangle$ $(10\bar{1}0)$ at high temperature
4. $\langle \bar{1}101 \rangle$ $(10\bar{1}0)$ at high temperature

An important twinning axis $(10\bar{1}2)$ exists at 1000°C under favorable orientation conditions. The system $(10\bar{1}1)$ $\langle \bar{1}2\bar{1}0 \rangle$ becomes important at high temperature. The system $(10\bar{1}4)$ $\langle \bar{1}2\bar{1}0 \rangle$ is active at 800 to 1000°C. These systems permit an explanation of certain aspects of the formation of textures which could not be interpreted with the aid of systems of deformation known before.

A marked alignment of $\langle 10\bar{1}0 \rangle$ directions in the direction of extrusion was found[32] in tubes prepared by warm (850°C) extrusion from billets machined from hot (1050°C) extruded rods and flats. The basal-plane concentrations varied only slightly and in general appeared to be affected only slightly by the conditions during the tube-extrusion stage.

Physical and Mechanical Properties of Beryllium

Measurements of thermal conductivity, electrical resistivity, Lorentz ratio, and thermoelectric power of beryllium at cryogenic (4 to 120°K) temperatures were reported by Powell et al.[33] and magnetic properties in the range 4 to 300°K by Verkin et al.[34]

The Canadians[35] have noted a sharp rise in ductility between 100 and 300°C, which suggests the occurrence of a brittle-ductile transition in this region. They also noted that water-quenched beryllium materials of the same average grain size showed the highest rupture life at all stresses.

Lockheed is continuing to develop extensive mechanical-property data[36–38] on beryllium, including fatigue properties and dynamic properties, as well as data on lug, joint, and fastener properties. From tensile tests on notched specimens, it is concluded that both beryllium block and sheet are somewhat notch sensitive up to 500°F, but neither is notch sensitive above this temperature. Surface twins in hot upset beryllium sheet, like those in hot-pressed material, can be removed[15] by a suitable annealing treatment. This could not be accomplished with hot-rolled sheet.

Yield strengths of about 64,000 psi and tensile strengths of about 81,000 psi, with elongations of 8.6 to 11.3 per cent, were obtained in a beryllium–1 wt.% copper alloy that was rolled at 1500°F with reductions[15] of about 3.5:1 or 4.5:1.

It was reported earlier [A. Brown et al., An Improvement in the Ductility of Beryllium at High Temperatures, *Nature*, 187: 494–496 (Aug. 6, 1960)] that the ductility of vacuum-cast beryllium that was subsequently extruded was much improved by an aging heat-treatment. Similar improvement could not be obtained at Nuclear Metals by the same aging treatment when applied to beryllium made from QMV powder material.[15]

A systematic study of the effects of heat-treating on cold-compacted and hot-extruded commercial (QMV) beryllium was reported[39] by Gelles and Wolff. Their specimens were heat-treated in evacuated sealed tubes at 1100°C for 1 hr and then were either water quenched or slow cooled, followed by various aging treatments on the quenched specimens. The slow-cooled specimens exhibited significantly higher tensile strengths and elongations at room temperature. Aging the quenched specimens at 400°C had no effect on tensile strength or elongation, but the material developed a yield point after 2 hr. Aging the quenched samples at 600°C improved their ultimate tensile strength and elongation. A yield point developed only after

24 hr at 600°C. The slow-cooled samples tested at elevated temperatures had better properties than the quenched and aged specimens, especially in the range from room temperature to 400°C.

The electrical resistivity of the quenched specimens showed essentially no change at 200°C, some decrease at 400°C, and a 78 per cent decrease after 168°C and reached essentially complete equilibrium after 15 min at 800°C.

No changes in hardness or in orientation were caused by the aging treatments. Electron-microbeam-probe analysis indicated the presence of chromium, manganese, and iron in the precipitated particles. Iron and some aluminum appeared to be segregated in the grain boundaries, and silicon in some beryllium oxide spots. The precipitates could not be identified, however.

Bastien and Pointu,[40] however, found that the ductility of thermally reduced beryllium was improved by heat-treatment. Their beryllium, extruded from powder, showed a decrease in ductility in the range 400 to 600°C, which was not found by the British in cast and extruded material.

Corrosion and Irradiation Behavior of Beryllium

Changes in the mechanical and physical properties of beryllium that result from neutron irradiation may be attributed to the displacements produced by energetic neutrons or the products from the $(n,2n)$ and (n,α) reactions with beryllium and to the effects of the agglomeration of the helium produced by these transmutations. According to Oak Ridge,[41] the mechanism for gas agglomerating into the large bubbles that cause swelling appears to be the migration of small gas-filled cavities (possibly cylindrical) to inclusions or other suitable nuclei where surface-tension restraining forces are small. Thus the swelling is probably controlled by the creep properties of the matrix and the rate of movement of the gas-filled cavities to the large bubbles.

Three grades of beryllium from Brush with oxide contents varying from 0.78 to 2.22 per cent, three from Pechiney with oxide contents varying from 0.25 to 0.55 per cent, and samples of zone-refined, bicrystal, and cast beryllium from Atomic Weapons Research Establishment (Aldermaston, England), all with 0.1 wt.% or less of oxide, were bombarded at 35°C and also at 600 to 750°C by alpha particles in the MIT cyclotron. No obvious dependence of the amount of bubble growth on oxide content was found.[42]

Hydrogen agglomerates were formed[43] in cyclotron-irradiated beryllium after heating for 1 hr in the temperature range 300 to 400°C. A hydrogen content of ~0.5 cm^3/cm^3 causes crack formation on heating above 800°C. Grain boundaries are highly preferred sites of nucleation for the agglomerates, and this behavior obscures the effects that are believed to be caused by bubble formation through vacancy diffusion mechanisms.

The chemistry and kinetics of the oxidation of electrolytic flake beryllium in moist carbon dioxide and in moist carbon monoxide (either gas, total pressure 10 cm Hg; partial pressure of water, 1.2 cm) have been investigated[44] at temperatures in the ranges 500 to 750°C and 600 to 700°C, respectively. In moist carbon dioxide, the reaction with water vapor predominates over that with carbon dioxide in the proportion of approximately 4 : 1; the reactions are $Be + H_2O = BeO + H_2$; $Be + CO_2 = BeO + CO$; and $2Be + CO_2 = 2BeO + Be_2C$. The oxidation is protective up to 600°C and nonprotective at 650°C and above; the reaction after breakaway takes place at the particle boundaries, giving rise to an interpenetrating region of oxide and unattacked metal. In moist carbon monoxide, the principal reaction is with water vapor, and the reaction $Be + CO = BeO + C$ only contributes about 3 per cent to the total weight gain. An investigation of the oxidation in a moist carbon monoxide–carbon dioxide mixture (partial pressures: water, 1.2 cm; carbon monoxide, 0.5 cm; carbon dioxide, 8.3 cm) at 700°C shows that the kinetics are the same as in moist carbon dioxide, the reaction with carbon monoxide only contributing 0.2 per cent to the total weight gain.

Beryllium brazed to stainless steel, nickel-clad beryllium, and nickel-plated beryllium metallographic samples were galvanically corroded, with the beryllium attacked in preference to the other metals, when the surfaces were prepared on a Syntron vibratory polisher with ethylene glycol as the vehicle for the abrasive.[45] This attack could be eliminated by the addition of small amounts of $NaNO_3$ to the abrasive slurry. However, the $NaNO_3$ reacted unfavorably with some components of the samples.

(W. Hodge)

Beryllium Compounds

University of California investigators have conducted a literature survey and compiled a bibliography[46] on properties of BeO ceramics pertinent to the thermal-shock parameter

$$\tau = \frac{K\sigma\,(1-\nu)}{E\alpha}$$

A compilation of published data on thermal conductivity (K), thermal expansion (α), modulus of elasticity (E), and Poisson's ratio (ν) of BeO bodies is given. The strength (σ) of ceramic bodies was recognized to be highly structure sensitive, and no generally applicable figure could be given.

Measurements of lattice parameters of BeO have been reported by investigators at Atomic International[47] and at Harwell.[48] Miller at Atomics International utilized lattice-parameter data at temperatures from 0 to 1700°C to measure the thermal-expansion coefficient of BeO. He reported the following:

Temp. range, °C	Coefficient of thermal expansion, 10^{-6}/°C	
	c axis	*a* axis
0 to 1700	10.95	11.32
1200 to 1700	14.95	14.79

Lattice parameters were given for temperatures up to 2050°C. Bellamy and associates at Harwell measured the lattice parameters at 21°C of BeO derived from various starting materials and having various impurity levels. Within the limits of experimental error, the observed lattice parameters were not sensitive to these variables or to the type of X radiation employed. The "best" values for lattice parameters and theoretical density at 21°C were

$$a = 2.6979 \pm 0.0001 \text{ A}$$
$$c = 4.3772 \pm 0.0002 \text{ A}$$
$$\rho = 3.0100 \pm 0.0003 \text{ g/cm}^3$$

Austerman and associates at Atomics International have employed radioactive O^{18} to observe diffusion of oxygen[49] in BeO. BeO surfaces were treated with O^{18}, and the specimens were then annealed at 1600 to 1900°C to cause the oxygen to diffuse inward. The O^{18} concentration as a function of depth was measured by procedures involving sectioning, vacuum fusion, and mass spectrometry. These workers observed two and possibly three distinct data regions, or apparent diffusion rates, as evidenced by plotting ln O^{18} concentration versus (section depth)^2. Also, oxygen was shown to diffuse more slowly, by several orders of magnitude, than beryllium in BeO. Thus it appeared that the kinetics of oxygen diffusion would control any mass-transfer phenomena. This conclusion is in reasonable agreement with recent sintering theory.

Investigators at several sites have observed a deterioration of certain properties in some beryllides when they are heated to an intermediate temperature (1000 to 2000°F). Owens et al. at Brush Beryllium Company have reported these effects[50] in (Zr, Nb, U-Zr)Be_{13}. Specifically, modulus of rupture and resistance to thermal stresses are decreased, and the tendency to spall and oxidize is enhanced. Similar effects were noted in $ZrBe_{13}$, Zr_2Be_{17}, and $NbBe_{12}$ at temperatures of 600 to 1000°C by Nachman and associates at Denver Research Institute.[51] No such effects were noted in Ta_2Be_{17} at temperatures[52] up to 2750°F. Brush investigators attributed these effects to an oxidizing atmosphere. The effects were lessened considerably when specimens were heated in moist argon and were not observed when atmospheres of dry argon, nitrogen, CO_2, or vacuum were employed. Brush scientists further learned that carbon and oxygen impurities in $ZrBe_{13}$ severely decreased its strength and thermal-stress resistance and increased its rate of oxidation[50] at 1600°F. Up to 1 wt.% iron, however, reduced spalling and oxidation in direct proportion to the amount of iron present. Experiments are continuing in this area.

In other work at Brush,[52] the ternary system tantalum-beryllium-silicon is being explored in a search for new high-temperature materials. Solid solutions were formed in this system, but the extent of solution was found to be limited. Three types of compounds were formed: (1) Ta(Be, Si)$_{12}$, isomorphous with $TaBe_{12}$; (2) Ta(Be, Si)$_2$, isomorphous with $TaBe_2$; and (3) a different form of Ta(Be, Si)$_2$, isomorphous with $MoSi_2$ and WSi_2. Current work at Denver Research Institute includes attempts to form zirconium beryllides by vapor-depositing beryllium on zirconium at high temperature.[51]

Russian investigators have studied the oxidation resistance of certain beryllium borides.[53] Compounds containing large amounts of boron (e.g., BeB_2, BeB_4, and BeB_6) were found to be more stable than Be_5B and Be_2B. Oxidation of boron to B_2O_3 and volatilization of the oxide was postulated to explain weight-loss data. The investigators suggested that a protective layer of B_2O_3 was formed on the specimens, indicating the existence of a diffusion-controlled reaction. These studies showed that even the most stable beryllium borides were inferior to the borides of the transition metals with regard to resistance to oxidation and carburization. (A. K. Smalley)

Solid Hydrides

Zirconium Hydride

Investigators at Atomics International[54] have completed the phase diagram of the zirconium-hydrogen system by dissociation-pressure measurements in the region of high hydrogen content. Figure II-1 shows the portion of the diagram of the system for compositions above $ZrH_{0.7}$. Dissociation pressures measured in the epsilon hydride region are given[55] in Table II-2.

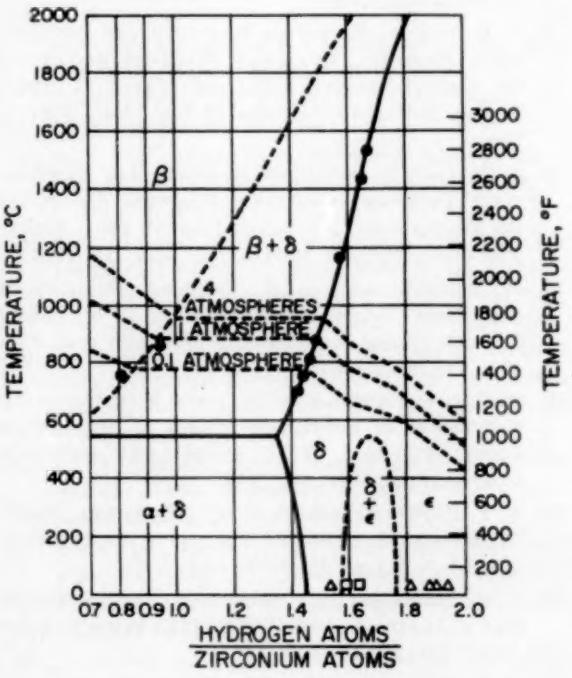

Fig. II-1 Phase diagram for the zirconium-hydrogen system.[55] ●, thermodynamic data. Δ, X-ray data (single phase). □, X-ray data (two phase).

Table II-2 DISSOCIATION PRESSURES OF EPSILON ZIRCONIUM HYDRIDE[55]

Temp., °F	Dissociation pressure, atm H/Zr ratio 1.85	H/Zr ratio 1.90	H/Zr ratio 1.95
850		0.03	0.46
900	0.01	0.07	1.30
950	0.03	0.17	2.90
1000	0.07	0.47	3.20
1050	0.16	1.00	10.0
1100	0.33	2.20	
1150	0.77	4.60	
1200	1.40	9.20	

Table II-3 TRANSVERSE RUPTURE STRENGTH OF ZIRCONIUM HYDRIDE (RECTANGULAR BARS)[56]

Temp., °F	Rupture strength, 1000 psi H/Zr ratio 0.62–0.67	H/Zr ratio 0.69–0.75
Room	21 ± 1	17 ± 3
500		18 ± 2
700	22.0	
800		19.0
1000	>23.0 (bent)	16.0

Measurements of transverse rupture strength made on zirconium hydride of low hydrogen content show a decrease in strength as the hydrogen-to-zirconium ratio is increased. Table II-3 presents the results of the study.[56]

Lithium Hydride

The viscosity of liquid lithium hydride was measured at Battelle[57] over the temperature range 1252 to 1578°F, under a hydrogen pressure of 20 psig. The viscosity is described by a straight line between 0.37 centipoise at 1252°F and 0.24 centipoise at 1570°F. The lithium hydride melted at about 1252°F, which is 10° lower than the reported value.

Austenitic stainless steels were exposed to molten lithium hydride at 1325°F for 100 hr by General Electric.[58] No significant changes in tensile strength or yield strength were found. The percentage elongation decreased slightly in all cases, type 301 showing the most. Chemical attack amounted to less than 0.001 in. Increasing the temperature to 1425°F increased the attack on all steels except type 301. All the steels showed lithium pickup, and type 321 showed nickel depletion, whereas type 316 lost both

nickel and chromium. However, the weight loss in 100 hr was negligible.

In another study[59] the effective thermal conductivity of cast lithium hydride was found to be increased slightly by finning the surface and further enhanced by introducing an inert gas to fill the cracks and voids.

Alloy Hydrides

The hydriding characteristics of 100 intermetallic phases were investigated at Denver Research Institute.[60] Intrinsic hydride formation was found with only eight of the compounds, whose composition and hydrogen-to-metal ratio are shown in Table II-4.

Table II-4 INTERMETALLIC COMPOUNDS THAT FORM INTRINSIC HYDRIDES[60]

Composition	Hydrogen-to-metal ratio
ZrV_2	1.38
$ZrCr_2$	1.16
$TiCr_2$	0.22
HfV_2	1.06
Ti_2Ni	0.96
Zr_2Al	0.90
Zr_3Al_2	0.52
Zr_2Al_3	0.21

At Atomics International[61] the thermal-expansion coefficient of zirconium–7 wt.% uranium hydride was found to be $6.12 \times 10^{-6}/°F$ for material having an N_H of 6.4 over the temperature range 77 to 1200°F. (H. H. Krause)

References

1. J. L. Jackson, The Effect of Irradiation on Siliconized-Silicon Carbide Coatings for Graphite, USAEC Report HW-68494, Hanford Atomic Products Operation, February 1961.
2. F. W. Albaugh, Reactor and Fuels Research and Development Operation Monthly Report, July 1961, USAEC Report HW-70658A, Hanford Atomic Products Operation, Aug. 15, 1961. (Classified)
3. Hawker Siddeley Nuclear Power Co., Ltd., The Production of Materials Based on Graphite with Reduced Permeability and with Improved Oxidation and Erosion Resistance, British Report NP-10213, November 1960.
4. R. E. Dahl, Evaluation of Chlorine Inhibition of Graphite Oxidation as a Gas-Cooled Reactor Safeguard, USAEC Report HW-67255, Hanford Atomic Products Operation, April 1961.
5. E. R. Stover, Effects of Annealing on the Structure of Pyrolytic Graphite, USAEC Report TID-12542, General Electric Research Laboratory, November 1960.
6. Hanford Atomic Products Operation. (Unpublished)
7. F. W. Albaugh, Reactor and Fuels Research and Development Operation Monthly Report, August 1961, USAEC Report HW-70872A, Hanford Atomic Products Operation, Sept. 15, 1961. (Classified)
8. K. G. Wikle and V. C. Potter, Beryllium Processing by Powder Metallurgy, *J. Metals*, 13(8): 537–544 (August 1961).
9. A. J. Martin and G. C. Ellis, The Relationship Between Powder Properties and Pressing and Sintering Behavior, *Powder Met.*, No. 7: 120–138 (1961).
10. W. Leszynski (Ed.), *Powder Metallurgy*, Interscience Publishers, Inc., New York, 1961.
11. L. R. Williams and P. B. Eyse, Beryllium, from *Materials for Nuclear Engineers*, Interscience Publishers, Inc., New York, 1960.
12. G. F. Silina et al., *Beryllium; Chemical Technology and Metallurgy*, Atomizdat, Moscow Berillii: Khimicheskaia Tekhnologiia i Metallurgiia, 1960.
13. U. R. M. Chadwick (Comp.), Bibliography on Beryllium and Beryllia, British Report NP-10472, June 30, 1961.
14. E. D. Hutchinson et al., Toxicology of Beryllium: A Bibliography, USAEC Report UR-570, University of Rochester, 1960.
15. S. H. Gelles, Beryllium Research and Development Program, Quarterly Progress Report for the Period January 1 Through March 31, 1961, Report NMI-9512, Nuclear Metals, Inc., July 7, 1961.
16. S. H. Gelles, Beryllium Research and Development Program, Quarterly Progress Report for the Period April 1 Through June 30, 1961, Report NMI-9515, Nuclear Metals, Inc., Aug. 11, 1961.
17. M. Herman and G. E. Spangler, Ductility of Beryllium Single Crystals Oriented for Basal Slip and Tested in Tension, *J. Franklin Inst.*, 271: 421–422 (May 1961).
18. A. P. Green and J. Sawkill, Some Thoughts on the Brittleness of Beryllium, Report No. 97, British Report NP-9946, Tube Investments Research Laboratories, Sept. 25, 1959.
19. A. F. Hayes, Beryllium Forging Program. Phase III. Interim Engineering Reports 4 and 5, March 1, 1960, to March 31, 1961, Ladish Co.
20. J. P. Denny and J. D. McKeough, Forging Unclad Beryllium, *J. Metals*, 13: 432–433 and *Light Metal Age*, 19: 11 (June 1961).
21. J. F. Sackman et al., Extrusion and Drawing of Beryllium, British Patent 868,064 (to United Kingdom Atomic Energy Authority), May 17, 1961.

22. A. D. Feith, Tapped Holes in Beryllium, USAEC Report APEX-649, General Electric Co., Flight Propulsion Laboratory Dept., July 10, 1961.
23. D. M. Atkinson, Beryllium Brazing, British Patent 870,780 (to Associated Electrical Industries, Ltd.), June 21, 1961.
24. D. R. Schwartzenberger, X-Ray Microscopy of Some Beryllium Alloys, British Report NP-8993, Tube Investments Research Laboratories, Mar. 1, 1960.
25. J. Sawkill and J. Meredith, The Metallography of Beryllium. A Summary Report, British Report NP-10116, Tube Investments Research Laboratories, Apr. 4, 1960.
26. J. Sawkill and D. R. Schwartzenberger, X-Ray Microscopy of a Zone-Refined Single Crystal of Beryllium, British Report NP-9919, Tube Investments Research Laboratories, July 29, 1959.
27. J. Sawkill et al., A Precipitation Reaction in Commercially Pure Beryllium, British Report NP-10385, Tube Investments Research Laboraties, Jan. 31, 1961.
28. J. Sawkill and J. E. Meredith, A Note on the Microfractography of Beryllium, British Report NP-9993, Tube Investments Research Laboratories, May 2, 1960.
29. G. S. Markevich et al., A New Phase in the Beryllium-Boron System, *Russ. J. Inorg. Chem.*, 5: 865–867 (August 1960).
30. N. I. Blok et al., Phase Studies in Nickel-Beryllium Alloys (in Russian), *Zavodskaya Lab.*, 27: 251–256 (1961).
31. P. Pointu et al., Determination of the Slip Elements by Analysis of the Asterisms of Laue Spots and Deformation Modes of Beryllium at High Temperatures (in French), *Compt. rend.*, 252: 1984–1986 (Mar. 27, 1961).
32. N. A. Hill, Textures in Beryllium Tubes Produced from Hot Extruded Rods, British Report AERE-R-3701, May 1961.
33. R. L. Powell et al., Low Temperature Transport Properties of Commercial Metals and Alloys—Reactor Grade Beryllium, Molybdenum, and Tungsten, *J. Appl. Phys.*, 31(7): 1221–1224 (1960).
34. B. I. Verkin et al., Magnetic Properties of Beryllium in Temperature Range 300 to 4.2°K (in Russian), *Zhur. Eksptl'. i Teoret. Fiz.*, 40: 670–671 (February 1961).
35. W. D. Bennett, Annual Report on Beryllium Research, 1960, Canadian Report CW-R&DL-14 (AECL-1236), February 1961.
36. Lockheed Aircraft Corp., Missiles and Space Div., Monthly Progress Report on Structural Design Data for Beryllium, Report LMSD-312201-16, June 1, 1961.
37. Lockheed Aircraft Corp., Missiles and Space Div., Monthly Progress Report on Structural Design Data for Beryllium, Report LMSD-312201-17, July 1, 1961.
38. Lockheed Aircraft Corp., Missiles and Space Div., Beryllium Design Data, Report LMSD-48472, Apr. 29–Aug. 1, 1959.
39. S. H. Gelles and A. K. Wolff, Impurity Effects in Commercially Pure Beryllium, USAEC Report NMI-1238, Nuclear Metals, Inc., Feb. 10, 1961.
40. P. Bastien and P. Pointu, Response to the Letter of A. Moore on the Improvement of the Mechanical Properties of Beryllium by Thermal Treatments, *J. Nuclear Materials*, 4(1): 113–114 (1961).
41. Oak Ridge National Laboratory, Metallurgy Division Annual Progress Report for Period Ending May 31, 1961, USAEC Report ORNL-3160, Aug. 17, 1961.
42. C. E. Ells, The Effect of Oxide Content on the Behavior of Helium in Beryllium, Canadian Report CRGM-1022(AECL-1253), May 1961.
43. Atomic Energy of Canada, Ltd., June 30, 1961. (Unpublished)
44. S. J. Gregg et al., The High Temperature Oxidation of Beryllium. Part V: In Moist Carbon Dioxide and Moist Carbon Monoxide, *J. Nuclear Materials*, 4(1): 46–58 (June 1961).
45. D. M. Hewette II, A Galvanic Corrosion Problem Associated with the Preparation of Multimetallic Samples, USAEC Report CF-60-4-111, Oak Ridge National Laboratory, Apr. 20, 1960.
46. J. Lillie, Some Properties of Beryllium Oxide, USAEC Report UCRL-6457, University of California Lawrence Radiation Laboratory, May 19, 1961.
47. K. T. Miller, High Temperature X-Ray Diffraction Investigation of BeO, USAEC Report NAA-SR-Memo-5934, Atomics International, Dec. 2, 1960.
48. B. Bellamy et al., The Lattice Parameter and Density of Beryllium Oxide Determined by Precise X-Ray Methods, British Report AERE-R-3774, July 1961.
49. S. B. Austerman et al., Oxygen Diffusion in Beryllium Oxide, USAEC Report NAA-SR-6427, Atomics International, Sept. 15, 1961.
50. L. Owens et al., Development of Intermetallic Compounds for Very High Temperature Applications, Quarterly Progress Report, April 1 Through June 30, 1961, USAEC Report BBC-111, Brush Beryllium Co., Aug. 1, 1961. (Classified)
51. J. F. Nachman et al., Study of Ceramic and Intermetallic Materials, Progress Report No. 12, USAEC Report TID-12505 (XDC-61-3-88), Denver Research Institute, Feb. 10, 1961. (Classified)
52. J. Booker et al., Investigation of Refractory Metal Beryllides and Silicides as Very High Temperature Materials, Progress Report No. 6, Covering January 1 to March 31, 1961, Report NP-10211, Brush Beryllium Co., Apr. 15, 1961.
53. G. S. Markevich and L. Ya. Markovakii, Chemical Stability of Beryllium Borides Against Attack by Oxygen, Nitrogen, and Carbon at High Temperatures, *Zhur. Priklad. Khim.*, 33: 1008–1012 (May 1960).

54. H. Rosenberg (Ed.), SNAP-8 Reactor Preliminary Design Summary, USAEC Report NAA-SR-6207, Atomics International, June 15, 1961. (Classified)
55. R. L. Wallerstedt (Ed.), SNAP-2 Nuclear Auxiliary Power Unit Development Progress Report, December 1960 to March 1961, USAEC Report NAA-SR-6292, Atomics International, June 15, 1961. (Classified)
56. R. L. Wallerstedt (Ed.), SNAP-2 Nuclear Auxiliary Power Unit Development Bimonthly Progress Report, October–November 1960, USAEC Report NAA-SR-6021, Atomics International, Mar. 1, 1961. (Classified)
57. F. H. Welch et al., Properties of Lithium Hydride: I. Viscosity of Liquid Lithium Hydride from 1252°F to 1578°F, USAEC Report TID-12738(XDC-61-4-59), General Electric Co., Flight Propulsion Laboratory Dept. and Battelle Memorial Institute, Mar. 16, 1961.
58. F. H. Welch, Properties of Lithium Hydride. V. Corrosion of Austenitic Stainless Steels in Molten LiH, USAEC Report APEX-673, General Electric Co., Flight Propulsion Laboratory Dept., May 31, 1961.
59. L. Manning and D. J. McKee, Investigation of the Effective Thermal Conductivity of Cast Lithium Hydride, USAEC Report APEX-744, General Electric Co., Flight Propulsion Laboratory Dept., June 5, 1961.
60. R. L. Beck, Investigation of Hydriding Characteristics of Intermetallic Compounds, Second Quarterly Report, Jan. 1 to Mar. 31, 1961, USAEC Report LAR-53, Denver Research Institute, Apr. 25, 1961.
61. J. D. Watrous, Thermal Expansion of SNAP Materials, USAEC Report NAA-SR-6047, Atomics International, July 30, 1961.

Section

III

Reactor Materials

Nuclear Poisons

Metallic Poison Materials

Figure III-1 shows a tentative type 304 stainless steel–gadolinium pseudobinary phase diagram as determined by the Bureau of Mines.[1]

(V. W. Storhok)

Dispersion Control and Poison Materials

Workers at Oak Ridge[2] have obtained promising results on borosilicate glass as a burnable poison in stainless-steel matrix fuel plates. No evidence of reaction or stringering of

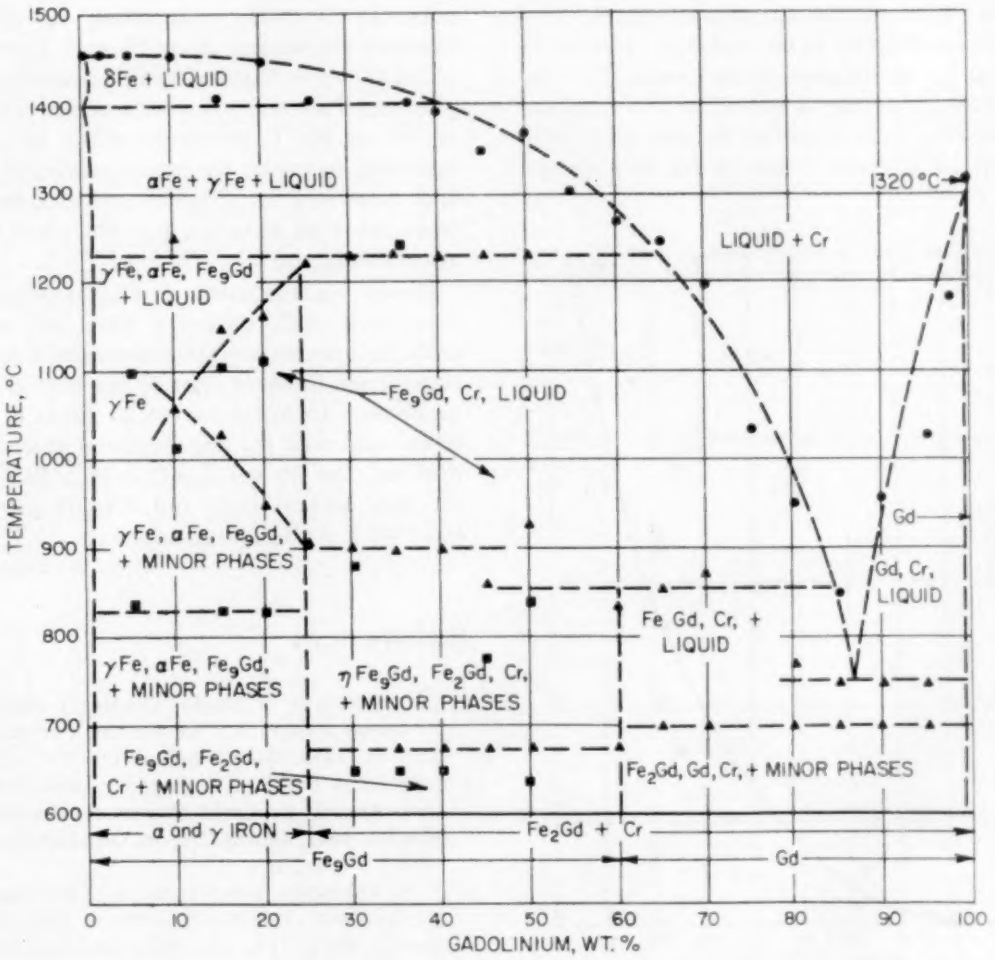

Fig. III-1 Tentative stainless steel–gadolinium pseudobinary diagram.[1] ●, liquidus, optical. ▲, thermal analysis. ■, hot stage.

glass shot containing 4 wt.% B_2O_3 was observed, and within the limits of chemical analysis no boron loss during fabrication was detected. An examination of 3 wt.% boron–iron absorber sections that were irradiated in the MTR at 170°F has been completed. A summary of results is shown in Fig. III-2. Changes in thickness were the only dimensional changes observed and were principally due to separation of the cores from the stainless-steel cladding. They conclude that 3 wt.% B^{10} in iron is limited to a maximum burnup of 5 at.%. Dispersions of 36 wt.% Eu_2O_3 in stainless steel showed no geometrical or microstructural changes at exposures estimated to be as high as 9×10^{20} nvt.

Deboronization[3] of stainless-steel matrix fuel plates containing boron as a burnable poison led to a study of the kinetics and mechanisms involved. The mechanism of loss during sintering was concluded to be oxidation of boron to B_2O_3 and its subsequent volatilization. On the basis of this premise, it was shown that, unless the compacts were sintered in hydrogen, oxygen must be present either in the atmosphere or in the sample for boron loss to occur. In hydrogen, a hydrogen-boron reaction was postulated.

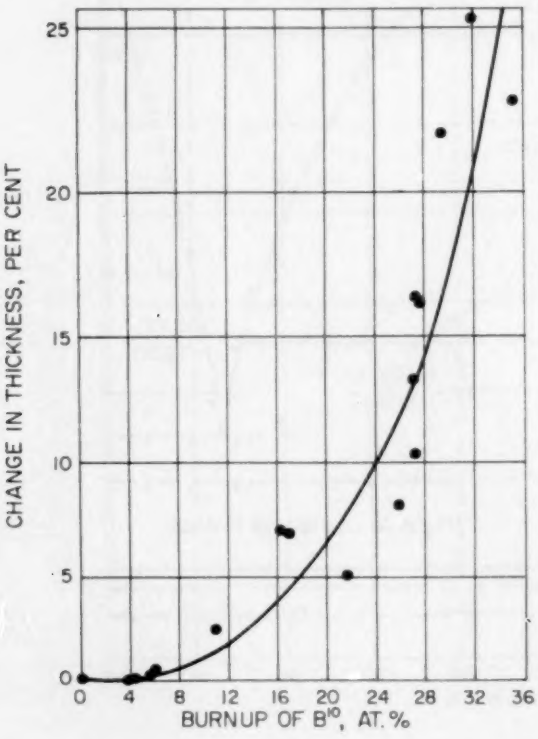

Fig. III-2 Effect of burnup on swelling in stainless-steel composite-plate specimens containing 3 wt.% B^{10} in iron.[2] Specimen size: 0.156 by 1 by 6.5 in.

A detailed report issued by Battelle[4] describes a method of incorporating a boron burnable poison in a UO_2–stainless steel fuel element. The process, which has been described in previous reviews, includes the use of ZrB_2 as a burnable poison and sintering of the compacts *in vacuo* to prevent boron loss. As a part of this study, an investigation was made of the thermodynamics of boron loss.[5] Detailed calculations have been made for the reaction of ZrB_2 with nitrogen, CO, oxygen, water, hydrogen, UO_2, and compounds of iron, chromium, nickel, niobium, and manganese.

Glasses containing rare-earth oxides and glass-bonded B_4C show promise as possible control materials, according to Handwerk.[6] Glasses containing up to 15 wt.% Eu_2O_3, Gd_2O_3, or Dy_2O_3 were found to resist devitrification for periods of seven days over a temperature range of 300 to 900°C. Mixtures of B_4C and glass, as sintered, had good mechanical strength, and control rods for an Argonne critical experiment were made by sintering B_4C and glass *in situ* in stainless tubes.

Bettis[7] is evaluating burnable-poison plates containing B_4C, depleted B_4C, B_4C in silicon carbide, and boron–stainless steel alloys. After irradiation to more than 90 per cent B^{10} burnup, increases in thickness of 27 to 31.8 per cent were observed for the depleted B_4C, 30.1 per cent for the 50 vol.% B_4C in SiC, 48.9 per cent for the natural B_4C, and 9 to 11 per cent for the 1 wt.% B^{10} in stainless steel.

(G. W. Cunningham)

References

1. U. S. Bureau of Mines, Quarterly Metallurgical Progress Report No. 11 for the Period April 1–June 30, 1961, USAEC Report USBM-U-839.
2. Oak Ridge National Laboratory, Metallurgy Division Annual Progress Report for Period Ending May 31, 1961, USAEC Report ORNL-3160, Aug. 17, 1961.
3. J. H. Cherubini, Determination of the Kinetics and Mechanisms of Deboronization at 1135°C, USAEC Report ORNL-3141, Oak Ridge National Laboratory, Sept. 15, 1961.
4. S. J. Paprocki et al., Incorporation of a Boron Burnable Poison and Spherical UO_2 in SM-2 Stainless Matrix Fuel Plates, USAEC Report BMI-1527, Battelle Memorial Institute, July 6, 1961.

5. J. J. Ward et al., Thermodynamics of Boron Loss in UO_2–Stainless Steel Dispersion Fuel Elements, USAEC Report BMI-1531, Battelle Memorial Institute, July 18, 1961.
6. Glass Bearing Fuels, Notes from Meeting Held at Germantown, Maryland, USAEC Report TID-12617, Jan. 31, 1961.
7. Westinghouse Electric Corp., Bettis Atomic Power Laboratory, Technical Progress Report, Pressurized-Water Reactor (PWR) Project for the Period April 24, 1961, to June 23, 1961, USAEC Report WAPD-MRP-92.

Section

IV

Reactor Materials

Cladding and Structural Materials

Corrosion

Niobium Oxidation

Emphasis in the protection of niobium from high-temperature oxidation is shifting from the development of oxidation-resistant alloys to studies on protective coatings. Although alloys are being developed which may be usable to 2500°F in air, the more oxidation-resistant compositions are generally weak or brittle. It is apparent that coatings will be required to protect high-strength alloys for service above 2000°F in oxidizing atmospheres.

Results from General Electric[1] have shown that superior oxidation resistance is obtainable in niobium-titanium-aluminum base alloys. At 2500°F, a typical oxidation-resistant alloy, niobium–34 wt.% titanium–28 wt.% aluminum, forms a very protective scale and has a weight gain of only 8 mg/cm^2 after a 450-hr exposure. Structurally, these alloys are based on the TiAl intermetallic, with niobium in solid solution. Additions of 3 to 6 wt.% chromium are beneficial in retarding spalling of the scale during exposure at 2100 to 2300°F, although Cr_2O_3 volatilizes at slightly high temperatures. The utility of these alloys as high-temperature structural materials is questionable, however, because of their high aluminum contents.

Protective coatings for niobium alloys are under study at Boeing Airplane Company, Chance-Vought Aircraft, Inc., Pfaudler Company, and Thompson Ramo Wooldridge, Inc., as described in the previous Review. These coatings are primarily silicide base and are protective to high-strength niobium alloys in air to 3000°F with no deleterious effects on the substrate. The TRW coating, a silicide modified with titanium and chromium, has been tentatively selected by Republic Aviation[2] for protecting refractory niobium-alloy fasteners.

Aluminide coatings are also attractive for protection of niobium alloys. Modification of the General Electric LB-2 slurry aluminide coating with silver has been shown to be beneficial in reducing the notch sensitivity of coated F-48 niobium alloy.[3] (W. D. Klopp)

Molybdenum Oxidation Protection

The effects of processing conditions on the protectiveness of silicide coatings on molybdenum have been studied at Chromalloy Corporation and Pfaudler Company.[2] Both companies have reported improved protectiveness for pack-cementation coatings applied in two cycles rather than in one cycle. The reasons for this interesting behavior are not understood but may be associated partly with improved coverage from the two-cycle treatment. These coatings afford protection to molybdenum for about 2 hr at 3000°F. (W. D. Klopp)

Tantalum Oxidation Protection

Sylcor[2] has developed a tin-modified aluminide coating that is protective for several hours up to 3200°F and also exhibits good self-healing properties. Defects in the coating are sealed at intermediate temperatures through flow of a liquid aluminum-saturated tin phase in the coating. The coating may be applied as a slurry or by hot dipping in an aluminum–50 wt.% tin bath.

Battelle[4] has shown that manganese additions to silicide coatings are beneficial, especially on tantalum alloys. A manganese-modified silicide coating made defective by a 0.04-in. hole was protective to an experimental tantalum alloy, tantalum–30 wt.% niobium–5 wt.% vanadium, for 10 hr at 2700°F. The protectiveness and self-healing abilities of this coating are

related to the formation of a viscous silicate scale that can bridge defects. (W. D. Klopp)

Tungsten Oxidation

The oxidation behavior of tungsten is reviewed in a recent report by the Defense Metals Information Center.[5] Tungstic oxide, WO_3, is volatile above about 1100°C, presenting a protection problem comparable with that for molybdenum. Alloying to improve the high-temperature oxidation resistance has been ineffective to date.

Thompson Ramo Wooldridge[2] has achieved protection for tungsten for about 10 hr at 3400° F through modified-silicide coatings. This degree of protection is similar to that previously observed at New York University for silicide-coated tungsten. (W. D. Klopp)

Zirconium Corrosion

Hydrogen uptake during the aqueous corrosion of zirconium continues to receive much attention. Recent work at Knolls with a zirconium–2 at.% tin–2 at.% niobium alloy in water and steam at 600 to 900° F indicates that the ratio of absorbed hydrogen to oxygen (weight gain) was 0.01322, and this ratio remained unchanged during the pre- and posttransition periods of the corrosion rate.[6] However, British workers have found that, with Zircaloy-2 in steam at 640 to 1110° F, the hydrogen-to-oxygen ratio is almost 0.125 in the posttransition period of corrosion.[7] Work performed at Chalk River[8] has been the basis for a novel suggestion that hydrogen absorption in zirconium is accomplished by the transfer of negative hydrogen ions through the oxide film rather than protons or atomic hydrogen as has generally been proposed.

In the field of alloy development, Knolls has recently completed a program involving binary zirconium alloys in which the additions were in alpha solid solution or just into the two-phase region.[9] It was concluded that the most favorable zirconium-alloy systems from the standpoint of corrosion resistance and mechanical strength were those with antimony, tellurium, and niobium additions. Argonne is using a corrosion-mechanism study as the basis for zirconium-alloy development for applications in 1000° F steam.[10,11] Approaches being studied include (1) combinations of low- and high-valence atoms which would produce spinel oxides and an average valence of +4 in the ZrO_2 corrosion film while resulting in a minimum disturbance in the structure and number of defects in the ZrO_2, and (2) additions that promote electronic conductivity in ZrO_2 without deleterious effects in the ZrO_2 structure. It is believed that the latter, in combination with noble-metal precipitates in the zirconium, could result in very rapid association of hydrogen atoms during corrosion and thus preclude damaging effects of hydrogen in the metal or as it passes through the oxide film. Results obtained appear promising, although no outstanding alloys have yet been developed. (W. E. Berry)

Aluminum Corrosion

Reported work on the aqueous corrosion of aluminum includes mechanism studies, effect of heat transfer, and effect of flow velocity.

Conclusions drawn from work conducted at Argonne[10] indicate that the corrosion-rate-determining barrier layer in the oxide on aluminum is close to the metal-oxide interface. The conclusion is based on experiments with precorroded 1 wt.% nickel–0.1 wt.% titanium alloy specimens in which the surface oxides were ground to varying depths; upon subsequent reexposure to high-temperature water, similar corrosion rates were obtained for all specimens.

Oak Ridge has investigated the effect of water velocity in the range of 20 to 107 ft/sec and temperature in the range of 170 to 290°C on the corrosion behavior of four aluminum alloys[12] (1100, 5154, 6061, and X-8001). At 170 to 200°C, all exhibited the same corrosion behavior, and corrosion rate increased with increasing flow rates. At 260 to 290°C, only the X-8001 alloy was free of selective attack. Penetration rates for X-8001 at 260°C ranged from 5 mils/year at 20 to 30 ft/sec to 200 mils/year at 107 ft/sec.

The effect of high heat flux on the corrosion behavior of 6061 aluminum[13] is also being studied. Workers conclude that, at a fixed *p*H, a flow rate of 40 ft/sec, a temperature range of 176 to 220° F, and a heat flux of 2×10^6 Btu/(hr)(sq ft), the rate of oxide formation (and presumably corrosion) is determined to a large extent by the specimen temperature.

(W. E. Berry)

Electrolytic Iron in Water

Argonne has produced temper films on electrolytic iron exposed to water at 212 to 500° F by adding up to 540 ppm oxygen to the water.[10]

Pitting occurred at oxygen concentrations just below the minimum amount which produced tarnish films, whereas at lower oxygen levels the attack was uniform but quite rapid. At about 0.1 ppm oxygen, the attack was uniform and the rate of attack was low, but the oxide film was loosely adherent and the corrosion rate was higher than under the optimum conditions with high oxygen. (W. E. Berry)

Corrosion of Base-Metal Alloys

Aqueous Corrosion. Alloy development efforts at Hanford[14] produced a series of alloys typified by 50 Ni–25 Cr–6 Mo–1 Cu–1 Ti–0.02 max. C–balance Fe that exhibited better resistance to corrosion by HNO_3, H_2SO_4, and acid fluoride solutions than current commercial iron- or nickel-base alloys. Further work at Hanford[15] showed that Hastelloy C exposed to 554°F lithiated (*p*H 10) water corrodes at a rate equivalent to 0.18 mil/year for about 1500 hr. After this initial exposure, the rate upon further exposure was doubled to 0.35 mil/year. This behavior verified prior experimental indications.

For potential use as cladding in the Molten-Salt Reactor (LiF-BeF_2-UF_4), INOR-8 is exposed to a potentially carburizing atmosphere via the graphite moderator used. In tests at Oak Ridge,[16] up to 14,000 hr at 1300°F, INOR-8 resisted carburization excellently. Inconel specimens, also included in the test, were severely attacked in 4000 hr.

The evaluation of carbon and low-alloy steels as alternative structural materials for stainless steel in PWR systems was the subject of work by Sargent and Lundy for Savannah River.[17] In mockup loop tests (oxygenated, 1000-psig water at 537°F, steam at 546°F), typical corrosion rates for steels were around 0.1 mil/year, compared with about 0.03 mil/year for stainless steels. These data indicate that low-alloy and carbon steels do corrode at higher rates than stainless steel, but the investigators concluded that the rates were not sufficient to jeopardize the functioning of the system considered. A problem reported in the past concerning substitution of carbon steel for stainless steel in certain PWR applications is finding effective decontamination procedures that are compatible with both plain and stainless steels. Sargent and Lundy also checked all anticipated aspects of Inconel corrosion in static and loop tests for primary and secondary PWR waters (normal corrosion, stress corrosion, crevice corrosion, galvanic corrosion, pitting, etc.). Their tests confirmed the excellence of corrosion properties of Inconel for the anticipated service and demonstrated that even abnormal heat-to-heat variation in chemistry does not result in any unusual corrosion effects.

Gaseous Corrosion. The 10,000-hr exposure of Hastelloy X and Inconel to 1750°F, 300-psi nitrogen containing 0.5 vol.% oxygen was completed at Aerojet-General.[18] Hastelloy X showed 2 mils of oxidation penetration in these tests (also in parallel air tests), compared with 7.5 mils for Inconel. Low-cobalt (0.07 per cent cobalt) Hastelloy X is currently under test in air (1750°F, 300 psi). After 5000-hr exposure, the low-cobalt variety exhibited intergranular penetration to a depth of 6 mils.

Work is also being initiated to study the corrosion behavior of reactivity shim materials.[20] Pertinent tests include 800°F, 300-psi reference-gas corrosion, quench tests (600°F reference gas to water quench), and water corrosion tests. Silver-plated stainless steel, a cobalt alloy (Nivco 10), and a silver alloy (Consil 995) are to be evaluated. Preliminary results indicate that the cobalt alloy lacks adequate corrosion resistance in the quench test.

Low-alloy steels were investigated for potential use in the Experimental Gas-Cooled Reactor (EGCR) at Oak Ridge.[16] Exposed to helium containing up to 1.25 per cent CO_2 + CO at temperatures from 600 to 1100°F and 45 psia for 900 hr, the steels oxidized rapidly (from 10 to 70 per cent of air oxidation rates).

The results of evaluation of austenitic and ferritic stainless steels, iron-chromium-aluminum alloys, and nickel-base superalloys were reported by Hanford.[19] The report offers general conclusions relative to the utility of these materials in various contemplated reactor media (gas and liquid).

General Electric[20] has initiated a program to investigate potential materials for fuel elements for service at temperatures in excess of 2200°F. Included in the program are iron-chromium-aluminum-yttrium alloys, niobium-aluminum-titanium alloys, and the platinum-group metals. Oxidation-test results determined for the platinum-group metals are summarized in Table IV-1. (E. S. Bartlett)

Corrosion by Molten Metals and Phosphates

A variety of capsule and loop experiments involving liquid, boiling, and superheated mercury were conducted to evaluate containment-materials compatibility problems.[21] Parameters included materials, surface treatments, additives, stress, and dissimilar metals. Many specific conclusions were formulated from the study, some of which are summarized below.

1. Materials exhibiting satisfactory corrosion resistance at 900°F:
   - Haynes 25 (most resistant material evaluated, with the exception of refractory metals and alloys)
   - Type 410 stainless steel (good to 1000°F)
   - Sicromo 55, PH 15-7 Mo, Neatro Tool Steel, and 17-4 PH
   - Tantalum, tungsten, molybdenum, and niobium
   - WC, TaC, Al_2O_3, ATJ graphite, and Pyroceram
2. Materials exhibiting unsatisfactory corrosion resistance at 900°F:
   - Type 300 stainless steels, Waspalloy, René 41, AF 1753, and A286 stainless steel
   - Aluminum, nickel, Inconel, chromium, zirconium, platinum, manganese, Sylvania No. 4, Kovar, Carpenter 20 Nb, and titanium
3. Chromium, nickel, and manganese are alloy constituents most susceptible to attack.
4. Interaction between dissimilar metals can increase corrosion effects.
5. Small additions of titanium to mercury greatly reduce the corrosion rate of some materials.
6. Corrosion fatigue failures can occur in mercury environments at temperatures below 200°F.

Boiling- and superheated-mercury corrosion experiments are also under way at Brookhaven; similar experiments with sodium are planned.[22] Two of the mercury boiling loops have operated slightly longer than 5000 hr with thermal conditions as follows: boiling fluid, 1000°F; superheated vapor, 1150°F; cold leg, 600°F. The mercury in each of these systems contained as a corrosion-inhibiting additive 50 ppm magnesium and a concentration of titanium equivalent to cold-leg saturation. After 5095 hr of operation, the first system, which was fabricated of carbon steel, exhibited very slight deposition at the condenser liquid level (as detected by radiography). The second system was fabricated of $2\frac{1}{4}$ chromium–1 molybdenum steel ($2\frac{1}{4}$ Croloy); after 5244 hr, the extent of deposition and corrosion seemed to be somewhat greater than that in the carbon steel system.

Table IV-1 DIMENSIONAL CHANGE OF PLATINUM-GROUP METALS[20] RESULTING FROM OXIDATION AT 2192, 2552, AND 2912°F

Material	Change in thickness, mils, after indicated time and temp.		
	350 hr at 2192°F	350 hr at 2552°F	350 hr at 2912°F
Rhodium	+0.25	–0.18	–0.42
Palladium	+0.09	High loss	Melts
Platinum–30 wt.% rhodium	+0.03	–0.2	–0.25
Platinum	–0.04	–0.26	–0.35
Iridium	Very high loss	Very high loss	Very high loss

Liquid-mercury corrosion studies at Argonne are directed toward the evaluation of lightweight alloys for containment purposes. Titanium is the material of current interest, and it has been found[23,24] from 370°C, 336-hr static exposures that (1) specimens of anodized titanium do not display accelerated attack on scratched and bent areas; (2) prenitrided titanium is immune to attack by mercury; and (3) additions of 500 ppm zirconium, copper, nickel, or iron to mercury reduce the attack on titanium by a factor of approximately 10.

In refluxing-capsule experiments at Oak Ridge, type 316 stainless steel in contact with boiling potassium has demonstrated corrosion resistance somewhat superior to that of Inconel, Haynes 25, or type 310 stainless steel. To explore this behavior further, boiling potassium loop experiments are being conducted[16] at 1500°F. After 3000 hr, a type 316 stainless-steel system exhibited a maximum attack of

about 2 mils near the liquid-vapor interface in the boiler. Weight losses occurred in the case of specimens suspended in the hot liquid and vapor regions, whereas weight gains and mass transfer characterized the cold-zone specimens; these effects are similar to those found for the refluxing-capsule experiments. Inconel and Haynes 25 loops are in operation and will be examined after the 3000-hr period.

Liquid-metal experiments at Aerojet-General have included the operation of pumped boiling rubidium loops. The first system was fabricated from type 316 stainless steel and was operated for 172 hr at various temperatures, the maximum being 1550°F boiling.[25] Corrosion of the stainless steel in this system was in the form of minor penetration and solution of the tube wall. There were no mass-transfer effects. For the second system, a niobium – 1 wt.% zirconium alloy was the construction material. After a total of 455 hr of 1840°F operation, the corrosion was negligible. The most noticeable effect occurred on the outer walls, presumably as a result of contaminants in the protective inert-gas blanket.

The solubilities of nickel, chromium, iron, titanium, and molybdenum in lithium were determined as a function of temperature in the 1200 to 1700°F range.[26] Results are presented in Fig. IV-1. A relation appears between solubility and atomic size; nickel, chromium, and iron, which have the smaller atomic diameters, have the higher solubilities. Solubilities of iron and nickel in lithium were also determined at United Nuclear Corporation.[27] In the 540 to 825°C range, the equilibrium nickel solubilities were correlated by the expression

$$\log C \text{ (ppm nickel)} = 8.44 - \frac{4600}{T(^\circ\text{K})}$$

The equilibrium solubility of iron was found to be 27 ppm in 662°C lithium and 85 ppm in 760°C lithium. Somewhat higher solubilities are indicated by these values than by the curves in Fig. IV-1. However, the differences are not great, assuming that the United Nuclear data are reported on a weight basis.

Mass-transfer effects in systems of niobium-sodium–type 316 stainless steel were investigated at Oak Ridge in isothermal (1500 to 1800°F) experiments of durations[16] up to 1000 hr. Whereas the transfer of iron, nickel, and chromium to the niobium was negligible, some transfer of carbon and nitrogen (to the niobium) occurred and appeared in the form of NbC and Nb_2N. The carbide was confined to the surface layer, but the nitride penetrated the entire 0.040-mil specimens. The stainless steel-to-niobium surface ratio, which varied from 0.1

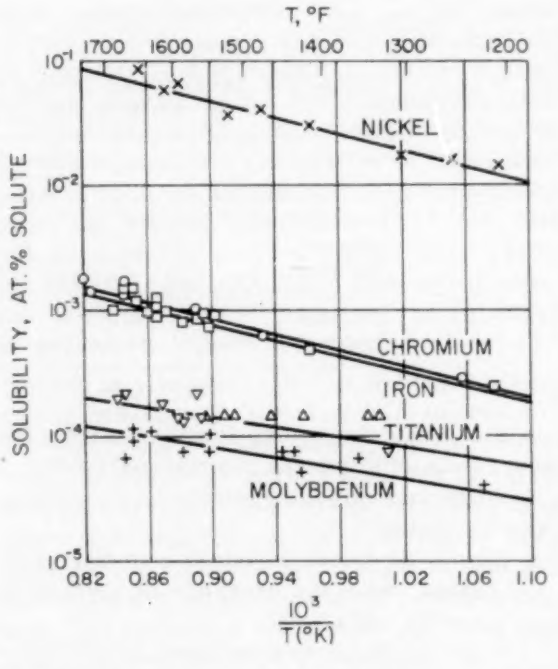

Fig. IV-1 Variation of the solubility, expressed as the atomic per cent solute, with the reciprocal of the absolute temperature.[26] Nitrogen contamination is 50 to 100 ppm. ×, nickel. ○, chromium. □, iron. +, molybdenum. ▽, titanium. △, titanium results reported as being <10 ppm.

to 20, was found to be a governing factor. In experiments where this ratio was held at the minimum, no carbon or nitrogen transfer occurred. In fact, the characteristic here was one of transfer of niobium to the steel surfaces.

An investigation of the feasibility of utilizing molten phosphates as high-temperature fuel carriers in homogeneous reactor systems has been under way at Atomics International for approximately two years. Some of the potential corrosion problems in such systems are being surveyed, and encouraging results are being developed. A recent report[28] presents data from a study of iron and Inconel in molten sodium polyphosphate (Na_2O/P_2O_5) at 900°F. Mass spectrographic determinations of evolved P_2, a cor-

rosion product, indicate that the corrosion rates, although initially quite high, taper off to rather low levels after 30 to 40 hr of exposure. Certain mechanisms for this effect, which reflects the possibility that corrosion in an engineering system might be controlled, are postulated. (J. H. Stang)

Metal-Water Reactions

The experimental program at Argonne[24,29,30] to determine rates of reaction of molten reactor fuel and cladding metals with water is continuing. One report[29] gives information on the zirconium-water reaction with initial metal temperatures from 1100 to 4000°C with 30- and 60-mil wires in room-temperature water. Runs were made also with 60-mil wires in water heated to 200°C (225 psia). The experimental method involves the rapid melting and dispersion of metal wires in a water environment by a surge current from a bank of condensers.

Results for the 60-mil wires in room-temperature water showed that progressively greater reaction occurred at higher initial metal temperatures, reaching 20 per cent reaction at 2600°C. Pressure traces showed that from one to several tenths of a second was required for reaction to reach a final value. At temperatures exceeding 2600°C, the reaction became violent and was 40 to 70 per cent complete in a few milliseconds. Generally finer particles resulted from the explosive runs. The change in character of the reaction was attributed to the formation of molten oxide, ZrO_2 (melting point, 2700°C), which did not stabilize large particles formed in early stages of the wire disintegration. Generally twice as much reaction occurred with 30-mil wires as with 60-mil wires at temperatures in the melting region and below.

Runs in heated water gave more extensive reaction at temperatures in the melting-point region (1840°C), reaching 50 per cent reaction for fully melted metal. The increased reaction was obtained with water heated to 100°C. Heating to 200°C, however, produced no additional reaction. This unusual pressure effect was attributed to an increased rate of diffusion of water vapor through the barrier of hydrogen surrounding reacting metal particles. At a later time the reaction becomes controlled by solid-state processes occurring within the partly oxidized particles (parabolic or other rate law). Reaction rates controlled by gaseous diffusion are normally independent of pressure, but only if the effective water temperature at the surface between liquid water and the steam-hydrogen blanket remains at the boiling point determined by the ambient pressure. Experimental results indicate that it does not. Hydrogen generated by reaction, therefore, tends to suppress further reaction with water at room temperature. With heated water, the vapor pressure is more nearly equal to the total pressure at all times, and therefore reaction is not suppressed.

The series of runs[30] with 60-mil zirconium wires at pressures up to 1500 psi is continuing. Runs made with water at 315°C (1500 psi) were identical in character to runs made in water from 90 to 200°C (10 to 225 psi). Explosive rates of pressure rise occurred at initial metal temperatures of 1900°C in heated water.

Results of previous studies at Battelle and Westinghouse were reexamined and shown to be consistent with rate data deduced from condenser discharge studies of the zirconium-water reaction. This is shown in Fig. IV-2. The following rate law was obtained:

$$V^2 = 4.82 \times 10^8 \left(\exp - \frac{45{,}500}{RT}\right) t$$

where V is cubic centimeters of hydrogen at standard temperature and pressure per square centimeter of surface and t is time in minutes.

The explosive reactions for zirconium at initial temperatures of 2600°C in room-temperature water and those at 1900°C in heated water could be explained by a critical particle diameter (500 μ in room-temperature water) below which rapid hydrogen evolution drives the particles through the water at high velocity. The high-speed motion results in rapid reactions. The reactions, however, are not complete because the increased velocity also increases the convective-heat-loss rate.

A series of condenser discharge runs[24] with uranium wires in water at 100°C was completed. It was not possible to study the reaction in water above 100°C because of rapid corrosion. Reaction reached 100 per cent in heated water when the initial metal temperature was 3000°C at a mean particle diameter of 200 μ.

Runs in room-temperature water gave only 40 per cent reaction under identical conditions.

A second experimental method[30] involves the rapid contact of steam with heated metal. In this method the metal receives a "pressure pulse" of water vapor. Runs with 1 atm of water vapor reacting with molten aluminum at 1000 and 1200°C are reported. Contact times varied from 0.1 to 1000 sec. The data can be represented approximately by the cubic rate law.

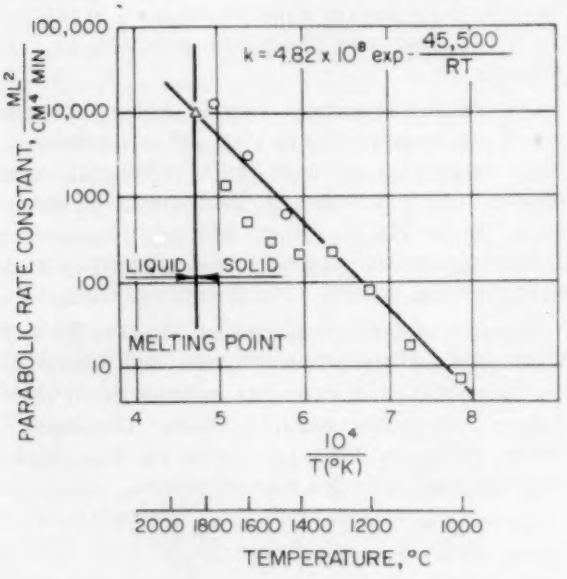

Fig. IV-2 Effect of temperature on the zirconium-water reaction.[30] Δ, condenser discharge method. ○, Bostrom, WAPD-104 (recalculated). □, Lemmon, BMI-1154 (recalculated).

A brief study of the sodium-steam reaction[24] at 200°C by the pressure-pulse method was begun. It was assumed that the rate of the sodium reaction would be limited only by gaseous diffusion and mixing processes with the reaction cell. Rates with sodium at 200°C were only slightly greater than those with uranium in the 1200 to 1600°C range, suggesting that observed uranium rates were also diffusion limited. Rates with sodium were considerably above those reported with aluminum. The aluminum data are therefore not limited by diffusion in mixing.

A recent literature survey by Du Pont[31] of metal-water reaction information has resulted in the publication of a bibliography.

(A. W. Lemmon, Jr.)

Radiation Effects in Nonfuel Materials

Defects: Structure and Properties

Metals. Films of annealed 99.998 per cent pure gold were observed with transmission electron microscopy after being bombarded with argon ions (Ar^+) having a maximum energy[32] of 75 ev. (The maximum energy transferable to gold here is 42 ev in a head-on collision.) Doses up to 3.5×10^{17} ions/cm² were used. Planar defects interpreted as dislocations, about 100 A in diameter, were observed to line up in ⟨111⟩ directions in suitably oriented crystals when bombarded at +22°C. Efficiencies at +22°C were of the order of 5×10^{-4} defects retained per incident ion. Other orientations, but more specifically the bombardments at −32°C, resulted in considerably higher densities of smaller defects. Since very little diffusion of argon has been observed below 100°C in gold and since there is a marked difference in the damage produced at −32°C and +22°C (vacancies are mobile in gold in this range), it is concluded that a vacancy diffusion mechanism has probably formed the defects observed.

Beevers and Nelson[33] used transmission electron microscopy to study thin aluminum foils (~2000 A) which were irradiated with 85-kev ions of hydrogen and helium at 40°C up to doses of 10^{18} ions/cm². Defect clusters in the form of spots (~30 A) and dislocations to a density of 5×10^{15}/cm³ were observed. Annealing *in vacuo* at 400°C for 1 hr removed all the observed damage. No effects due to the presence of hydrogen and helium ions in the aluminum are observed here, since their path length (7500 A) is at least four times the thickness of the sample. Neutron irradiations of 7.5×10^{18} neutrons/cm² have shown no observable damage. Differences here can be explained by the rate of damage produced by the two types of particles. Neutrons produce damage by hard sphere collisions with a cross section of $\sim 5 \times 10^{-24}$ cm², whereas the positively charged ions produce displacements by Rutherford collisions with an average cross section of the order 10^{-17} to 10^{-18} cm².

Beryllium of 98.5 per cent purity has been studied after irradiations up to 10^{21} thermal neutrons/cm² at temperatures[34] of 350 and 600°C. Little damage was observed until doses

exceeded 10^{19} neutrons/cm^2, at least 10 times that required for most metals. This increase in dose necessary for damage might be due to the relatively low purity of the material. Thin foils observed with transmission electron microscopy after irradiation at 350°C showed 1.2×10^{14} dislocation loops/cm^3 about 200 to 500 A in diameter. Annealing for 1 hr at 600°C removed these loops. After 1 hr at 700°C, gas bubbles were observed ~100 A in diameter with a density of $\sim 10^{14}$/cm^3. The bubbles grew with increase in temperature, until an anneal of 1 hr at 1000°C resulted in 2×10^{13} bubbles/cm^3 with diameters ranging from 400 to 1200 A. The samples irradiated at 600°C showed 100 A bubbles ($\sim 10^{14}$/cm^3) in the grains and up to 600 A bubbles in the grain boundaries ($\sim 10^{10}$/cm^3). In general, annealing at high temperatures increased the size of the holes in both regions, but bubbles less than 100 A in diameter were still observed in the grain boundaries even after annealing at 1000°C.

In continuing their studies of fission tracks in thin films, Kelsch et al.[22,35] have reported on detailed analysis of individual tracks in a 50 A layer of platinum. High-magnification electron micrographs showed "empty regions" (low density) with an average spacing of 207 A from center to center. This agrees with other calculations, which resulted in mean free paths for fission fragments (between major collisions) of 200 A. In these experiments this distance corresponds to 50 atoms of platinum. The same investigators have also reported on variations in track registration with film thickness and explain their results in terms of dissipation of thermal energy. Similar experiments are being studied in a continuing program by Bierlein and Mastel,[36,37] who point out the importance of the free surface to the registration of events. Some other conclusions drawn from their work are that (1) damage in a material is a function of mass of the fragment as well as the specific nature of the material and its thickness, and (2) damage in fine-grained material is similar to that in coarse-grained foils and is the same qualitatively if the fragment is produced by either an external (to the material) or an internal source.

Energy of formation of vacancies in silver is reported[38] as 1.06 ± 0.07 ev, as determined in quenching experiments by measuring the change in electrical resistivity produced by the defects. A Russian report[39] states that neutron irradiation produced a 0.03 per cent increase in the lattice constants of molybdenum as observed with X rays. Lefort et al.[40] have discussed 82- and 150-Mev-proton-induced spallation damage in thorium.

Defects in Metal Alloys. Stainless-steel foils have been held between natural or enriched uranium plates and irradiated at 1.3×10^{12} nvt up to doses[41] of 10^{19} neutrons/cm^2 at 60°C. The fission damage was observed with transmission electron microscopy. Fueling and rate of exposure resulted in fission fragment doses of 1.2×10^8 or 1.6×10^{10} fragments/(cm^2)(sec). Small defects about 25 A in diameter were seen at doses of 1.8×10^{14} fragments/cm^2. Increasing the dose increased the defect size and number until dislocation loops were formed. No defects were observed in the electron microscope after neutron irradiation up to 10^{19} neutrons/cm^2; however, tensile tests did show the characteristic increase in yield stress which is associated with increased number of defects. Plotting the number of defects observed (obtained from the integrated area of the defects and the thickness of the foils) versus the fragment dosage results in an estimate of 45 defect pairs produced per fission event at 60°C with a dose of 1.8×10^{14} fragments/cm^2 at a rate of 1.6×10^{10} fragments/(cm^2)(sec). Similar experiments at 60°C with a dose rate of 1.2×10^8 fragments/(cm^2)(sec) have yielded the value of 250 defect pairs per fission event. The lower number of defect pairs observed at the higher dose rate is felt to be due to a greater number of unobserved pairs. Lowering the dose rate or increasing the temperature should allow the defect clusters to grow to an observable size.

The influence of impurity atoms on the annealing of point defects in metals has been studied[42] in pure copper (spectrographic) and three dilute copper alloys containing about 0.05 at.% silver, cadmium, and beryllium, respectively. Defects were introduced by irradiation with 4-Mev electrons at −196°C, and the annealing was studied up to 50°C. Recovery was measured in terms of the electrical-resistance changes measured at liquid-helium temperatures. Annealing peaks at −140, −80, and 0°C were observed in all samples; however, they were significantly different in form. The tentative explanation proposed is concerned with defect trapping at impurity sites. In the case of the two lower-temperature peaks, the

trapped defects are interstitials and the 0°C peak is altered because of vacancy trapping. Westmacott et al.[43] have also observed vacancy trapping by solute atoms. In these experiments, quenched aluminum alloys were studied.

Schindler[44] has supplied a considerable amount of additional data to support his proposal that neutron irradiation causes ordering in nickel-iron alloys.[45] Conclusions are drawn from the changes in magnetic properties measured both during and after irradiations. Ferrite materials have also been studied this period. Dekhtyar and Shalaev[46] have also produced ordering in nickel-iron (24.96 wt.% iron) with gamma irradiation. Increase in coercive force and decrease in the galvanomagnetic effect similar to those produced during thermal ordering, as well as the fact that no changes were observed in ordered specimens, verified that the gamma rays did produce ordering. Annealing of this damage occurs in the region of 300 and 550°C, which is explained in terms of a new phase separating because of the presence of point defects. Gamma-irradiated pure iron shows an increase in coercive force and magnetization which does not anneal until temperatures in excess of 580°C. This high temperature suggests dislocation loops as the damage-produced defect. The character of the increase in coercive force in the nickel-iron alloys also supports this suggestion. However, Biorci and his coworkers,[47] in continuing their studies[48] of neutron-produced effects in high permeability iron, suggest that the observed annealing kinetics preclude the possibility that the defects produced are either free-iron interstitials or dislocation loops. They have characterized the defect as anisotropic, interacting with the magnetization vector and moving with an activation energy of 1.2 ev in the temperature range 100 to 200°C.

Enhanced diffusion of zinc in 10 wt.% zinc–90 wt.% copper was observed in samples irradiated with 30-kev Ne^+ ions.[49] The results can be explained in terms of a vacancy mechanism for zinc diffusion. The activation energy and the dependence on flux of the enhanced diffusion suggests that the steady-state vacancy concentration under bombardment is limited by linear annealing of defects to surfaces and dislocations as well as by direct recombination of interstitials and vacancies.

Effects of neutron irradiations at low temperatures on the austenitic $\rightleftharpoons$ martensitic transformation in chrome steels has been studied[50] at doses up to 10^{18} neutrons/cm^2. The results are discussed in terms of thermodynamics and Cohen's recently proposed theory [*Radex Rundschau*, No. 6: 318–322 (1960)].

Defects in Other Materials. Fission tracks in biotite, muscovite, artificial fluorophlogopite, and muscovite annealed at 900°C (above the point where it loses its crystallization water) have been observed with transmission electron microscopy.[51] Initially, samples 30 μ thick were coated with a thin evaporated layer of uranium and irradiated to doses of 10^{15} neutrons/cm^2 (thermal). A few minutes after irradiation, the samples were placed in liquid nitrogen and stored until observed. The observations were actually made in samples cleaved from the irradiated specimens to a thickness of 1000 to 2000 A. Tracks were not observed in biotite and varied in size in the other samples in correspondence to the resistance each of the materials has to thermal decomposition. The largest-diameter tracks (240 A) were observed in muscovite, which loses its crystallization water at 750°C; thinner tracks (150 A) were seen in the fluorophlogopite, annealed at 1200°C; and still thinner tracks (115 A) were observed in the dehydrated muscovite, which does not show further decomposition until 1400°C. The biotite decomposes at 500°C; thus the lack of observed tracks is probably explained by too rapid a recovery. These results are used to support the suggestion that thermal processes, as opposed to ionization processes, are responsible for the registration of events that are characterized as cylindrical thermal spikes. Calculations from thermal-conductivity considerations, where the ionization effects are minimized, show general agreement with the observed results. Recovery effects have also been observed in the muscovite. When heated under the beam, some of the tracks transform into dotted lines or completely disappear. No such effects were observed in the fluorophlogopite or dehydrated muscovite.

Fission tracks up to 250 A wide have been observed in platinum phthalocyanine[52] by transmission electron microscopy. These crystals have a $(20\bar{1})$ lattice spacing of 11.94 A which can be resolved directly in the microscope. Fueling was accomplished by placing the crystals in contact with thin uranium foils and irradiating for periods between 5 min and 20 hr

in the BEPO reactor at a pile factor of 12. The observed damage is explained in terms of a thermal-spike mechanism. Similarly fueled and irradiated samples of silver cyanamide have also been studied[53] with direct transmission electron microscopy. Here fission tracks about 120 A in diameter were observed. Indications are that silver produced during the damage process diffuses (or migrates) away from the sites where it is liberated. The specific studies here were concerned with other properties of the silver cyanamide. Izui and Fujita[54] observed fission tracks about 100 A wide in molybdenite crystals using transmission electron microscopy. Fueling was accomplished with evaporated layers of uranium on one side of the crystal. Irradiations were of the order of 10^{16} neutrons/cm^2. Thermal spikes are suggested as the explanation of the observed events, especially for some of the tracks that appear as individual dots as opposed to continuous straight lines. The dots are produced by nonuniform solidification of the molten material in the spikes, which were initially uniform cylinders. Similar techniques were used to reveal fission damage in graphite.[55] The thermal spikes were observed to have produced areas up to 2000 A in diameter between the layers of the graphite structure.

The energy stored in graphite from fission damage has been measured[56] in a 92-g sample of Pechiney graphite (density 1.75 ± 0.04 g/cm^3) which was impregnated with 1.61 g of U^{235} (0.0332 g/cm^3) in the form of UO_2. The resulting UO_2 particles were so small that all the fission fragments came to rest in the graphite. Irradiation was to a level of 1.3×10^{18} nvt (thermal) at about 32°C. Calorimetric measurements indicated a stored energy of 31.2 ± 3.2 cal/g after a 3 Mwd/ton exposure. Neutron irradiation alone would have produced about 1 cal/g. In explaining the stored energy due to neutron irradiation, the suggestion was made that the energy is stored in atoms that have been displaced by carbon atoms. Previous results show stored energy of 0.45 cal/g from a 1 Mwd/ton exposure which was explained in terms of 5×10^{-5} displaced atoms per carbon atom. From similar considerations, estimates were made that each fission event produced 30,000 displaced carbon atoms. The authors suggest alternative possibilities to explain the large energy storage in fission damage: (1) larger numbers of displaced atoms, (2) different processes of storage because of high density of damage due to a fission fragment, or (3) a different type of damage resulting from the high charge on the fission particle.

Some of Muller's[57] data on spin-resonance lines in neutron-irradiated single-crystal graphite have been correlated with recent data of Bollmann's[58] on direct observation of neutron damage in the same system. At neutron fluxes up to 9.6×10^{18} nvt at 300°K, Muller is able to conclude that, on the average, about 30 carbon atoms were displaced per nvt per cubic centimeter.

Electrical-resistance change of graphite irradiated with electrons at liquid-nitrogen temperatures resulted in a determination of the energy for lattice displacements[59] of 30 ev. (Measurements are reproducible to 0.05 per cent.) This is slightly higher than the value reported from neutron-damage experiments at room temperatures. A 2-Mev Van de Graaff with a maximum electron current of 100 μa was used. Annealing of the electron damage is complete after about 15 min at 200°C. The temperature region corresponds to an annealing peak in the neutron damage also. Resistance changes of about 8 per cent were observed at exposures of 200 μa-hr. Damage increased with increase of electron energy, and the displacement energy was determined from the threshold energy by plotting the percentage resistance change against electron energy, using an 800 μa-min exposure. The threshold energy for lattice displacement found in this manner was 150 kev.

Silica glass was irradiated in excess of 5×10^{19} nvt (fast) and measured by means of ultrasonic attenuation[60] from 7 to 50 Mc/sec in the temperature range 1.5 to 200°K. A large number of defects in the form of elongated Si-O-Si bonds were observed with two equilibrium positions available for the oxygen bridge. The conclusion made is that thermal-spike mechanisms are necessary to explain this damage. The elongated bonds can be produced thermally and cannot be explained in terms of an increase in point defects only. (T. G. Knorr)

Theories of Radiation Effects

Three reports[61–63] have appeared which include papers presented at the Faraday Society's Discussions on Radiation Effects in Inorganic Solids held at Saclay on Apr. 11 and 12, 1961.

Vineyard's[61] general introduction is an excellent survey of interests in the complete field, whereas Levy's[62] paper is concerned with defect annealing in reactor-irradiated Al_2O_3. Dienes and Damask[63] reported on specific results, extending the theory of annealing of mono-, and divacancies to pure metals. Further machine calculations are reported in this paper. General results show that the mobility of divacancies is always less than that of single vacancies and that the combination of vacancies to form divacancies increases as the annealing temperature increases. Other results require a detailed analysis of the equations. Comparison with experiments at this time, they say, is limited by the small amount of experimental data.

Taimuty[64] proposes the use of sputtered copper as a reactor-radiation-damage monitor. The sputtered atoms can be collected on foils adjacent to or even in contact with the emitting surfaces, and their number can be determined by thermal-neutron activation. Piling up these sandwiches can easily result in 100 cm^2 of emitting area. Using the present experimental data for sputtering yields, Taimuty concludes that measurable amounts of copper will be transferred after irradiations of the order of 10^{18} neutrons/cm^2. Additional experiments and theory are necessary, but he feels that the presently available data are sufficient for the purposes of this device.

Calculations of the change in lattice constants and internal energy of a graphite crystal containing Frenkel defects have been made in the Russian literature.[65] The theoretical results are compared with experimental data. Calculations have also been developed to show that vacancies in graphite (formed by various processes) condense to form cavities 100 to 1100 A in diameter between (0 0 1) planes.[66] Internal surface energy and configurational entropy require the formation of these large cavities, which are expected to grow and collapse into prismatic dislocation loops because of higher stresses in the *c* direction. The criterion for this change is found by comparing the self-energy of the dislocation loop with the sum of the surface energy of the original cavity and the compressive strain energy to be released by the collapse.

Mitchell and Whitehouse[67] have published a short note indicating their attempts to study defects by means of the refractivity of light scattered from damaged crystals. Their theory is compared favorably to some results obtained in neutron-irradiated quartz. However, they state that there is no possibility of distinguishing between point defects, combinations of point defects, and disordered regions less than about 1000 A by these methods.

Kikucki[68] has considered the dissipation of incident energy in a nuclear medium by calculating the nuclear reactions produced by fast nucleons. Such energy dissipation is similar to the diffusion of neutrons in an absorbing medium. Because of the similarity, analogy is incorporated so that a diffusion equation is developed for the energy and spatial distribution of the incident beam and for the nucleons excited by the incident nucleon. The formula obtained from this classical model is used to calculate the energy spectrum of all nucleons emitted, with particular concern for successive collisions of the incident nucleons. The energy spectra and cross sections determined are in fair agreement with experiments where the energy spectra of protons emitted from tin and lead bombarded with 40-Mev protons were studied.

(T. G. Knorr)

Surveys on Radiation-Induced Defects

Amelinckx[69] has discussed in detail the effects produced by radiation in ionic crystals. Because of the lack of data in other materials, his analysis is limited to the alkali halides. Sections of particular interest here are concerned with dimensional and density changes as well as stored-energy and magnetic-susceptibility studies. Extensive bibliographies are included in each section.

Bibliographies of radiation damage of various interests have appeared: (1) 39 papers reporting on damage[70] in Al_2O_3-Al_2O_3MgO-MgO up to April 1961, (2) 24 papers of effects[71] in CaF_2 up to April 1961, and (3) 129 papers concerned with effects in inorganic glasses[72] from 1910 to 1959. The effects of radiation on the mechanical properties of steels have been surveyed in a list of 112 references covering a period[73] through 1960. (T. G. Knorr)

Effects of Radiation on Mechanical Properties

The effect of irradiation on the magnetic properties of a structural steel, SA-212B, has

been investigated by Argonne.[74] Four groups of specimens received exposures, the maximum of which was 2.8×10^{21} nvt (>1 Mev) and a minimum of 1×10^{20} nvt (>1 Mev). It was found that the hardness increased as a result of the irradiation, but the coercive force was relatively unaffected. These properties will again be measured for a portion of these samples after annealing at 900°F for 1 hr.

The Canadians[75] are investigating the effect of irradiation on a number of structural materials, including type 410 stainless steel and magnesium in the form of foils, Invar, and beryllium in more massive forms. The annealed foil materials showed no change after irradiation to 4.4×10^{19} neutrons/cm^2 at 50°C. Invar showed a 0.042 per cent increase in length after exposure to 1.5×10^{20} neutrons/cm^2 (>500 ev) at 45°C. It has been found that hydrogen will agglomerate in cyclotron-irradiated beryllium after 1 hr at 300 to 400°C and a hydrogen concentration of about 0.5 cm^3/cm^3 can cause crack formation upon heating above 800°C.

Workers at Oak Ridge[76] report additional data for the rupture strength of type 304 stainless steel during irradiation at 1500 and 1600°F. These data are given in Table IV-2 and indicate a 25 and 15 per cent reduction in rupture strength at 1500 and 1600°F, respectively, when compared with tests made out of reactor. This reduction in rupture strength was not noted for tests made at 1300°F. Specimens showed a reduction in ductility at all test temperatures. Another investigation to determine the effect of boron on the in-reactor burst strength of Inconel has shown recent results which both do and do not support the argument that boron will have a deleterious effect on Inconel during irradiation. These and previous data are shown in Tables IV-3 and IV-4.

The tensile properties of aluminum and several aluminum alloys have been determined by Du Pont[77] after irradiation to 8×10^{20} nvt (fast). Fast-neutron energies have been defined to include those neutrons with energies >0.1 Mev. The room-temperature properties after irradiation are shown in Table IV-5. The usual increases in yield strength, ultimate strength, and hardness are noted after irradiation, along with decreases in total elongation and reduction in area.

In an investigation at Hanford[78,79] to evaluate the effects of irradiation on Zircaloy-2, the tensile properties of a cold-worked unirradiated and cold-worked irradiated material were determined at room temperature and 300°C. The specimens were cut from a tube exposed in the KER reactor at 200 to 250°C. The tube was cold worked 70 per cent by tube reducing before irradiation. Tables IV-6 and IV-7 give the results of the test. Significant increases in strength and decreases in ductility

Table IV-2 STRESS-RUPTURE AND TANGENTIAL STRAIN DATA FOR IN-PILE AND CONTROL TUBE-BURST SPECIMENS OF TYPE 304 STAINLESS STEEL (SUPERIOR TUBE CO., HEAT NO. 2399x)[76]

Test temp., °F	Specimen identification	Stress, 1000 psi	Time to rupture, hr	Tangential strain, %	
				Av.	Max.
1300	15-2	13	127	1	1.4
	15-3	13	217*	0.4	0.6
	15-6	13	141	1.1	2.1
	15-8	13	116	0.85	1.15
	126 control	13	144	1.57	2.33
	127 control	13	144	2.72	3.49
	15-4	11	502	0.9	1
	15-7	11	470	1.1	1.9
	15-10	11	452	0.8	1.1
	124 control	11	470	3.57	4.12
	128 control	11	550	2.86	4.21
	15-1	9	1642	1	1.1
	15-5	9	>1860	0.85	1.1
	15-9	9	>1860	0.8	1
1500	9-7	5	337	3.3	3.8
	9-8	5	518	3.2	3.8
	73 control	~5.25	1130	8.1	9.3
	239 control	~5.25	1025	12.5	15
	9-6	4	673	3.8	5.3
	17-3	4†	851	1.3	3.6
	72 control	~4.2	1670	9.6	11.5
	240 control	~4.2	2450	9.2	12.4
	17-1	3	>1600	0.5	0.6
	17-9	3	>1600	0.7	0.85
	310 control	~6.3	520	10	15
	537 control	~6.3	184	7	9
1600	17-8	5	50	1.1	1.5
	1066 control	~4.6	82	7.5	9.8
	Control	~4.3	175		
	1112 control	~4.2	63	11	17
	Control	~3.8	180		
	Control	~4.1	142		
	360 control	~3.7	265	10.2	13.5
	718 control	~3.2	243	18.5	24.2
	1068 control	~2.2	197		
	17-5	3	414	3.3	5.8
	17-6	2.6	870	3.2	5.6
	17-4	2.2	1430	2.2	3.8
	17-7	2.2	>1500	1.5	1.8

* Irradiated more than 500 hr at 1300°F and 16 Mw prior to stressing.

† Irradiated more than 500 hr at 1500°F and 30 Mw prior to stressing.

Table IV-3 STRESS-RUPTURE AND TANGENTIAL STRAIN DATA FOR IN-PILE AND CONTROL TUBE-BURST SPECIMENS OF INCONEL TESTED[76] AT 1500°F (INCO HEAT NO. NX 8962)

Specimen	Stress, 1000 psi	Time to rupture, hr	Tangential strain, % Av.	Tangential strain, % Max.
11-5	5	173*	0.45	0.6
11-6	5	73	2.7	5
11-7	5	140*	2.5	4.4
11-8	5	91	1	1.6
9-4	5	117†	0.55	0.8
4-5	5	109‡	1.5	2.3
4-6	5	110§	4.7	5.6
35 (control)	5	473		11.2
41 (control)	5	487		8.4
28 (control)	5	410		5.7
43 (control)	4	801		13.8
44 (control)	4	797		10.7
4-10	3	774	0.65	0.8
37-2-71	3	784		0.8
37-2-73	3	>870		1.25
48 (control)	3	>2850		9.6

* Stressed 48 hr prior to start of irradiation.

† Irradiated more than 1000 hr at 1500°F prior to stressing out of pile.

‡ Irradiated 100 hr at 1500°F prior to stressing.

§ Irradiated 550 hr at 1500°F prior to stressing.

were noted at both test temperatures. Some recrystallization was observed in the tube after irradiation.

Also at Hanford,[79] the in-reactor creep properties of Zircaloy-2 are being investigated at elevated temperature. A test in progress in reactor at 260°C and 30,000 psi has shown an average unit creep rate over a one-month period of 1.69×10^{-6}/hr, as compared with the ex-reactor rate of 1.5×10^{-7}/hr. In contrast, an in-pile creep test for 500 hr made by the Canadians[75] under similar conditions (30,000 psi at 300°C) on 18.5 per cent cold-worked Zircaloy-2 showed no effect of the irradiation on the creep rate. Several tests have also been made at Oak Ridge[16] comparing the rupture strength of Zircaloy-2 at 700 and 900°F in and out of reactor environment. The rupture strengths are determined by tubular-burst tests in a flux of approximately 1×10^{13} nv (> 1 Mev). These tubes are exposed to approximately 4×10^{18} nvt before pressurizing with helium. The results, given in Fig. IV-3, suggest that the effect of neutrons is to reduce the rupture life at high stresses and increase it at lower stresses.

Table IV-4 EFFECT OF NEUTRON BOMBARDMENT ON STRESS-RUPTURE CHARACTERISTICS OF "BORON-ADJUSTED" HEATS OF INCONEL IRRADIATED AT 1500°F IN AIR[76]

Specimen heat	Boron content	Specimen identification	Stress, 1000 psi	Time to rupture, hr	Comments on effect of irradiation on time to rupture
OB	<10 ppm, natural boron	Control	6	155	Reduced by a factor of 2 to 3
		Control	5	320	
		28-6	5	140	
		Control	4	1250	
		28-2	4	473	
		Control	3	1950	
4B11	40 ppm, 98% B^{11}	Control	5	105	No change
		28-9	4.5	186	
		Control	4	250	
		28-5	3.2	617	
		Control	3	980	
6B11	60 ppm, 98% B^{11}	28-4	5.5	56	Reduced by a factor of 10
		Control	5	610	
		28-10	4.5	133	
		Control	3.8	1500	
10B	100 ppm, natural boron	28-3	6	52	Reduced by a factor of 5 to 10
		28-8	5	58	
		Control	5	580	
		Control	4	1750	
6B10	60 ppm, 95% B^{10}	Control	5	195	Reduced by a factor of 3 to 5
		28-1	4.5	80	
		Control	4	255	
		28-7	3.5	229	

Table IV-5 EFFECT OF IRRADIATION ON MECHANICAL PROPERTIES OF ALUMINUM AND ALUMINUM ALLOYS[77]

	Preirradiation		Postirradiation, 8×10^{20} fast* nvt
	Measured	Handbook	
Aluminum (99.9–99.99%), annealed:			
Ultimate tensile strength, psi	6,600		12,200
Yield strength at 0.2% offset, psi	2,100		5,500
Total elongation to fracture, %†	46		30
Uniform elongation, %†	23		12
Reduction of area at fracture, %	86		94
Elastic modulus, 10^6 psi	7.8		9.4
Hardness, DPH‡	35		37
1100 alloy, H12 temper:			
Ultimate tensile strength, psi	17,600	16,000	22,000
Yield strength at 0.2% offset, psi	15,100	15,000	18,700
Elastic modulus, 10^6 psi	10.1	10.0	10.1
Hardness, Rockwell H	35		61
6063 alloy, annealed:			
Ultimate tensile strength, psi	19,400	13,000	24,200§
Yield strength at 0.2% offset, psi	8,200	7,000	33,900
Total elongation to fracture, %	24		13
Uniform elongation, %	12		11
Reduction of area at fracture, %	83		41
Elastic modulus, 10^6 psi	9.3	10.0	9.4
Hardness, Rockwell H	67		97
6063 alloy, T4 temper:			
Ultimate tensile strength, psi	28,500	25,000	48,200
Yield strength at 0.2% offset, psi	14,100	13,000	39,400
Reduction of area at fracture, %	71		29
Elastic modulus, 10^6 psi	10.8	10.0	9.7
X2219 alloy, as received:			
Ultimate tensile strength, psi	38,100		47,000
Yield strength at 0.2% offset, psi	28,500		32,800
Total elongation to fracture, %	12		12
Uniform elongation, %	8		7
Reduction of area at fracture, %	40		30
Elastic modulus, 10^6 psi	10.6		10.3
Hardness, Rockwell K	31		49
X2219 alloy, T6E46 temper:			
Ultimate tensile strength, psi	57,800		63,800
Yield strength at 0.2% offset, psi	38,300		47,200
Total elongation to fracture, %	12		11
Uniform elongation, %	10		6
Reduction of area at fracture, %	39		16
Elastic modulus, 10^6 psi	10.4		10.6
Hardness, Rockwell A	39		39
X8001 alloy, as received:			
Ultimate tensile strength, psi	17,200		17,200
Yield strength at 0.2% offset, psi	9,400		7,600
Total elongation to fracture, %	31		27
Uniform elongation, %	17		14
Reduction of area at fracture, %	84		78
Elastic modulus, 10^6 psi	9.8		9.6
Hardness, Rockwell H	40		54
X8001 alloy, H14 temper:			
Ultimate tensile strength, psi	21,200		22,700
Yield strength at 0.2% offset, psi	20,300		20,600
Total elongation to fracture, %	15		14
Uniform elongation, %	4		4
Reduction of area at fracture, %	78		74
Elastic modulus, 10^6 psi	10.6		10.0
Hardness, Rockwell H	74		79

* Fast neutrons defined to include those with energies greater than 0.1 Mev.

† In 2-in. gauge length.

‡ 0.2-kg load.

§ Exposure of annealed specimens of 6063 alloy is 2×10^{20} fast nvt.

Table IV-6 TENSILE PROPERTIES OF ZIRCALOY-2 SPECIMENS CUT FROM UNIRRADIATED AND IRRADIATED KER TUBES[78]

Specimen	Tube section	Gamma activity	Strength, 1000 psi		Total elongation, %*	Modulus of elasticity, 10^6 psi
			0.2% yield	Tensile		
C-1	Control	0	88.7	96.8	7.6	11.8
C-2	Control	0	87.8	95.1	6.3	12.7
1-1	1	500 mr	91.7	102.0	6.8	*
1-2	1	500 mr	70.1	89.4	5.4	14.6
1-3	1	500 mr	91.3	101.0	3.0	16.1
4-1	4	3 r	50.4	78.6	10.9	12.6
4-3	4	3 r	97.5	103.5	>2.1†	14.7
5-1	5	10 r	82.7	96.5	6.4	12.1
5-2	5	10 r	92.4	105.3	7.2	*
2-2	2	15 r	102.0	108.7	3.7	12.6
3-1	3	25 r	100.3	110.9	4.6	12.3
3-2	3	25 r	84.8	99.3	3.2	14.9
3-3	3	25 r	98.4	109.6	>1.8†	16.8

* Poor resolution of initial elastic strain.
† Broke outside of gauge length.

Table IV-7 300°C TENSILE PROPERTIES OF ZIRCALOY-2 SPECIMENS CUT FROM UNIRRADIATED AND IRRADIATED KER TUBES[73]

Specimen	Tube section	Gamma activity	Ultimate strength, 1000 psi	Total elongation, %
B-2*	Control	0	53.4	4.7
B-8*	Control	0	58.9	4.7
E-4	Control	0	61.7	4.2
D-8	Control	0	60.0	3.5
1-4	1	500 mr	48.8	3.3†
1-5	1	500 mr	47.8	3.7
4-4	4	3 r	50.9	2.4
4-5	4	3 r	60.8	2.5
5-3	5	10 r	63.4	4
5-4	5	10 r	54.9	3.3
2-3	2	15 r	55.3	3.5
2-4	2	15 r	47.6	7.4†
3-4	3	25 r	65.3	2.6
3-5	3	25 r	66.0	3.5

* Tested at 275°C.
† Known to be partially recrystallized.

The effects of annealing temperatures on the properties of irradiated molybdenum, zirconium, and high-purity nickel are being investigated by Hanford.[78,79] Both irradiated and unirradiated samples have been annealed for equal times to temperatures as high as 550°C. Changes in electrical resistivity and hardness were noted. The results are discussed in terms of vacancy diffusion. (F. R. Shober)

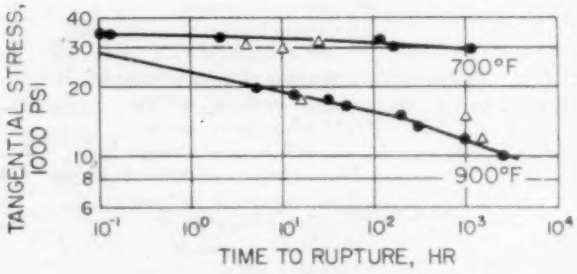

Fig. IV-3 Results of Zircaloy-2 tube-burst tests at 700 and 900°F in helium.[16] ●, control tests. Δ, in-pile tests.

Selected Mechanical Properties of Cladding and Structural Materials

Nickel-Base Alloys

The effects on Inconel of the application of relatively high-frequency thermal oscillations were studied at Oak Ridge,[80] under conditions generating significant transient stress in the surface fibers. Fatigue type cracking is observed in 214 hr at 1.0 cps for a surface-temperature amplitude of ±64°F (17,800-psi maximum elastic surface stress). Incipient cracking occurs in 23 hr at 0.4 cps for an amplitude of ±104°F (31,300 psi). Application of ±46°F surface-temperature oscillations

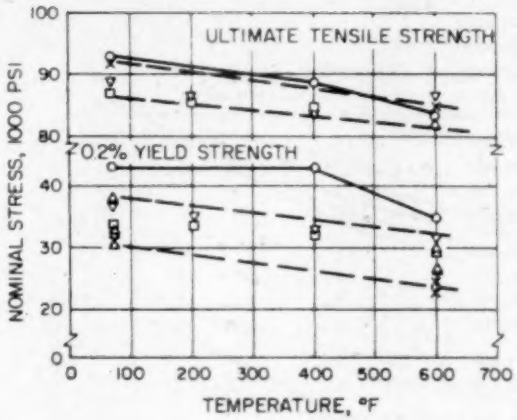

Fig. IV-4 Tensile properties of air-melted Inconel.[81] ○, vacuum melted, air melted. Δ, NX 2027. ×, NX 2026. □, NX 1186. ▽, NX 728.

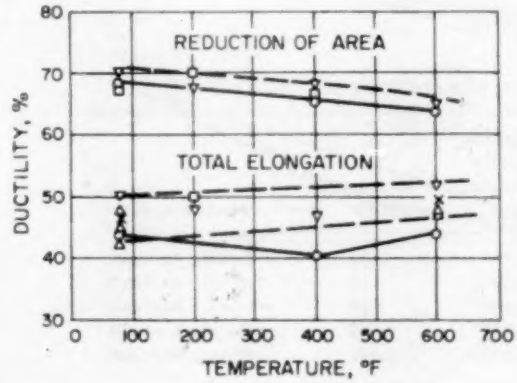

Fig. IV-5 Ductility of air-melted Inconel.[81] ○, vacuum melted, air melted. Δ, NX 2027. ×, NX 2026. □, NX 1186. ▽, NX 728.

(12,800 psi) at 1.0 cps for 612 hr produces accelerated intergranular corrosion in a fused-salt environment. These results are correlated in terms of the maximum calculated elastic surface stress.

The tensile properties of vacuum-melted Inconel, as determined by Knolls,[81] are summarized in Figs. IV-4 to IV-6. The vacuum-melted material is slightly stronger than air-melted material. The ductility decreases slightly with increasing temperature and is practically identical for each material.

Iron-Base Alloys

The short-time tensile strength of Fe–25 Cr–4 Al–1 Y alloys is said to drop rapidly with

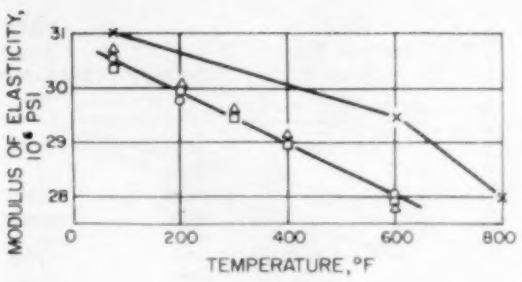

Fig. IV-6 Modulus of elasticity of air-melted Inconel.[81] NX 728: ○, static determination; □, dynamic determination. NX 1186: Δ, dynamic determination; ×, published data.

increasing temperature above 1500°F. In addition, General Electric reports[82] that the material elongates in excess of 100 per cent at rupture. The stresses to produce rupture in 1000 hr are approximately 1200 psi at 1500°F, 600 psi at 1750°F, and 300 psi at 2000°F. At 2200°F, the alloy is subject to stress oxidation at loads greater than 200 psi.

An AGARD (NATO)[83] report has been released which lists 348 references to crack initiation and propagation in high-strength alloy sheets.

Refractory-Metal Alloys

A recent Battelle report[84] summarizes the creep strength of three high-strength niobium-

Table IV-8 STRESSES TO PRODUCE CREEP RATES OF 0.001, 0.01, AND 0.1 PER CENT PER HOUR IN THREE NIOBIUM-BASE ALLOYS[84]

Alloy composition (balance Nb), wt.%	Stress, psi, to produce creep rate shown		
	0.001%/hr	0.01%/hr	0.1%/hr
	At 650°C		
2.37 Cr	47,800	53,200	58,700
3.34 Zr	41,400	41,800	42,300
5.21 V	52,700	58,800	64,700
	At 800°C		
2.37 Cr	35,000	37,800	40,600
3.34 Zr	31,300	40,200	42,200
5.21 V	40,000	42,500	25,000
	At 1000°C		
2.37 Cr	10,800	17,000	23,200
3.34 Zr	9,000	15,300	20,800
5.21 V	15,500	20,300	25,000

Table IV-9 TENSILE PROPERTIES OF NIOBIUM ALLOYS WITH OXYGEN ADDITIONS[85]

Alloy composition (balance Nb), wt.%	Temp., °F	Yield strength (0.2% offset), psi	Ultimate tensile strength, psi	Elongation, %	Reduction of area, %
1 Zr–0.25 O	–76	68,000	76,900	16	54
	RT		88,700	17	>15
	1800	42,000	45,300	17	
	2000	32,000	34,500	10	
3 Zr–0.25 O	–76	73,000	85,500	19	36
	RT	52,000	64,800	19	48
	1400	49,000	56,000	7	41
	1600	53,000	55,700	6	40
3 Zr–0.50 O	1800	47,000	4,800	2	
	2000	39,000	42,500	5	
1.5 Ti–0.50 O	–76	64,000	93,400	29	59
	RT	60,000	73,500	29	74
	1600	40,000	44,600	19	65
	1800	33,000	36,500	14	
	2000	29,000	31,400	13	
	2200	24,000	26,900	20	

Table IV-10 TENSILE PROPERTIES OF SOME REFRACTORY-METAL ALLOYS[86]

Alloy composition, wt.%	Temp., °F	Yield strength (0.2% offset), psi	Ultimate tensile strength, psi	Elongation, %	Source of data
Nb–1 Zr	RT	35,400	48,100	15	Boeing Aircraft
	2000	20,700	22,800	14	Boeing Aircraft
	2500	6,600	8,400	>48	Boeing Aircraft
	2700	4,800	6,000	>44	Boeing Aircraft
	3000	2,100	3,200	>41	Boeing Aircraft
Ta–8 W–4 Hg	2700	30,000	32,000		Westinghouse
Ta–5 Hg–10 W	3000		28,500		Battelle
88 W–6 Mo–6 Nb	3000		62,000		Crucible Steel
44 W–44 Ta–12 Nb	3000		54,000		Crucible Steel
25 W–75 Ta	3000		37,000		Crucible Steel
88 Ta–12 Mo	3000		29,000		Curcible Steel

Table IV-11 ROOM-TEMPERATURE TENSILE PROPERTIES OF TANTALUM-TUNGSTEN ALLOYS[87]

Condition	Yield strength (0.2% offset), psi	Ultimate tensile strength, psi	Elongation, %		
			½ in.	1 in.	2 in.
		Ta–0.1 Wt.% W			
As rolled	83,900	84,400	4	1	1
Annealed ½ hr at 1500°C	39,500	49,400	36	32	26
		Ta–3.0 Wt.% W			
As rolled	101,500	102,400	4	4	2
Annealed 1 hr at 1300°C	48,200	59,200	36	29	25

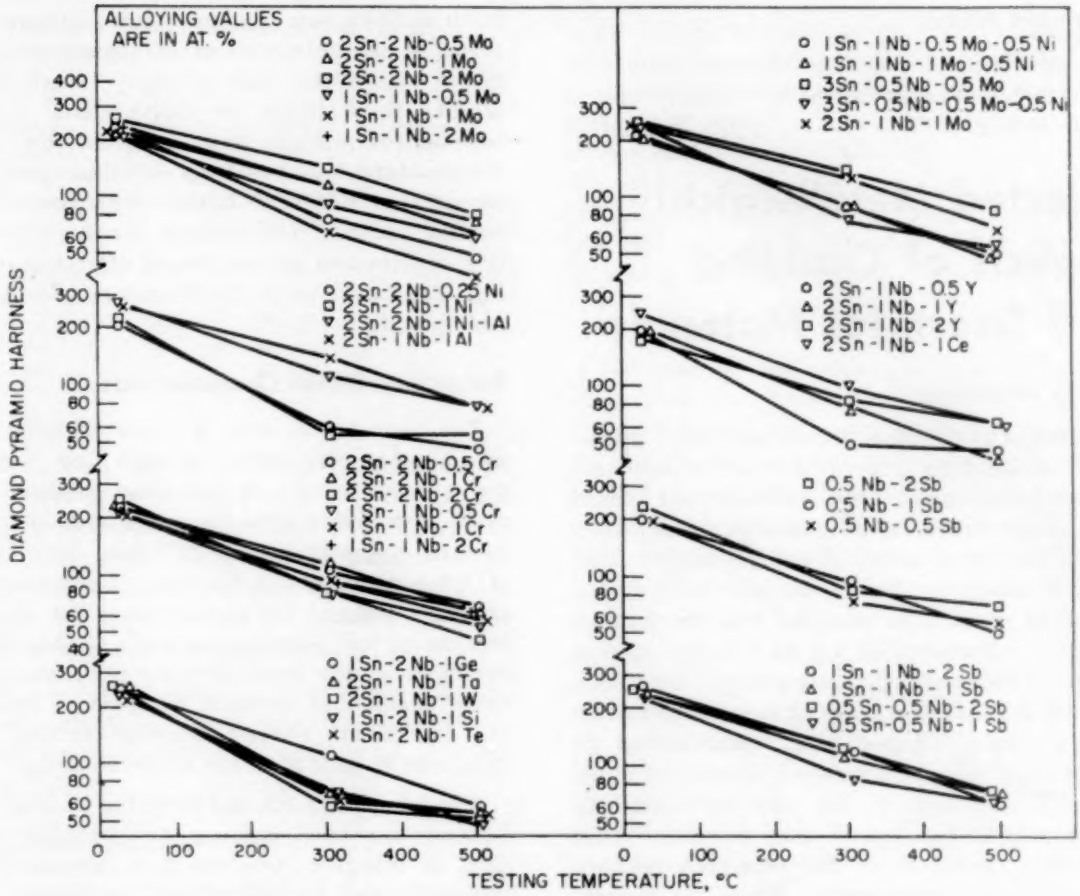
ALLOYING VALUES
ARE IN AT. %
o 2 Sn - 2 Nb - 0.5 Mo
Δ 2 Sn - 2 Nb - 1 Mo
□ 2 Sn - 2 Nb - 2 Mo
▽ 1 Sn - 1 Nb - 0.5 Mo
× 1 Sn - 1 Nb - 1 Mo
+ 1 Sn - 1 Nb - 2 Mo
o 2 Sn - 2 Nb - 0.25 Ni
□ 2 Sn - 2 Nb - 1 Ni
▽ 2 Sn - 2 Nb - 1 Ni - 1 Al
× 2 Sn - 1 Nb - 1 Al
o 2 Sn - 2 Nb - 0.5 Cr
Δ 2 Sn - 2 Nb - 1 Cr
□ 2 Sn - 2 Nb - 2 Cr
▽ 1 Sn - 1 Nb - 0.5 Cr
× 1 Sn - 1 Nb - 1 Cr
+ 1 Sn - 1 Nb - 2 Cr
o 1 Sn - 2 Nb - 1 Ge
Δ 2 Sn - 1 Nb - 1 Ta
□ 2 Sn - 1 Nb - 1 W
▽ 1 Sn - 2 Nb - 1 Si
× 1 Sn - 1 Nb - 1 Te
o 1 Sn - 1 Nb - 0.5 Mo - 0.5 Ni
Δ 1 Sn - 1 Nb - 1 Mo - 0.5 Ni
□ 3 Sn - 0.5 Nb - 0.5 Mo
▽ 3 Sn - 0.5 Nb - 0.5 Mo - 0.5 Ni
× 2 Sn - 1 Nb - 1 Mo
o 2 Sn - 1 Nb - 0.5 Y
Δ 2 Sn - 1 Nb - 1 Y
□ 2 Sn - 1 Nb - 2 Y
▽ 2 Sn - 1 Nb - 1 Ce
□ 0.5 Nb - 2 Sb
o 0.5 Nb - 1 Sb
× 0.5 Nb - 0.5 Sb
o 1 Sn - 1 Nb - 2 Sb
Δ 1 Sn - 1 Nb - 1 Sb
□ 0.5 Sn - 0.5 Nb - 2 Sb
▽ 0.5 Sn - 0.5 Nb - 1 Sb
DIAMOND PYRAMID HARDNESS
TESTING TEMPERATURE, °C

Fig. IV-7 Hardness of zirconium alloys.[79]

base alloys under development. The results are shown in Table IV-8.

Workers at Armour[85] report the following results on studies of the addition of oxygen, together with titanium or zirconium, to niobium. They say that this is an excellent method of preparing forgeable niobium alloys having good high-temperature strength and adequate low-temperature ductility. Tensile strengths are shown in Table IV-9.

The tensile properties of a number of promising high-temperature alloys are presented in a recent DMIC report.[86] These are listed in Table IV-10.

The tensile properties of tantalum–0.1 wt.% tungsten and 3.0 wt.% tungsten alloys are reported by Los Alamos[87] in the as-rolled and annealed conditions. The values are presented in Table IV-11.

An investigation of dispersion strengthening of a molybdenum–1.5 wt.% titanium alloy by the New England Materials Laboratory[88] has produced the following results. The alloy was strengthened by internal oxidation, which depends on the oxidation of the solute element in a dilute solid solution with a resultant fine oxide dispersion throughout the metal matrix. The completely recrystallized material at 2200°F in argon had yield and ultimate tensile strengths of 21,900 and 31,900 psi, respectively.

The tensile and notch-tensile properties of molybdenum, tungsten, niobium, tantalum, and molybdenum–0.5 wt.% titanium alloy have been investigated at Battelle.[89] These properties were studied at five temperatures selected to encompass the brittle-to-ductile transition range. Specimen failures are classified according to fracture mechanism. The notch sensitivity of each material is evaluated by analyzing the notch and unnotched tensile strength, the ductility transition, and the fracture transition.

Zirconium Alloys

A plot of the hardness of several zirconium-base alloys was prepared by Knolls[81] and is shown in Fig. IV-7. (J. A. DeMastry)

Selected Metallurgical Aspects of Cladding and Structural Materials

Slip in Aluminum

Workers at the Max-Planck Institute,[90] utilizing a combination of X-ray diffraction with light and electron-microscope examinations, found that nonoctahedral slip occurs relatively often during the deformation of polycrystalline aluminum samples. Almost 30 per cent of the examined aluminum samples with an average crystallite diameter of 0.1 to 0.5 mm showed {1 0 0}, {1 1 0}, and {1 3 3} slip planes. This nonoctahedral slip takes place at deformation rates of less than 2.5 per cent. Observations on crystallites with an average diameter of more than 0.5 mm lead to the conclusion that the tendency for octahedral slip increases with increasing grain size. The observed relative frequency of nonoctahedral planes is closely related to the ratio of Burger's vector and slip-plane spacing.

Constitution of Iron-Base Alloys

The liquidus and solidus relations in iron-rich alloys of the iron-niobium and iron-molybdenum systems were investigated by the British,[91] using alloys of high purity. They confirm the general form of the earlier iron-niobium diagram but report that the composition of the delta eutectoid is at a lower percentage of niobium than was previously imagined. For the system iron-molybdenum, the general form of the earlier diagram is again confirmed, but the freezing range of the delta-phase alloys is narrower than was previously supposed. In the systems iron-niobium and iron-molybdenum, the delta liquidus and solidus curves pass through minima at almost the same composition (~20 at.% solute), in spite of the larger size of the molybdenum atom.

Additional constitution-diagram work by the British[92] is reported for the chromium-niobium-molybdenum system. The diagram derived is characterized by an extensive miscibility bay within the primary single-phase (alpha) field, based on molybdenum. Lattice segregation effects are involved, the high-temperature alpha matrix dividing into isomorphs of different lattice dimensions; this entails various intermediate stages, with lattice strains and age-hardening effects developing. The Laves phase Cr_2Nb enters as a further precipitant.

Refractory-Metal Characteristics

The surface tension of solid niobium was measured by Manufacturing Labs., Inc.,[93] utilizing a modification of the Udin method. The value obtained is 2100 dynes/cm at 2250°C in a vacuum of approximately 10^{-5} mm. This result is consistent with a theoretical estimate and provides support for estimates of the surface tension of the refractory metals. From measurements of the dihedral angle of grain boundaries formed in niobium by thermal etching, the interfacial energy (gamma prime) was computed to be 0.36 of the surface energy.

A niobium-data manual prepared by English[94] authors has been revised and brought up to date. In addition, two chapters containing information on the effects of irradiation and equilibrium diagrams have been added.

The niobium-base alloys F-48 and F-50 are reported by General Electric[95] to be typically precipitation hardenable in the presence of sufficient interstitial content. The F-48 (Nb–15 W–5 Mo–1 Zr) alloy age hardens extensively in the temperature range of 1800 to 2100°F; the optimum aging temperature range of F-50

Table IV-12 PHASE IDENTIFICATION (PROBABLE) OF F-48 AND F-50 ALLOYS[95]

Alloy	Condition	Phases
F-48	As cast	ZrO_2, monoclinic Nb_2C, hexagonal
	Extruded at 3000°F	(Zr, Nb, W) C, cubic, Nb_2C
	Annealed at 3500°F	(Zr, Nb, W) C, ZrO_2, Nb_2C
F-50	As cast	ZrO_2, TiC, cubic*
	Extruded at 2800°F and swaged at 2500°F	(Zr, Nb, Ti, W) C, cubic
	Annealed at 3500°F	ZrO_2, NbC, cubic (rare)†

* Titanium-rich monocarbide.
† Niobium-rich monocarbide.

Table IV-13 RECRYSTALLIZATION VERSUS ANNEALING CONDITIONS FOR TANTALUM–0.1 WT.% TUNGSTEN

Annealing temp., °C	Annealing time, hr	Recrystallization, %	Hardness, DPH
As rolled		As worked	177
1200	1	40–50	107
1300	1	60–70	121
1400	1	75	96
1400	2	75–80	115
1500	½	80–90	98
1550	½	80–90	93
1600	¼	80–90	103

(Nb–15 W–5 Mo–1 Zr–5 Ti) is found to be 200 to 300°F lower. The lower solutioning and aging temperature ranges of F-50 appear to result primarily from the titanium addition rather than its lower interstitial contents. In addition, a tentative phase identification has been made and is shown in Table IV-12.

The recrystallization and annealing conditions for a tantalum–0.1 wt.% tungsten alloy, as reported by Los Alamos,[87] are shown in Table IV-13.

Zirconium Characteristics

A study[96] by Nuclear Metals of the deformation processes active in zirconium crystals deformed at 77, 300, 575, and 1075°K has been completed. Specimens studied were large grained and of relatively high purity and wide orientation distribution. The only slip system observed at any of the temperatures was of the form $(10\bar{1}0)[\bar{1}2\bar{1}0]$ with a critical resolved shear stress of about 1.0 kg/mm² in tension at 77°K, 0.65 kg/mm² in tension at 1075°K. The slip planes were found by the usual two-trace technique, and the slip direction was found from a detailed analysis of Laue spot asterism. The active twin planes were $\{10\bar{1}2\}$, $\{11\bar{2}1\}$, $\{1122\}$, and $\{11\bar{2}3\}$ with varying frequencies at the different test temperatures. The most active at all temperatures was $\{11\bar{2}1\}$, with $\{11\bar{2}2\}$, $\{11\bar{2}3\}$, and $\{\bar{1}012\}$ twins unobserved at 1075°K.

Savannah River[97] has published a rather comprehensive literature search of X-ray-diffraction studies on zirconium and Zircaloy-2. The report on classified and unclassified literature contains 85 abstracts.

The aging kinetics of zirconium-niobium alloys are the subject of a study at Knolls.[81] The major hardening of the zirconium-niobium al-

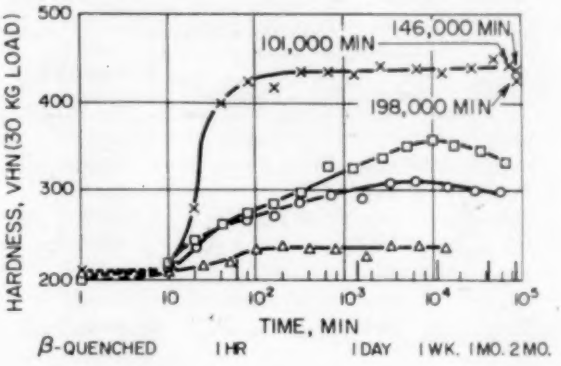

Fig. IV-9 Quench aging[81] of crystal-bar alloy 90 wt.% Zr–10 wt.% (94 Nb–6 V). ×, 400°C. □, 500°C. ○, 550°C. △, 600°C.

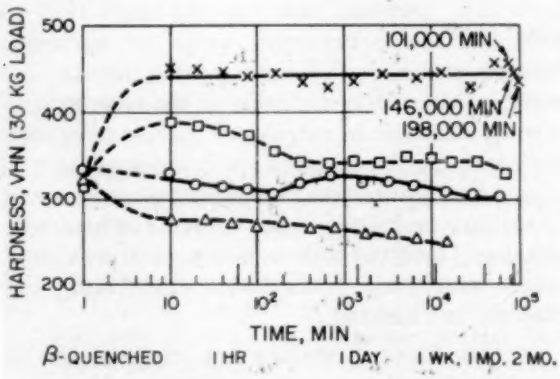

Fig. IV-8 Quench aging[81] of sponge-base alloy 90 wt.% Zr–10 wt.% (94 Nb–6 V). ×, 400°C. □, 500°C. ○, 550°C. △, 600°C.

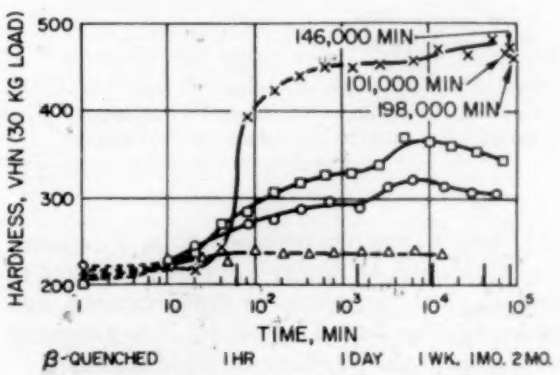

Fig. IV-10 Quench aging[81] of sponge-base alloy 82.5 wt.% Zr–17.5 wt.% (94 Nb–6 V). ×, 400°C. □, 500°C. ○, 550°C. △, 600°C.

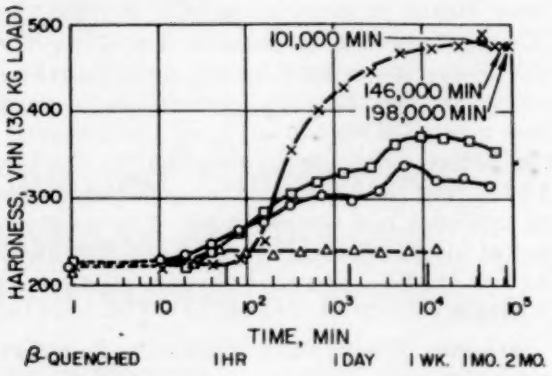

Fig. IV-11 Quench aging[81] of sponge-base alloy 80 wt.% Zr–20 wt.% (94 Nb–6 V). ×, 400°C. □, 500°C. ○, 550°C. △, 600°C.

Table IV-14 COMPATIBILITY OF COMPOUNDS WITH HYDROGEN AND TUNGSTEN[98]

Material	Temp., °F, at which material was observed to be		
	Stable in H_2	Unstable	Incompatible with tungsten
HfB_2		4400	4600
NbB_2	4450		4410
TaB_2	4660		4400
TiB_2		4400	4550
WB	4600		4600
ZrB_2	4510		4550
HfC	4290	4840	
Mo_2C	4250		4410
NbC	4680		4800
SiC			
TaC	4300	4630	4960
TiC	4520	4870	4640
UC			4420
WC	4250		4250
ZrC	4600	4780	4780
HfN	4000	4720	
NbN	3760		
TaN		4570	
TiN		4370	
ZrN	4450	5070	4890
ZrO_2	4230	4700	5690

loys results from the decomposition of retained beta zirconium to omega plus beta enriched in niobium. The hardness results obtained are shown in Figs. IV-8 to IV-11. The following conclusions were drawn from their studies:

1. Increased niobium increases the incubation period for the formation of the omega phase in beta-quenched zirconium-niobium alloys.

2. Short-time aging at 400°C after beta quenching results in extreme hardening of the zirconium-niobium alloys.

3. Oxygen has a profound influence on the quench-aging characteristics of the zirconium-niobium alloys; oxygen decreases the incubation period for omega-phase formation.

4. Aging zirconium-niobium alloys at 600°C results in only small increases in hardness because the quenched omega decomposition is very rapid.

Stability of Refractory Compounds

The stability in hydrogen and compatibility with tungsten of a number of high-temperature compounds were investigated[98] by NASA. The results are summarized in Table IV-14.

(J. A. DeMastry)

Diffusion Studies

A number of quite complete surveys on diffusion in certain types of systems have been published. An excellent monograph on diffusion in uranium, its alloys, and compounds has been published by Argonne.[99] The report surveys research that has been conducted in this field and includes over 150 references up to September 1960. Areas that still require investigation are also discussed. Subjects included in the monograph are diffusion in pure uranium, diffusion in uranium alloys, kinetics of layer growth, diffusion of hydrogen and rare gases in uranium, and self-diffusion and diffusion of rare gases in UO_2. Atomics International[100] has issued a bibliography consisting of 47 references to books, journals, and reports from 1955 to 1960 on the permeation rates of hydrogen through ceramics, ceramic-coated metals, and metals. Also, data available in the open literature on diffusion in refractory metals have been reviewed and evaluated in a comprehensive report.[101] Information on 95 binary systems and 13 ternary or higher order systems of tungsten, tantalum, molybdenum, niobium, platinum, hafnium, zirconium, vanadium, chromium, and titanium is reported.

At Oak Ridge,[16] studies are in progress on the diffusion of zirconium, niobium, and strontium in zirconium and in uranium dioxide, but significant results are not yet available. In another study, Oak Ridge reports data for the

diffusion coefficient of Al^{26} or Mn^{54} in aluminum which fit the following equations:

$$D_{Al^{26}}(T) = 1.3 \exp(-33{,}600/RT)$$

$$D_{Mn^{54}}(T) = 3.2 \exp(-33{,}500/RT)$$

The intermediate zone formed between arc-cast uranium monocarbide and hot-pressed beryllium at temperatures from 700 to 1000°C is also being investigated in diffusion studies at Oak Ridge. The zone formed has been identified as consisting of the reaction product UBe_{13}. A finely dispersed precipitate observed within this zone is believed to be free carbon. A large increase in the width of the UBe_{13} zone has been observed with increasing temperature in the range 750 to 800°C.

An exhaustive treatise in Russian on diffusion processes in alloys has been translated.[102] Results are presented for experiments on the effects of carbon, aluminum, titanium, tungsten, and molybdenum on the diffusion rate of chromium in nickel-base heat-resistant alloys and of tungsten, molybdenum, niobium, titanium, and vanadium on the self-diffusion of iron in iron-nickel alloys. The effect of the structure of nickel-tungsten alloys on the diffusion rate is also discussed. At Oak Ridge[103] the self-diffusion coefficients of Cr^{51} in Inconel and INOR-8, which are alloys suitable for use at high temperatures, were measured in an interesting manner by contacting the alloys with fused-salt mixtures containing radioactive chromous fluoride. The data, which are pertinent to a corrosion-behavior application, were determined over the temperature range of 600 to 900°C, where relatively low diffusion coefficients (10^{-16} to 10^{-12} cm^2/sec) were obtained.

(D. C. Carmichael)

References

1. General Electric Co., Flight Propulsion Laboratory Dept., Nuclear Materials and Propulsion Operation, High-Temperature Materials Program, Progress Report No. 1, May 1–June 30, 1961, USAEC Report GEMP-1. (Classified)
2. W. D. Klopp, Recent Developments on Oxidation-Resistant Coatings for Refractory Metals, Report DMIC-Memo-137, Defense Metals Information Center, Nov. 8, 1961.
3. S. Foldes, Oxidation Resistant Aluminide Coating on Columbium Alloy F-48, Paper Presented at Fall Meeting, AIME, Detroit, October 1961.
4. W. D. Klopp and H. R. Ogden, Protective Coatings for Tantalum and Its Alloys, Paper Presented at Fall Meeting, AIME, Detroit, October 1961.
5. V. D. Barth and G. W. P. Rengstorff, Oxidation of Tungsten, Report DMIC-155, Defense Metals Information Center, July 17, 1961.
6. H. A. Fisch, Hydrogen Absorption by Zirconium–2 At.% Tin–2 At.% Niobium Alloy During Corrosion, USAEC Report KAPL-2149, Knolls Atomic Power Laboratory, Jan. 19, 1961.
7. B. Cox, The Oxidation and Corrosion of Zirconium and Its Alloys. XII. Hydrogen Absorption by Zircaloy-2 and Some Other Alloys During Corrosion in Steam, British Report AERE-R-3556, January 1961.
8. S. B. Dalgaard, The Corrosion Resistance of Zr-Nb and Zr-Nb-Sn Alloys in High-Temperature Water and Steam. Part II. Canadian Report CRGM-1030 (AECL-1308), July 1961.
9. A. E. Bibb et al., Investigations of Binary Zirconium Alloys, USAEC Report KAPL-2162, Knolls Atomic Power Laboratory, Nov. 1, 1960.
10. Argonne National Laboratory, Annual Report for 1960, Metallurgy Division, USAEC Report ANL-6330.
11. R. D. Misch and C. Van Drunen, Corrosion Studies of Ternary Zirconium Alloys in High-Temperature Water and Steam, USAEC Report ANL-6370, Argonne National Laboratory, July 1961.
12. J. L. English et al., The Corrosion of Aluminum Alloys in High-Velocity Water at 170 to 290°C, USAEC Report ORNL-3063, Oak Ridge National Laboratory, June 15, 1961.
13. Oak Ridge National Laboratory, June 7, 1961. (Unpublished)
14. R. F. Maness, Corrosion Evaluation of Nickel-Base Alloys Developed to Contain Power Reactor Fuel Elements, USAEC Report HW-68426, Hanford Atomic Products Operation, February 1961.
15. F. W. Albaugh, Reactor and Fuels Research and Development Operation Monthly Report for July 1961, USAEC Report HW-70658A, Hanford Atomic Products Operation, Aug. 15, 1961. (Classified)
16. Oak Ridge National Laboratory, Metallurgy Division Annual Progress Report for Period Ending May 31, 1961, USAEC Report ORNL-3160, Aug. 17, 1961.
17. W. A. Chittenden and G. F. Hoveke, Engineering Evaluation Studies, Heavy Water Moderated Power Reactor Plants, USAEC Report SL-1873, Sargent and Lundy, June 30, 1961.
18. Aerojet-General Nucleonics, Army Gas-Cooled Reactor Systems Program, Semiannual Progress Report, January 1–June 30, 1961, USAEC Report IDO-28573, Aug. 10, 1961.
19. H. J. Pessl, Evaluation of Iron- and Nickel-Base Alloys for Medium and High-Temperature Reactor Applications. Part I. USAEC Report HW-

67715, Hanford Atomic Products Operation, February 1961.

20. General Electric Co., Flight Propulsion Laboratory Dept., High-Temperature Materials Program, Progress Report No. 3, Part A, July 1–August 31, 1961, USAEC Report GEMP-3A, Sept. 15, 1961.
21. J. J. Owens et al., The Snap II Power Conversion System Topical Report No. 7. Mercury Materials Evaluation and Selection, USAEC Report TID-11307, Thompson Ramo Wooldridge, Inc., Oct. 26, 1960.
22. Brookhaven National Laboratory, Nuclear Engineering Department Progress Report, Jan. 1–Apr. 30, 1961, USAEC Report BNL-671 (S-58), August 1961.
23. Argonne National Laboratory, Reactor Development Program Progress Report, September 1961, USAEC Report ANL-6433, Oct. 15, 1961.
24. Argonne National Laboratory, Reactor Development Program Progress Report, July 1961, USAEC Report ANL-6399, Aug. 15, 1961.
25. Aerojet-General Nucleonics, Rubidium: Corrosion and Physical Properties Evaluation Program, Final Report (No. 16) for Period Feb. 1, 1960, Through May 31, 1961, USAEC Report AGN-8034.
26. H. W. Leavenworth and R. E. Cleary, The Solubility of Ni, Cr, Fe, Ti, and Mo in Liquid Lithium, *Acta Met.*, 9: 519–520 (May 1961).
27. B. Minushkin, Solution Rates and Equilibrium Solubility of Nickel and Iron in Liquid Lithium, Report NDA-2141-1, United Nuclear Corp., June 30, 1961.
28. L. F. Grantham et al., Molten Phosphate Reactor Fuels. IV. *In Situ* Corrosion Studies of Metals in Molten Sodium Polyphosphate, USAEC Report NAA-SR-5928, Atomics International, Aug. 15, 1961.
29. L. Baker, Jr., et al., Studies of Metal-Water Reactions at High Temperatures: I. The Condenser Discharge Experiment: Preliminary Results with Zirconium, USAEC Report ANL-6257, Argonne National Laboratory, May 1961.
30. Argonne National Laboratory, Chemical Engineering Division Summary Report, January, February, March 1961, USAEC Report ANL-6333, June 1961.
31. E. U. Kauer, Metal-Water Reactions. A Literature Survey, USAEC Report TID-12746, Savannah River Laboratory, Mar. 17, 1961.
32. D. G. Brandon and P. Bowden, The Low Energy Ion Bombardment of Gold, *Phil. Mag.*, 8(6): 707–710 (1961).
33. C. J. Beevers and R. S. Nelson, Conference on Property Changes in Reactor Materials and Radiation Damage at CEGB, Berkeley Nuclear Laboratories, May–June 1961, proceedings to be published.
34. J. B. Rich and G. P. Walters, Conference on Metallurgy of Beryllium, Institute of Metals, October 1961 (Paper 3), proceedings to be published.
35. J. J. Kelsch et al., Electron Microscopy of Fission Damage in Metal Matrices, *J. Appl. Phys.* 32(8): 1627 (August 1961).
36. T. K. Bierlein and B. Mastel, Experimental Evidence of Fission Fragment Damage in Some Metals and Nonmetals, USAEC Report HW-68919, Hanford Atomic Products Operation, March 1961.
37. T. K. Bierlein and B. Mastel, Some Observations of Fission Fragment Damage in Metals, *J. Appl. Phys.*, 32(8): 1627 (August 1961).
38. Y. Quere, Freezing-In of Holes in Silver, *Compt. rend.*, 251: 367–369 (July 18, 1960); also French Report CEA-1711.
39. F. P. Botra, Influence of Neutron Irradiation on the Structure of Mo, *Fiz. Metal. i Metalloved., S.S.S.R.*, 10(2): 223–225 (1960).
40. M. Lefort et al., Réactions Nucléaires de Spallation Induites sur le Thorium par les Protons de 150 et 82 Mev, *Nuclear Phys.*, 25(2): 216–247 (May 1961).
41. P. R. B. Higgins and A. C. Roberts, Damage in Stainless Steel Due to Fission Fragments, *Nature*, 191: 1158–1160 (Sept. 16, 1961).
42. D. G. Martin, The Influence of Impurity Atoms on the Annealing Kinetics of Electron Irradiated Copper, *Phil. Mag.*, 6(67): 839–846 (July 1961).
43. K. H. Westmacott et al., Vacancy Trapping in Quenched Aluminum Alloys, *Phil. Mag.*, 6(67): 929–935 (July 1961).
44. A. I. Schindler, The Effects of Irradiation on Magnetic Properties of Alloys and Ferrites, Report NRL-5686, U. S. Naval Research Laboratory, Aug. 11, 1961.
45. A. I. Schindler and E. I. Salkovitz, Effect of Applying a Magnetic Field During Neutron Irradiation on the Magnetic Properties of Fe-Ni Alloys, *J. Appl. Phys.*, 31 (Suppl.): 245S (1960).
46. I. Ya. Dekhtyar and A. M. Shalaev, Effect of Gamma Radiation on Certain Magnetic Properties of Iron and Its Alloys, *Ukraïn. Fiz. Zhur.*, 5: 677–681 (September–October 1960).
47. G. Biorci et al., On the Nature of Radiation Damage Due to Fast Neutron Bombardment in Ferromagnetic Materials: Very High Permeability Pure Iron and Nickel, *Nuovo cimento*, 10(20): 617–637 (May 16, 1961).
48. G. Biorci et al., Effect of Neutron Bombardment on the Magnetic Properties of Very High Permeability Iron, *J. Appl. Phys.*, 31: 2046 (1961). See also *Reactor Core Materials*, 4(2): 36 (May 1961) and 4(1): 55 (February 1961).
49. R. A. Arndt and R. L. Hines, Radiation Enhancement of Bulk Diffusion in 10% Zn–90% Cu by 30-Kev Ne^+ Ion Bombardment, *J. Appl. Phys.*, 32(10): 1913–1919 (October 1961).

50. G. Weiss-Hollerwoger, Der Einfluss von Neutronenbestrahlung auf die Phasenumvandlungen in Chromstählen, *Nukleonik*, 2(6): 222–227 (1960).
51. G. Bonfiglioli et al., Electron Microscope Investigation on the Nature of Tracks of Fission Products in Mica. Technical Note No. 3, Report AFOSR-981, Istituto Elettrotecnico Nazionale Galileo Ferraris, May 1961.
52. F. P. Bowden and L. T. Chadderton, Molecular Disarray in a Crystal Lattice Produced by a Fission Fragment, *Nature*, 192: 31–34 (Oct. 7, 1961).
53. F. P. Bowden and H. M. Montaqu-Pollock, Slow Decomposition of Explosive Crystals and Their Damage by Fission Fragments, *Nature*, 191: 556–559 (Aug. 5, 1961).
54. K. Izui and F. E. Fujita, Observation of the Tracks of Fission Fragments in Molybdenite, *J. Phys. Soc. Japan*, 16: 1779 (September 1961).
55. K. Izui and F. E. Fujita, Observation of Lattice Defects in Fission Fragment-Irradiated Graphite, *J. Phys. Soc. Japan*, 16: 1032–1033 (1961).
56. A. H. Willis et al., Stored Energy in Fuel-Bearing Graphite, *J. Appl. Phys.*, 32(8): 1622–1623 (August 1961).
57. K. A. Muller, Spin Resonance in Neutron-Irradiated Graphite, *Phys. Rev.*, 123(5): 1550–1552 (Sept. 1, 1961).
58. W. Bollmann, Electron Microscope Study of Radiation Damage in Graphite, *J. Appl. Phys.*, 32: 869 (1961).
59. I. I. Myers et al., Resistivity Changes in Electron Irradiated Graphite, USAEC Report HW-SA-2207, Hanford Atomic Products Operation, 1960.
60. R. E. Strakna, Low Temperature Ultrasonic Absorption in Fast-Neutron Irradiated SiO_2 Glass, *Phys. Rev.*, 123(6): 2020–2026 (Sept. 15, 1961).
61. G. H. Vineyard, The Faraday Society Discussion on Radiation Effects in Inorganic Solids, April 11 and 12, 1961, General Introduction, USAEC Report BNL-5453, Brookhaven National Laboratory, 1961.
62. P. W. Levy, Annealing of the Defects and Color Centers in Unirradiated and in Reactor Irradiated Al_2O_3, USAEC Report BNL-5218, Brookhaven National Laboratory, 1961.
63. G. J. Dienes and A. C. Damask, Theory of Annealing of Vacancies and Divacancies in Pure Metals, USAEC Report BNL-5214, Brookhaven National Laboratory, 1961.
64. S. I. Taimuty, Proposed Reactor Radiation Damage Monitor, *Nuclear Sci. and Eng.*, 10(4): 403–404 (August 1961).
65. Vm. Agranovich and L. P. Semenov, K. peorii vlianiia oblucheniia na nekotorze svoistva grafita, *At. Energ.*, 10(6): 572–576 (June 1961).
66. I. Isuzuka, Cavity Growth by Vacancy Condensation and Transformation to Dislocation Loop in the Graphite Structure, *J. Phys. Soc. Japan*, 16: 407–413 (March 1961).
67. E. W. J. Mitchell and J. W. Whitehouse, The Refractivity and Light Scattering of Crystals Containing Defects, *Phil. Mag.*, 6(67): 947–949 (July 1961).
68. K. Kikuchi, Excitation of Heavy Nuclei by Fast Nucleons, *Nuclear Phys.*, 20: 601–613 (1960).
69. S. Amelinckx, Radiation Effects in Ionic Crystals, Belgian Report NP-9483, 1960.
70. O. Liskowsky, Radiation Effects on Al_2O_3-Al_2O_3MgO-MgO, German Report NP-10397, April 1961.
71. M. Wittenberg, Radiation Effects on CaF_2, German Report NP-10398, April 1961.
72. O. Liskowsky, Radiation Damage in Inorganic Glasses, Bibliography, 1910–1959, German Report NP-10399, 1959.
73. L. F. Porter (Comp.), Effect of Radiation on the Mechanical Properties of Steels. Bibliography, Report NP-9927, United States Steel Corp., Feb. 7, 1961.
74. Argonne National Laboratory, Reactor Development Program Progress Report, August 1961, USAEC Report ANL-6409, Sept. 15, 1961.
75. Atomic Energy of Canada, Ltd., June 30, 1961. (Unpublished)
76. Oak Ridge National Laboratory, Gas-Cooled Reactor Program, Quarterly Progress Report for Period Ending June 30, 1961, USAEC Report ORNL-3166, Aug. 28, 1961.
77. J. W. Joseph, Mechanical Properties of Irradiated Aluminum, USAEC Report DPST-60-285, Savannah River Laboratory, Apr. 21, 1960. (Classified)
78. Hanford Atomic Products Operation, Quarterly Progress Report, Fuels Development Operation, October, November, December 1959, USAEC Report HW-64863, Jan. 15, 1960. (Classified)
79. Hanford Atomic Products Operation, Quarterly Progress Report, Fuels Development Operation, January, February, March 1960, USAEC Report HW-66094, Apr. 15, 1960. (Classified)
80. J. J. Keyes, Jr., and A. I. Krakoviak, High-Frequency Surface Thermal Fatigue Cycling of Inconel at 1405°F, *Nuclear Sci. and Eng.*, 9: 462–474 (April 1961).
81. Knolls Atomic Power Laboratory, Reactor Technology Report No. 16, Metallurgy, USAEC Report KAPL-2000-13, July 1961.
82. J. F. Collins and N. McConnaughey, Iron-Chromium-Aluminum-Yttrium Alloys for Cladding Applications to 2400°F, USAEC Report APEX-681, General Electric Co., Flight Propulsion Laboratory Dept., June 12, 1961. (Classified)
83. G. Sertour, Crack Initiation and Propagation in High Strength Alloy Sheets, Report NP-10067, NATO Advisory Group for Aeronautical Research and Development, October 1960.

84. J. A. DeMastry et al., High-Temperature Niobium-Base Alloys for Sodium Cooled Reactors, USAEC Report BMI-1513, Battelle Memorial Institute, Apr. 14, 1961.
85. J. B. McAndrew and C. R. Simcoe, Hardening of Columbium by Interstitials, Final Report, March 4–December 3, 1960, Report ARF-2196-9 (AD-248580), Illinois Institute of Technology, Armour Research Foundation, Dec. 23, 1960.
86. E. S. Bartlett and F. F. Schmidt, Review of Recent Developments in the Technology of Columbium and Tantalum, Report DMIC-Memo-130, Defense Metals Information Center, Oct. 10, 1961.
87. R. W. Keil et al., Metallurgical Evaluation of Tantalum Alloys, USAEC Report LAMS-2496, Los Alamos Scientific Laboratory, Dec. 1, 1960.
88. A. S. Bufferd et al., Hard Particle Strengthening of Refractory Metals for High Temperature Use Through Internal Oxidation, Report NP-10243, New England Materials Laboratory, Inc., May 29, 1961.
89. A. G. Imgram et al., Notch Sensitivity of Refractory Metals, Report WADD-TR-60-278, Battelle Memorial Institute, September 1960.
90. R. J. Hartman and E. Macherauch, Non-Octahedral Slip in Multicrystalline Aluminum, *Z. Metallk.*, 52: 353–358 (May 1961).
91. W. S. Gibson et al., Liquidus-Solidus Relations in Iron-Rich Iron-Niobium and Iron-Molybdenum Alloys, *J. Iron Steel Inst.*, 198: 64–66 (May 1961).
92. H. J. Goldschmidt and J. A. Brand, The Constitution of the Chromium-Niobium-Molybdenum System, *J. Less-Common Metals*, 3: 44–61 (February 1961).
93. S. V. Radcliffe and H. Udin, Surface Tension of Refractory Metals, Report WADD-TR-60-566, Manufacturing Laboratories, Inc., Aug. 31, 1960.
94. E. L. Francis (Comp.), Niobium Data Manual, British Report IGR-R/R-304(Amend.), April 1961.
95. W. H. Chang, A Study of the Influence of Heat-Treatment on Microstructure and Properties of Refractory Alloys, Quarterly Report No. 5, March 1–May 31, 1961, Report NP-10351, General Electric Co., Flight Propulsion Laboratory Dept., May 31, 1960.
96. E. J. Rapperport and C. S. Hartley, Deformation Modes of Zirconium at 77°K, 300°K, 575°K, and 1075°K, USAEC Report NMI-1243, Nuclear Metals, Inc., Oct. 6, 1960.
97. M. S. Feldman, X-Ray-Diffraction Studies on Zirconium and Zircaloy-2, a Literature Search, USAEC Report DP-551, Savannah River Laboratory, May 1961.
98. C. E. May and P. D. Hoekstra, Stability of Refractory Compounds in Hydrogen Between 4500 and 5000°F, and Their Compatibility with Tungsten, Report NASA-TN-D-844, National Aeronautics and Space Administration, Lewis Research Center, July 19, 1961.
99. S. J. Rothman, Diffusion in Uranium, Its Alloys, and Compounds, USAEC Report ANL-5700(Pt. C), Argonne National Laboratory, May 1961.
100. M. J. Chapman, Permeation Rates of Hydrogen Through Metals and Ceramic-Coated Metals and Ceramics—Unclassified Bibliography, USAEC Report NAA-SR-Memo-5686, Atomics International, Aug. 13, 1960.
101. N. L. Peterson, Diffusion in Refractory Metals, Report WADD-TR-60-793, Advanced Metals Research Corp., Dec. 1, 1960.
102. L. M. Mirskii, Diffusion Processes in Alloys, Russian Translation NP-tr-686, from State Publishing House of Defense Industry, 1959.
103. W. R. Grimes et al., Diffusion of Chromium in Nickel-Base Alloys, in Nuclear Reactor Chemistry, First Conference, Gatlinburg, Tennessee, October 12–14, 1960, USAEC Report TID-7610, pp. 63–82.

Section V

Reactor Materials

Special Fabrication Techniques

Melting and Casting

The effect of processing variables (furnace pressure and feed materials) imposed during the remelting of uranium on the chemistry and yield of fuel elements fabricated from vacuum-induction-melted ingots has been scrutinized by the Feed Materials Production Center.[1] In particular, such subjects as level and distribution of impurities in the ingots, the effect of furnace pressure on yields and level of impurities in the ingots, and the joint effects of furnace pressure and feed materials on ingot impurities were studied. The following are among the more important conclusions drawn: (1) crude ingot yield varies directly with charge purity, i.e., lowered impurity in feed gives higher yields; (2) with good quality feed, good core yield varies inversely with furnace pressures; (3) the impurity content tends to vary with furnace pressure, for all pressures with a hydrogen atmosphere, above 350 mm Hg for oxygen, or above 3 mm Hg for nitrogen; (4) the effect of furnace pressure on carbon content depends on the type of feed material charged; (5) the impurity contents are higher at the center than at the edges of the ingots; and (6) a general increase in hydrogen content occurs during ingot fabrication to cores, the greatest increase being observed after the ingots are preheated in a salt bath prior to blooming. The Feed Materials Production Center also reports on efforts to develop techniques for the production of centrifugal-cast heavy-walled uranium tubes. Good tubes, 6 ft long with a maximum taper end-to-end of 0.03 in., were produced.[2]

The interest in melting processes and development of techniques remains high. A recent British patent relates to the use of a hollow electrode to introduce a flowing material into an electric-arc furnace in a manner such that a reduction, purification, or melting and consolidation operation is effected and gas is continuously removed.[3] The elements titanium, zirconium, nickel, beryllium, molybdenum, tungsten, silicon, and selenium were cited as examples of materials appropriate for this type processing.

Knolls reports on two activities relating to elimination of intermediate steps in the production of zirconium and hafnium metal.[4] For zirconium, the elimination of the drip melting step was attempted. Although an expected reduction in final ingot cost of 3 to 5 per cent was envisioned, an increase of about 5 per cent has been experienced, mainly due to the low yield encountered. Other problems, particularly in handling, met in this endeavor were introduced by the presence of the metallic sodium before (in sponge) and after (in furnace) melting.

The production of hafnium metal meeting rigid properties specifications usually includes a so-called crystal-bar step (iodide decomposition) to attain the purity required. An attempt to eliminate this process step in the interest of scheduling and cost was not successful, again due in part to low yield. This low yield stemmed mostly from hardness variations within ingots, which were responsible for fabrication difficulties. The variations in hardness were due to variable oxygen content of the sponge feed. Some optimism is still held for the elimination of the iodide step if sponge oxygen content can be controlled.

Of general interest in the arc melting of refractory metal is a report by LaMarche dealing with efforts to develop tungsten alloys for rocket nozzles.[5] Among the results cited were a measured temperature of 10,000 to 11,000°F for a tungsten arc, distribution of heat up to 17 to 1 between anode and cathode of a consumable electrode with a d-c straight (electrode nega-

tive) polarity, and the direct relation between the purity of the tungsten and its ability to be vacuum arc melted.

Research into the use of electron beam in the melting of material continues active due to its capacity for obtaining high temperature in low pressures. Studies of the ability of EBM (electron-beam melting) to purify or alter the properties of boron, boron-carbon alloys, boron-silicon alloys, tantalum carbide, titanium carbide, zirconium diboride, hafnium, tungsten, cobalt, vanadium, and beryllium were reported by Martin et al.[6] In addition, studies of the effects of deoxidation by additives to beryllium, vanadium, cobalt, and molybdenum were noted. In the attempts to melt compounds, the products were either brittle or could not be melted. For metals, the interstitial content was reduced. With the addition of deoxidants, the interstitial content of molybdenum and beryllium was reduced. In this same manner the tensile properties of vanadium and molybdenum were improved. (E. L. Foster, Jr.)

Fabrication and Heat-Treatment

Bridgeport Brass reported on studies of the effect of temperature and grain structure on the formability of uranium.[7] The formability of fine-grained (as extruded) and coarse-grained (beta or gamma annealed) uranium samples was tested on a drop-hammer impactor in the alpha- and beta-phase temperature ranges (25 to 750°C). The experimenters concluded that: (1) the equicohesive temperature (ECT), where the deformation resistance of fine-grained and coarse-grained uranium is equal, is below the recrystallization temperature; (2) the deformation resistance of fine-grained uranium is lower than that of coarse-grained uranium in the hot-work range (above the ECT); (3) the formability of beta uranium is equivalent to alpha uranium in the range of temperature between 200 and 300°C; (4) data from the hot hammer tests can be used to estimate the extrusion resistance of uranium having a variety of grain structures; (5) the surface quality of formed uranium depends to some extent on the grain size of the uranium stock; and (6) the impacting of uranium held in the beta temperature range produces some grain refinement.

Interesting in the working of metals was a report on a technique developed in Scotland by Watkins et al. for determining the temperature distribution set up inside a metal slug during extrusion.[8] Using lead, copper, aluminum, and 70/30 brass, they found that the major factors in the rise of temperature in the metal slugs during extrusion were reduction and punch speed.

The fabrication of rare-earth metals was the subject of research at Knolls[4] in which small cast ingots of samarium, europium, gadolinium, dysprosium, and erbium were rolled into narrow strips of 50- and 100-mil sheet. Although no information on the purity of the rare earth was cited, the material could be considered typical, or better than typical, of the available grades. All of the five lanthanons were worked by techniques now considered standard for reactive metals. Samarium, gadolinium, and erbium could be hot worked, and about 10 per cent cold work could be imposed before any cracking was noticed. Attempts to anneal the cold-worked strip were unsuccessful (due apparently to the need for extremely slow cooling rates). Dysprosium was cold worked to about 38 per cent before annealing was required, and europium was capable of withstanding an unlimited amount of "cold work" (suspect recrystallization below room temperature). In addition to the protection required for reactive metals during fabrication, europium was also protected from room-temperature oxidation by immersing it in high-grade paraffin oil between fabrication steps.

A state-of-the-art survey concerned with the technology of, and extrusion practices for, tantalum-base alloys was completed.[9] This summary was the first phase in a broad study designed to further refractory-metal technology. From the limited number of tantalum-base alloys for which data exist, the tantalum–10 wt.% tungsten alloy was chosen for further study of differences in as-cast and wrought materials. On the basis of findings of the survey, a duplex melting practice was recommended, consisting of electron-beam melting followed by consumable-electrode arc melting.

Three compilations worthy of note, in that they provide a convenient reference for fabrication information, were published recently. The Office of Technical Services was responsible for two volumes[10,11] on *Metal Working*, covering casting, forging, rolling, drawing, and extrusion. Also, the AEC published a literature

survey on the extrusion of uranium, uranium alloys, and uranium compacts.[12] Unclassified reports listed in *Nuclear Science Abstracts* for the period 1951 to May 31, 1961, were used as the source. (E. L. Foster, Jr.)

Cladding

Cladding by Rolling and Swaging

Major emphasis this quarter was placed on roll bonding of fuel-element assemblies. Interesting work was reported on drawing of duplex tubing for reactor applications. Reports on swage cladding were many but dealt entirely with densification of UO_2. No significant advances were noted in this area.

Process specifications for the roll bonding of fuel elements for the Organic-Moderated Reactor Experiment (OMRE) third core loading were published by Atomics International,[13] and Battelle described the procedure necessary for the roll cladding of SM-2 type irradiation specimens.[14] These fuel systems are both stainless-steel-clad stainless steel–UO_2 dispersions.

As a result of some diffusion studies using vacuum hot-pressing techniques, Atomics International is studying the roll bonding of a niobium-clad uranium–10 wt.% molybdenum fuel system.[15] The hot-pressing studies indicated that good core-to-cladding bonds could be obtained at 1550°F. Experimental fuel plates were roll bonded in an evacuated mild-steel pack from 1550°F with a 3:1 reduction. Examination revealed a partial bond between the core and cladding, but niobium self-bonds were good. It was concluded that spotty bonding in the core was due to impurities in the material. (H. D. Hanes)

Pressure Bonding

The process that involves the use of gas pressures at elevated temperatures to produce bonds has been termed pressure bonding, gas-pressure bonding, or hot isostatic pressing. This process is currently being used to bond or clad numerous similar and dissimilar metals, ceramics, cermets, and composite systems. It is also being employed to compact metallic, ceramic, and cermet materials under a hydrostatic gas pressure at elevated temperatures.

A detailed survey[16] of the field of gas-pressure bonding has been issued by the Defense Metals Information Center (DMIC). In this report the gas-pressure-bonding process and many of its applications for cladding, joining, and densification of numerous metallic and ceramic materials are described. Included are photomicrographs, photographs, and references to research performed at various installations.

Preliminary studies conducted at Battelle on the bonding of beryllium-clad UO_2 fuel elements have been summarized in a topical report.[17] In these studies, gas-pressure bonding was investigated as a fabrication technique for the solid-state bonding of beryllium. Bonding parameters, surface-preparation methods, and compatibility of beryllium with UO_2 and with several container and barrier materials were studied. It is reported that beryllium-to-beryllium bonds were obtained after 2 to 4 hr at 1550 to 1650°F at 10,000 psi. Bonds produced with grit-blasted and abraded surfaces exhibited recrystallization of grains at the original interface. The interface did not appear weaker than the parent metal during limited mechanical testing. It was also found that chromium or pyrolytic carbon coatings on UO_2 cores prevented significant UO_2-beryllium reaction during bonding for 4 hr at 1650°F and at 10,000 psi. Reaction products formed on the beryllium surface during compatibility experiments with other materials were easily removed by acid pickling.

Fabrication of instrumented fuel plates of the SM-1 type designed by Alco Products utilizing the blocked-channel method of plate instrumentation has been developed by use of the gas-pressure-bonding process at Battelle.[18] Two such instrumented plates will be contained in an instrumented fuel-element assembly and will occupy the same space as three standard fuel plates and two water channels in the SM-1. The plate consists of a low-cross-section Zircaloy-2 filler plate which is contained in a type 304L stainless-steel picture-frame jacket. To prevent any eutectic reactions between the Zircaloy-2 and stainless steel during the bonding cycle, niobium strips 20 mils thick were employed as a barrier. This assembly was covered on top and bottom with SM-1 type fuel plates of one-half standard thickness, each of which embodied a 3-mil barrier layer of niobium to prevent Zircaloy-iron eutectic formation during bonding. Gas-pressure bonding of the composite was accomplished at 2100°F and 10,000 psi for 3 hr.

The topical report by Sylvania[19] on stainless-steel-clad UO_2 fuel elements made by gas-pressure bonding (hot isostatic pressing), reported in process in the last Review, has been issued. In this study, 100 per cent fused UO_2 powder was consolidated in a stainless-steel tube by tamping, sonic vibration, or ultrasonic vibration and was then further densified by gas-pressure bonding at temperatures up to 1250°C. Resulting core densities of 87 to 90 per cent of the theoretical density and mechanical bonds between the ceramic core and the metal cladding were obtained.

The study of gas-pressure bonding of ceramic fuel elements by Battelle[20] for the AEC Fuel Cycle Program is being continued with three major areas of research. The first area involves the fabrication of UO_2 fuel elements by direct pressure bonding for irradiation testing in the Vallecitos Boiling-Water Reactor (VBWR). Four full-scale VBWR fuel rods consisting of UO_2 clad with stainless steel have been gas-pressure bonded for this test. The other two areas of research are cooperative programs with Hanford and with Gladding, McBean & Company. In these programs, studies have been initiated to evaluate the gas-pressure-bonding process as combined with vibratory-packing techniques and the UO_2 sheet-rolling techniques.

The basic investigation of the mechanism of pressure bonding and factors affecting it is being continued.[20] This Battelle study is concerned with the effect of temperature, pressure, time, grain growth, impurities, and surface roughness on the bonding mechanism. A topical report[21] has been issued on the first phase of the program and describes extensive studies made principally using copper. In this investigation the basic mechanism of the solid-phase bonding of two components under the application of heat and pressure has been established. For a metallurgically sound bond, i.e., no discontinuities or changes in the structure in the bond region, the first requirement is the application of sufficient pressure to place the surfaces in intimate contact. For copper, it was found that the pressure required could be related directly to Meyer hot-hardness values. Grain growth across the bond interface, and thus elimination of the interface, has been found to be dependent on the presence or absence of microvoids in the bond region. Microvoids can be created during bonding by insufficient flow of metal or by condensation of excess vacancies at impurity nuclei. At high temperatures the driving force to straighten the irregularly shaped interface is sufficient to provide grain growth across the bond region if there are only a few microvoids. Decreasing the number and size of microvoids to a level permitting grain growth depends on the availability of vacancy sinks in the metal. In copper the most effective sinks were found to be grain boundaries. If the number of microvoids is large, grain growth can occur only if the grain size is smaller than the size usually existing at that temperature or if recrystallization or an allotropic transformation occurs during bonding. The mechanism is now being studied in more detail and in other metals.

(E. S. Hodge)

Diffusion Bonding

The study of the fundamentals of diffusion bonds between dissimilar metals has been continued by Castleman and coworkers, and their Sixth Annual Progress Report has been issued.[22] As reviewed here in 1960, emphasis in this study has been on the effects of pressure on the kinetics of growth of intermetallic layers in binary diffusion couples. It has been found recently that pressure diminishes beta-brass layer growth in saturated alpha-brass versus saturated gamma-brass diffusion couples, both above and below the critical transition temperature for ordering. The effect of pressure is reported to be less in the ordered temperature range. Refinements in experimental procedures have permitted some corrections to be made in the data reported in last year's progress report for this copper-zinc system. An attempt by the authors to apply to this system a proposed method for determining chemical diffusion coefficients at the interface boundaries of an intermetallic phase from measurements of the interface displacements has not been successful. Their results indicate that available techniques for measuring the concentration gradients at the interfaces, specifically the presently available electron-probe-microanalysis techniques, are not sufficiently accurate in these regions. Disagreement found between interface displacement values obtained experimentally and by theoretical calculations is attributed by the authors to relatively large variations in the chemical diffusion coefficient in the immediate vicinity of the interfaces.

Further consideration is being given to this interface situation in their present work.

In this study the investigation of the aluminum-uranium system has also been continued. It has been found that the growth of the UAl_3 intermetallic layer, contrary to expectation, is not diminished in the pressure range of 10 to 100 tsi. An argument is advanced, based on the activation volume concept, that the aluminum ions diffuse in UAl_3 by an interstitial mechanism. An exploratory study of layer growth in copper-gold diffusion couples has been discontinued because of the extremely slow growth rates. In future work the investigators plan also to study the kinetics of layer growth in ternary systems, a field that is markedly interesting, difficult, and unexplored. It should also be noted here that a basic study of the mechanism of pressure bonding of similar metals[20,21] which is being conducted is discussed above under the heading "Pressure Bonding."

Through metallographic and X-ray-diffraction techniques, the diffusion zones that occur in aluminum-nickel-uranium bonds in nuclear fuel elements have been identified.[23] In this study reported at the recent National Metal Congress in Detroit, identification of the zones was accomplished by correlating their appearances with those of similar zones developed in diffusion couples. Four zones were identified: Al_3Ni, Al_3Ni_2, U_6Ni, and UNi_5. The limiting factor in the quality of the bonds was reported to be the presence of an unidentified oxide within the uranium-nickel portion. When this oxide occurred as a continuous layer, bond strength averaged less than 10,000 psi. Furthermore, the bond corroded rapidly in pinhole tests. However, when the oxide occurred as dispersed particles, it was found that the bond strength was greater (averaging over 15,000 psi) and that the corrosion resistance was much better.

(D. C. Carmichael)

Electroplating

Resistance to wear and galling of nickel-chromium-iron alloys such as Inconel was improved by chromium plating. A new specification (KAPL-S-3083, "Chromium Plating for Service in Pressurized-Water Vessels") was prepared by Knolls Atomic Power Laboratory to require electroplaters to adopt the necessary techniques for producing satisfactory deposits. Sleeves electroplated at four independent sites failed to meet thickness requirements because of improper anode design, inadequate use of "thieves," or some other improper procedure capable of being corrected.[24]

Important steps in improved procedures identified at Battelle[25] for electroplating thorium and uranium to increase corrosion resistance include the following:

1. Removal of 3 to 4 mils from the surface of thorium or uranium by electropolishing
2. Anodic etching in hydrochloric acid solution for thorium or in a phosphoric-hydrochloric acid solution for uranium
3. Pickling in a nitric deoxidizer solution to remove smut
4. Making electrical contact to the thorium before immersion
5. Adding a leveling agent to the nickel bath to promote pore filling by the nickel plate
6. Outgassing at 500°F to remove hydrogen
7. Electroplating 2 mils of nickel plus 0.03 mil of chromium

Thorium specimens plated with these steps resisted corrosion for more than 600 hr in water-saturated air at 200°F and for more than 2000 hr in a warehouse at Daytona Beach. Uranium specimens resisted corrosion for more than 400 hr in water-saturated air at 200°F. Specimens that were not outgassed showed blistering after less than 150 hr. Early-stage blistering in the case of thorium specimens not outgassed after plating occurred within the thorium. While outgassing, the temperature had to be raised slowly to permit gradual diffusion outward. Soldered joints prepared with lead-tin alloy withstood corrosion when the nickel-plated surfaces were plated with copper and tin before soldering.

The most protective of several electroplated cermet coatings on molybdenum heated to 2000°F was a 5-mil nickel coating containing particles of zirconium oxide.[26] Oxidation of molybdenum with this coating was first observed after 408 hr, whereas a 5-mil nickel electroplate protected molybdenum for only 35 hr. At 2500°F, a cermet of nickel and silica particles protected molybdenum for 5 hr. To prepare such coatings, oxide particles up to 3 μ in diameter were dispersed by air or centrifugal agitation in conventional Watts type nickel baths. Cermets of chromium, cobalt-tungsten alloy, platinum, and rhodium were prepared analo-

gously. An electrophoretic effect is believed to be responsible for the inclusion of a large amount of aluminum, silicon, and zirconium oxide particles in the cathode deposits. Weight-change data indicate a lower oxidation rate for some of the cermet coatings as compared with electroplates containing no refractory oxide particles.

Sintered uranium oxide can be electroplated with copper, nickel, silver, or gold as dense coatings free of visible pores with a thickness of only 5 μ (0.0002 in.), according to the results of experiments at Chalk River.[27]

Polycrystalline deposits of uranium oxide on cathodes in fused-salt mixtures were described by Hanford personnel as being of good quality.[28] With mixtures of lead and potassium chlorides, bath temperatures from 500 to 750°C were studied. Single crystals as long as 8 mm were formed in melts of potassium and sodium chlorides. A crystal density as high as 98 per cent of the theoretical UO_2 density was observed. Density was influenced by the atmosphere over the melt.

A recent patent[29] claims that films of Np^{239} can be deposited on the cathode in either aqueous or ethereal solutions. Polonium has been electrodeposited in films described as suitable for an intense source of alpha particles, from hydrofluoric acid solutions.[30]

Uranium, beryllium, zirconium, and several other metals can be electrolytically precipitated in a finely dispersed metallic form in a mercury cathode. The electrolyte is a mixture of a fused-salt eutectic of alkali and alkaline-earth halides and uranium (or other recoverable metal) halide.[31]

A method for preparing uranium for plating with other metals, which was patented, includes an anodic treatment for 30 sec to 15 min with a current density of 60 to 100 amp/sq ft in an aqueous solution containing 10 per cent polycarboxylic acid (preferably oxalic acid) and 1 to 5 per cent hydrochloric acid.[32]

(W. H. Safranek)

Nonelectrolytic Chemical-Plating Techniques

The use of chemical-vapor-deposition techniques to produce high-purity metals, refractory-metal compounds, and coatings on both metallic and nonmetallic bases was reviewed by Schultze.[33] A discussion of current commercial applications and future potential of the process also was presented. Investigation of the preparation of ultrapure molybdenum by reduction of the chloride was continued at the Alloyd Corporation.[34] Powdery deposits, consisting of a mixture of fine, pyrophoric molybdenum and lower chlorides, were obtained.

Graphite surfaces can be coated[35] with nickel by exposure to an atmosphere of nickel carbonyl and heating to 200 to 500°C. The nickel-coated surfaces subsequently are joined to each other or to other metal surfaces by brazing. A process was described for coating various materials in powder form by hydrogen reduction of solutions[36] containing nickel. Surface activation is required for noncatalytic powders. Test coupons of uranium-molybdenum alloy were successfully coated with niobium by hydrogen reduction[15] of NbCl. Flash coatings of nickel and copper were employed to protect the alloy from atmospheric attack. Use of nickel led to localized eutectic melting with uranium.

The metallizing of ceramics with titanium and zirconium by thermal decomposition of the respective hydrides at temperatures near 900°C was reviewed.[37] The coating of beryllia and beryllia-tungsten nozzle inserts with tungsten was investigated.[38] Six graphite nozzle inserts, three of which were precoated with rhenium, also were coated with tungsten.

Interest in pyrolytic carbon and its modifications as new construction materials continues to expand. "Hard" carbon layers can be deposited on graphite by pyrolysis of volatile hydrocarbons.[39] Smooth layers result which are not graphitized but can be graphitized by heating in vacuum at 2300 to 2400°C. The thickness and uniformity of pyrolytic graphite coatings are extremely sensitive to gas dynamics in the deposition zone.[40] Studies were made of the effects of gas dynamics, substrate geometry, and surface finish using a standard cylindrical substrate that was 1 in. in inside diameter. An atmosphere consisting of 2.5 to 7 vol.% methane with an inert diluent was used at a flow rate of 20 scfh at temperatures near 2000°C. Deposition rates of 4 to 15 mils/hr were achieved. Experimental difficulties encountered in preparing thick deposits of pyrolytic graphite for scaled-down model studies indicated that inserts 0.100 in. thick would give less trouble than inserts 0.150 in. thick.[41,42] This result is a direct consequence of the low interplanar shear strength and lack of ductility of pyrolytic graphite at low temperatures, which render it sus-

ceptible to cracking when the ratio of thickness to radius of curvature exceeds a critical value.

In continuing studies at High Temperature Materials, Inc., on the formation of NbC and TaC coatings,[43] a 27-sec test life was obtained for an NbC-coated specimen. Difficulties encountered with cracked or buckled coatings were eliminated by development of a carbide with a metal-to-carbon ratio higher than stoichiometric. Such a carbide has greater high-temperature ductility and an improved rupture strength that increases linearly with excess metal content.

The deposition of the refractory oxides Al_2O_3, BeO, and ZrO_2 by vapor-phase chemical reactions is particularly useful for a number of nuclear applications. Alumina is formed by the reaction[44]

$$2AlCl_3 + 3H_2 + 3CO_2 \rightarrow Al_2O_3 + 3CO + 6HCl$$

Deposition conditions include: 0.5 liter/min gas flow with $H_2:CO_2 = 10:1$ to 8:1 (by volume); $AlCl_3$ volatilization rate, 50 g/hr at 15 per cent utilization; deposition rate, 0.18 g Al_2O_3/hr; deposition time, 1 hr; work surface temperature, 1120°C.

Diffusion coatings, applied by pack methods, as well as by straight vapor-deposition methods, were investigated by numerous industrial laboratories. One review article[45] discussed the parameters involved in coating metallic materials by substitutional and interstitial diffusion using metal halides. The various exchange reactions were described, and the kinetics and thermodynamics of the diffusion process were examined. A broad study of pack diffusion was made[46] which covered the use of halides of 15 metallic elements and 3 nonmetals. Coating processes studied included boronizing, chromizing, and siliciding, with by far the greatest emphasis on siliciding.

Use of a 1:4 (parts by volume) mixture of BCl_3 and hydrogen at 900°C for periods up to 10 hr was described as a means of securing boron-enriched surfaces on nickel.[47] The limiting factor of the process is the diffusion of boron atoms from the gas phase to the surface of the metal. The rate of coating formation was independent of the BCl_3 concentration for $BCl_3:H_2$ ratios between 1:4 and 1:10. A three-layer coating is obtained, the outer layer of which has a hardness of 1700 kg/mm^2.

An up-to-date survey of chromizing processes has been presented.[48] An article by Sprinz and Wachtel[49] described the use of a proprietary process for protecting molybdenum from oxidation. Siliconizing of steel, although an older process, still is of interest.[50] Formation of a silicide coating on tungsten in a pack consisting of 90 per cent 325-mesh silicon powder and 10 per cent NaF at 1050°C with an external, but permeating, hydrogen atmosphere was reported.[51] A coating rate of 4 mils in 16 hr was obtained. Sodium fluoride losses, by volatilization, amounted to 50 wt.%. No satisfactory diluent for the pack has been found. The variables for scaleup of a laboratory process designed to yield a 2- to 3-mil, oxidation-resistant silicide coating for molybdenum are under study by the Pfaudler Company.[52] The siliconizing pack contained a small amount of niobium powder as well as the silicon source material. Alloy specimens of vanadium–5 wt.% titanium–20 wt.% niobium were silicided in a silicon powder pack[53] activated with KF, NaF, or NH_4Cl. Coatings formed with alkali-metal fluoride activators were 0.0005 to 0.001 in. thick. In other work,[54] coatings of silicide, aluminum-modified silicide, and boron-modified silicide were applied to tantalum–10 wt.% tungsten alloy specimens by a two-cycle pack-cementation process at 1200°C. The use of coarse (5-mil) Al_2O_3 as a pack diluent led to slightly increased coating formation rates and improved protective lives at 1480°C. A manganese-modified silicide coating was exceptionally protective at 1480°C. This coating was formed by siliconizing manganese-coated tantalum.

In a review of recent developments in the field,[55] attention was called to the formation of coatings in a fluidized-bed process. The specimen is supported in a heated fluidized bed of silicon into which volatilized iodine flows. Other investigations were primarily concerned with duplex coatings, applied by pack methods. Such coatings include (1) a silicide layer overcoated with chromium-boron or chromium-aluminum or (2) an undercoat of chromium or chromium-aluminum overlaid with silicon, silicon-chromium, or silicon-chromium-aluminum.

(E. M. Sherwood)

Ceramic Coatings

Ames Laboratory[28] found that a frit composed of 71.0 wt.% SiO_2, 5.8 wt.% CaO, 18.8 wt.% Na_2O,

and 4.4 wt.% TiO_2 with 15 wt.% Cr_2O_3 formed an adherent protective enamel on yttrium when fired in air for 1 or 2 min at 1025°C.

(B. W. King)

Explosive Forming

A program has been conducted to determine the feasibility of explosive forming refractory metals, particularly molybdenum and molybdenum–0.5 per cent titanium.[56] Several tests were run using different types of explosives and various weights of charge. The optimum weight of charge of a given type of explosive required to form a specific thickness of these materials was determined during these tests. These data are shown in Table V-1.

Table V-1 OPTIMUM CHARGE FOR FORMING MOLYBDENUM[56]

Material		Explosive	
Type	Thickness, in.	RDX, g	15% dynamite, g
Pure Mo	0.010	15	35
Mo–0.5% Ti	0.010	25	35
Pure Mo	0.020	30	50
Mo–0.5% Ti	0.020	30	45–50
Pure Mo	0.040	40–45	70
Mo–0.5% Ti	0.040	35	70

Various transfer media, including water, 325-mesh powdered alumina, 140-mesh glass beads, and synthetic mica, were also tested. Of these materials, the best results were obtained with water. However, water possesses obvious temperature limitations. The temperature of the workpiece during forming was varied from ambient to 1000°F in 200°F intervals. It was found that, as the forming temperature was increased, the results obtained improved.

The data obtained during these tests revealed that greater elongation and formability in molybdenum and a molybdenum–0.5 per cent titanium alloy can be achieved by explosive forming than by conventional forming methods. The maximum elongation was obtained at a strain rate of 0.7 to 0.9×10^7 μin./(in.)(sec). These materials were, however, found to be very susceptible to "notch effect," and extreme care must be taken in their fabrication to avoid scratches and scribe lines where elongation of the metal is required.

Tests were also conducted on tungsten during this program. The results of these tests revealed that as the rate of strain was increased the per cent elongation (and hence formability) increased.

A program is presently being conducted to determine the optimum strain rate to be used for the explosive forming of specific refractory metals.[57] Also included in this program will be the determination of the most suitable transfer media for achieving maximum formability and the effects of temperature up to a maximum of 1000°F.

The materials to be tested during this program are (1) arc-cast molybdenum–0.5 per cent titanium, (2) tungsten, (3) columbium alloy Cb-74, and (4) columbium alloy CT-2WZ. Both unidirectional tests in a trough die and multidirectional tests in a cup die will be conducted. Draw rings will be used in these tests since draw-ring pressure is thought to be of the utmost importance. The types of explosives to be used during this testing are RDX and 40 per cent dynamite. The testing temperature will be held constant at 1000°F, whereas the draw-ring pressure will be varied. The transfer media to be tested will be selected according to forming characteristics and price.

Strict dimensional control of both types of tubing was easily achieved, with the values consistently being held to 0.003-in. variations. The surface quality of both types of tubing, in the absence of excessive banding, was considered satisfactory. In most instances defects were difficult to detect.

A program is presently being conducted to develop the basic high-energy-rate extrusion operation for steel and titanium and to evolve a process for manufacturing extrusions of the materials equivalent to those normally supplied by industry.[58]

Grease and graphite were used as lubricants in these tests; however, they were found to be satisfactorily effective only when extruding aluminum. Many of the extrusions produced were scored and, in some instances, fused to the entry cones of the dies. Glass compounds, applied to the billet prior to heating, may be found to provide adequate lubrication.

Aluminum was extruded at billet temperatures ranging from ambient to 150°C and at fire pressures ranging from 300 to 400 psi. As was anticipated, the shear orifice produced the longest extrusion in each case.

Billets of AISI 1020 steel were heated to 900 and 1100°C and extruded at 500- and 800-psi fire pressure. The relative ram velocity and energy for these fire pressures are: for 500 psi, 33 ft/sec and 22,000 ft-lb; for 800 psi, 46 ft/sec and 45,000 ft-lb. When extruding under these conditions, 90° and 120° orifices produced the longest extrusions. AISI 4340 and type 304 stainless steel behaved in a manner similar to that of AISI 1020 steel during high-energy-rate extrusion.

The billets of a 6 wt.% aluminum–4 wt.% vanadium–90 wt.% titanium alloy proved to be quite difficult to extrude. It was found that an extrusion temperature of 900°C produced cracked extrusions, whereas 1000°C did not. A billet that was heated to 1100°C and extruded at 800-psi fire pressure through a 90° orifice produced a long extrusion. A method that is described in this report has been devised to determine the energy developed by the Dynapak when various combinations of fire pressure, backpressure, and stroke length are employed.

Electrodeposited crystals of approximately −28 +48-mesh UO_2 and −6-mesh UC have been compacted by high-energy impact at 500,000 psi and 1100 and 1200°C to 99.2 and 97.4 per cent of theoretical density, respectively.[59] A machinable solid was produced with the UC.

Tests have been conducted for the purpose of defining the roles of temperature, pressure, and oxygen-to-uranium ratio on the high-energy impacting of UO_2. Preliminary results indicate that (1) temperature has very little effect in the 1000 to 1200°C range at 500,000 psi; however, as pressures are decreased and oxygen-to-uranium ratios are increased, the tendency is toward higher densities with increasing temperature; (2) higher oxygen-to-uranium ratios (in the range studied, 2.01 to 2.26) in the starting material produce greater densities; and (3) a pressure of about 400,000 psi is required to compact uranium oxide to 99 per cent of theoretical density.

A study is presently being conducted to determine the feasibility of employing explosive techniques for achieving a mechanical or metallurgical bond between Zircaloy-2 and type 410 stainless steel.[60] Initial studies were conducted with $2\frac{1}{2}$- by $2\frac{1}{2}$-in. flat-plate assemblies for the purpose of determining the optimum surface preparation and charge density required to produce a sound bond. The results of this initial study were then used as a basis for conducting a series of tests using mockup tubular components of mild steel and aluminum approximating those of the CANDU configuration. Bonding was achieved during this testing by employing a combination of the roll-forming and explosive-joining techniques. A photomicrograph of the bond produced is shown in Fig. V-1.

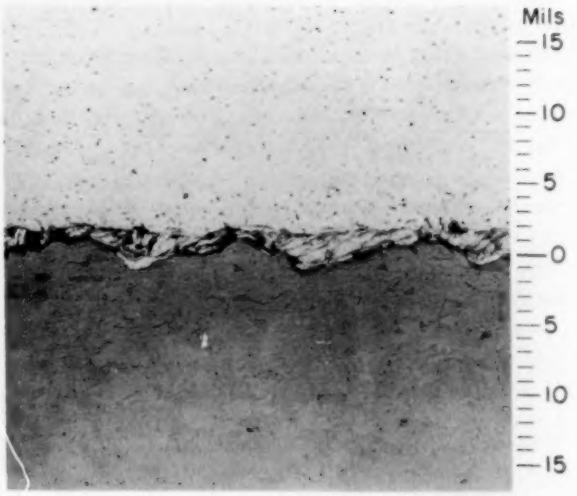

Fig. V-1 Interface of mild steel (bottom)-to-aluminum (top) joint produced by a combination of roll-forming and explosive joining.[60]

(C. C. Simons)

Welding and Brazing

A comprehensive study of the mechanical properties of Zircaloy-2 weld metal has been made at Knolls.[61] Tensile, strain-fatigue, and creep-rupture properties of weld metal deposited by the consumable-electrode inert-gas-shielded (MIG) process were determined. It was found that weld-metal properties were essentially the same as corresponding base-metal properties. Therefore base-metal properties can be used in design calculations for weld metal. However, this conclusion should be limited to the properties investigated. In particular, the bend ductility of Zircaloy-2 weld metals is usually lower than that of base plate.

A patented method of bonding aluminum involves the use of silicon powder.[62] The powder is placed between the joint surfaces, which are then moved relative to each other. The abrasive action of the powder breaks up the oxide surface on the aluminum. Subsequent application of heat and pressure produces a bond.

Table V-2 RESULTS OF BRAZING STUDIES ON NIOBIUM T-JOINTS[64]

Composition of brazing alloy,* wt.%	Flow point, °C
67 Zr–29 V–4 Fe	1300
60 Zr–25 V–15 Cb	1280
48 Zr–48 Ti–4 Be	1050
63 Ti–27 Fe–10 Mo	1250
63 Ti–27 Fe–10 V	1280
68 Ti–28 V–4 Be	1250
45 Ti–40 Zr–15 Fe	1050
75 Zr–19 Cb–6 Be	1050
80 Zr–17 Fe–3 Be	1000
46 Ti–46 Zr–4 V–4 Be	1000
95 Zr–5 Be	1000
62 Ti–26 Fe–8 Mo–4 Zr	1250

*All alloys exhibited excellent flow and no cracking.

An investigation is being made by Aeroprojects of the use of ultrasonic welding for cladding plate type elements.[63] Only preliminary results have been obtained using a higher energy (5 kw) ultrasonic unit. The experiments involve attempts to bond X8001 aluminum sheet or foil to cores consisting of a U_3O_8 dispersion in X8001 aluminum.

Development of brazing alloys for niobium at Oak Ridge has progressed to the selection of the compositions shown in Table V-2 for further study.[64] These alloys survived theoretical and experimental screening for favorable behavior, based on the following four requirements:

1. Melting point between 1000 and 1300°C
2. Good flowability
3. Freedom from compound formation with niobium
4. Good corrosion resistance in liquid metals

The effects of interstitial carbon, nitrogen, and oxygen on the bend ductility of welds in niobium and tantalum are being studied by the Bureau of Mines.[65] Sixteen niobium ingots containing from 130 to 710 ppm carbon, <10 to 90 ppm nitrogen, and 410 to 860 ppm oxygen were processed to weldments. All the welds had satisfactory bend ductility. Generally the weld metals exhibited a loss of carbon and an increase in nitrogen. Similar tantalum ingots contained from 10 to 1700 ppm carbon, 120 to 730 ppm nitrogen, and 180 to 880 ppm oxygen. Weldments prepared from these alloys generally had poor bend ductility if the carbon was higher than 90 to 150 ppm. However, since all three interstitial elements were not varied individually, it is not possible to establish this limit or limits on nitrogen or oxygen accurately. Further studies are in progress.

Another study of tantalum welding has been completed at Los Alamos.[66] Resistance seam welds were made in 0.020-in.-thick sheet from three heats of tantalum-tungsten alloy material. Both as-rolled (cold worked) and annealed sheet were used. Some copper pickup from the electrodes was observed when welding the as-rolled sheet, but no copper pickup occurred in welding the annealed sheet. The welded overlap area was 10 times as large as the base-metal area. The results of tension tests and metallographic examinations are shown in Table V-3. Annealing before or after welding had little effect on the weld strength observed. (R. E. Monroe)

Nondestructive Testing

Ultrasonic Techniques

Symposia such as the Symposium on Physics and Nondestructive Testing held at Argonne National Laboratory[67] on October 4 and 5, 1960, can be of considerable value to persons con-

Table V-3 CHARACTERISTICS OF RESISTANCE SEAM WELDS IN TANTALUM-TUNGSTEN ALLOYS[66]

Nominal tungsten content, wt.%	Condition	Approximate tensile strength, psi	Bond appearance
0.1	As rolled	68,600–72,300	No apparent bond
0.1	Annealed (1500°C, ½ hr)	41,400–51,300	No apparent bond
0.1	As rolled	85,500–89,800	Some evidence of good bonds
0.1	Annealed (1500°C, ½ hr)	46,700–55,200	Some evidence of good bonds
3.0	As rolled	104,700–106,100	No apparent bond
3.0	Annealed (1300°C, 1 hr)	57,700–61,100	No apparent bond

cerned with nondestructive testing. The five papers on ultrasonics which appear in the proceedings of this meeting are fine reference material.

Various investigators have considered the use of ultrasonic pulses of almost rectangular envelope resulting in the simultaneous transmission of a wide band of ultrasonic frequencies in ultrasonic testing. When and if a suitable system is developed, it should be very useful not only in the field of nondestructive testing but also for other applications of ultrasonics.

Maguire of Watertown Arsenal[68] claims that, with square input pulses, either the contour of the reflected ultrasonic pulse or a spectrum analysis of the ultrasonic energy reflected from cylindrical flaws will distinguish between flaws of various diameters. The response of the transmitting transducer is from 5 to 90 Mc/sec. The rectangular pulses are 0.1 μsec long, and the repetition rate is 500/sec. Morris of National Lead[69] found that the square "short-pulse" technique can be used to evaluate the quality of the bond between two interfaces from the shape of the returned signal.

In fundamental studies involving attenuation measurements in liquids and other materials over a range of frequencies, a single measurement using the square-pulse technique could conceivably replace a long, laborious study, as the one now in progress at Hanford[70] to ultrasonically analyze Zircaloy-2 samples for hydride over a wide range of frequencies. Although present methods of determining grain sizes seem to be adequate, the use of square waves might result in even more accurate data.

Libby of Hanford reports[69] that "Ultrasonic pulses have been generated and detected in nonmagnetic metals by electromagnetic means. The pulses are generated using a send coil driven by a hydrogen thyratron at one end of the sample, and detected at the opposite end by a coil in a magnetic field." No elaboration was given regarding the practical application of this technique.

In work at Argonne[71–73] which compares shear waves and Lamb waves to detect transverse outside surface flaws, the amplitude of response is approximately the same whether the angle of incidence is that necessary to generate shear waves or Lamb waves. This is believed to be because the phenomenon used is neither shear nor Lamb waves but direct reflection from the defective surface; thus there appears to be no advantage in using Lamb waves when looking for outer surface defects. In cases where internal defects can be located by both shear waves and Lamb waves, the amplitude of the received signal is always greater with Lamb waves than with shear waves. In this work, Argonne has found that Li_2SO_4 transducers are more satisfactory than quartz. This is in agreement with the growing acceptance of Li_2SO_4 as a transducer material. (D. Ensminger)

Eddy-Current and Other NDT Techniques

Argonne[73,74] has resumed work on pulsed-field reflection systems. This electromagnetic test method replaces the sinusoidal currents and test coils or probes of older eddy-current test systems with pulsed fields emanating from small apertures in special masks. Test information about the metallic specimen being examined is received as a series of reflections from the surface and from the inside of the metal. Recent experiments revealed that the system possesses a pronounced sensitivity to the orientation of flaws in a metal passing under the aperture. The mask-aperture-pickup assembly can be oriented to achieve maximum pickup of defects of one orientation while minimizing indications from flaws that are oriented differently. The authors feel that, although their data thus far are limited, the results are significant. The system represents a possible new approach to the problems of electromagnetic testing. More work is indicated and is in progress to provide a clearer understanding of this effect.

A review[75] indicated that pulse eddy-current techniques are not yet competitive with the conventional a-c methods. However, the development of suitable filters along the lines suggested by Hanford to separate the measured parameters might result in a useful laboratory tool.

A new eddy-current system under development at Hanford[76,77] is capable of reading out a multiplicity of specimen parameters instead of the conventional two normally associated with eddy-current testing. The principle employed involves the use of broad-band techniques, with a multiple analyzing system reading as many electrical variables of the complex, broad-band, eddy-current signals as possible. A device has been built which provides a series of direct readout measurements. Experimental

work with this equipment, although not yet complete, indicates that the technique will be a definite contribution to the better understanding of eddy-current testing systems as applied to the nondestructive measurement of material parameters.

Neutron techniques in nondestructive testing have been improved at Argonne[78] where, on the basis of image resolution studies, gains in image sharpness can be obtained by the use of a single, metal converter screen. Some decrease in speed is experienced and is not appreciably changed by the use of one screen configuration over another. However, over-all image quality can be improved by the use of a 10-mil rhodium screen with the film located on the neutron side of the screen, with a factor of about 2 sacrifice in speed. For neutron beams having a large neutron-to-gamma ratio, this is reported to be the preferred method of obtaining high-quality neutron radiographs.

An extremely small eddy-current pickup coil has been developed[79] for the purpose of inspecting very small zones to pinpoint defects and property variations in specimens where the surface to be inspected is difficult to reach with conventional techniques. Three of these U-shaped coils can be mounted on the head of a pin. The coils consist of 200 turns of No. 56 gauge wire (0.00065 in. in diameter) wound on a 0.008-in.-diameter, U-shaped, iron core. The use to which this coil has been put to date is limited; however, it is felt that many applications will become apparent.

A document[80] has been published from a meeting (October 25–30, 1956) of the all-union, scientific, technical conference on magnetic methods of industrial control and new methods of magnetic measurements created at the instigation of the Institute for the Physics of Metals and the Commission of the Academy of Sciences, USSR. Not much that would be considered new was discussed; however, those in the nondestructive testing field should find this document interesting. (C. L. Seale)

References

1. H. M. Eikenberry et al., Effects of Furnace Pressure and Feed Material on Uranium Ingot Quality, USAEC Report NLCO-831, National Lead Co. of Ohio, Dec. 1, 1960.
2. R. Burgett (Ed.), Summary Technical Report for the Period April 1, 1961, to June 30, 1961, USAEC Report NLCO-830, National Lead Co. of Ohio, Aug. 4, 1961. (Classified)
3. R. J. Fletcher, Arc-Melting Furnace for Melting Reactive Refractory Metals, British Patent 871,715, June 28, 1961.
4. Knolls Atomic Power Laboratory, Reactor Technology Report No. 16, Metallurgy, USAEC Report KAPL-2000-13, July 1961.
5. A. E. LaMarche, Manufacturing Development of Tungsten Alloys for Rocket Nozzles, Mid-Year Report on Phase II, Report AD-245350, Westinghouse Electric Corp., Materials Manufacturing Dept., Sept. 1, 1960.
6. R. L. Martin et al., A Study of the Effects of Electron Beam Melting on Compounds and Metals, Report WADD-TR-60-404, Reactive Metals, Inc., July 14, 1960.
7. Bridgeport Brass Co., Process Development Quarterly Report, April–June 1960, USAEC Report BRB-59, Mar. 1, 1961. (Classified)
8. M. T. Watkins et al., The Slow Extrusion of Metals. Part III. British Report NP-8368, December 1954.
9. Battelle Memorial Institute, Tantalum Extrusion Program, State-of-the-Art Survey, Interim Technical Report No. 1, December 2, 1960–March 2, 1961, Report NP-10275.
10. Office of Technical Services, Metalworking. Part III. Casting and Forging, Report SB-462, April 1961.
11. Office of Technical Services, Metalworking. Part IV. Rolling, Drawing, and Extrusion, Report SB-463, April 1961.
12. T. F. Davis (Comp.), Extrusion of Uranium, Uranium Alloys, and Uranium Compacts. A Literature Search, USAEC Report TID-3563, June 1961.
13. E. Peters and M. H. Binstock, Fabrication Modification Development for OMRE Third Core Loading, USAEC Report NAA-SR-5616, Atomics International, July 15, 1961.
14. S. J. Paprocki et al., Fabrication and Irradiation of SM-2 Core Materials, USAEC Report BMI-1528, Battelle Memorial Institute, July 12, 1961.
15. Atomics International, Annual Technical Progress Report, AEC Unclassified Programs, Fiscal Year 1961, USAEC Report NAA-SR-6370, Aug. 15, 1961.
16. S. J. Paprocki et al., Gas-Pressure Bonding, Report DMIC-159, Defense Metals Information Center, Sept. 25, 1961.
17. S. J. Paprocki et al., Preliminary Studies of Bonding of Beryllium-Clad UO_2 Fuel Elements, USAEC Report BMI-1545, Battelle Memorial Institute, Sept. 20, 1961.
18. S. J. Paprocki et al., Process Development for Making SM-1 Instrumented Fuel Plates by Gas-Pressure Bonding, USAEC Report BMI-1544, Battelle Memorial Institute, Sept. 18, 1961.
19. I. Sheinhartz and J. Fugardi, Ceramic Fuel Elements Made by Hot Isostatic Pressing, USAEC

Report SCNC-311, Sylvania-Corning Nuclear Corp., September 1960.
20. R. W. Dayton and C. R. Tipton, Jr., Progress Relating to Civilian Applications During August 1961, USAEC Report BMI-1541, Battelle Memorial Institute, Sept. 1, 1961. (Classified)
21. G. W. Cunningham and J. W. Spretnak, The Mechanism of Pressure Bonding, USAEC Report BMI-1512, Battelle Memorial Institute, Apr. 6, 1961.
22. L. S. Castleman et al., Fundamentals of Diffusion Bonding. VI. Sixth Annual Progress Report, July 1, 1960–June 30, 1961, USAEC Report SEP-258, General Telephone and Electronics Laboratories, Inc., July 26, 1961.
23. C. L. Angerman, Metallographic Studies of Al-Ni-U Bonds in Nuclear Fuel Elements, in Proceedings of the 43rd National Metal Congress (to be published).
24. M. A. Gerardi, Evaluation of Chrome Coatings, Electrodeposited on Inconel, USAEC Report KAPL-M-MAG-5, Knolls Atomic Power Laboratory, May 3, 1961.
25. J. G. Beach and C. L. Faust, Electroplates on Thorium and Uranium for Corrosion Protection and To Aid Joining, USAEC Report BMI-1537, Battelle Memorial Institute, Aug. 14, 1961.
26. J. C. Withers, Electroplated Cermet Coatings for Oxidation Protection of Substrates in Excess of Excess of 2000°F, Report WADD-TR-60-718, American Machine and Foundry Co., October 1960.
27. H. R. Longfield (Comp.), Atomic Energy of Canada, Ltd., April 1961. (Unpublished)
28. Hanford Atomic Products Operation. (Unpublished)
29. G. T. Seaborg and A. C. Wahl, Electrodeposition of Neptunium, U. S. Patent 2,951,018 (to USAEC), Aug. 30, 1960.
30. R. F. Wehrmann, Method for Electrodepositing Polonium, U. S. Patent 2,951,020 (to USAEC), Aug. 30, 1960.
31. B. Kopelman and R. B. Holden, Electrolytic Process for Producing Metals, U. S. Patent 2,987,454 (to USAEC), June 6, 1961.
32. R. F. Wehrmann, Pretreating Uranium for Metal Plating, U. S. Patent 2,982,702 (to USAEC), May 2, 1961.
33. H. W. Schultze, Chemicals in Metallurgy — Vapor-Phase Deposition, *Ind. Eng. Chem.*, 53: 48A–51A (June 1961).
34. The Alloyd Corp., Research on the Production of Ultrapure Molybdenum, Progress Report No. 4, May 3–June 3, 1961.
35. H. W. Davidson and J. W. Ryde, Improvements in or Relating to Methods of Joining Graphite to Graphite and Graphite to Metal Surfaces, British Patent 865,592 (to General Electric Co., Ltd.), Apr. 19, 1961.
36. W. Leszynski (Ed.), *Powder Metallurgy*, pp. 775-798, Interscience Publishers, Inc., New York, 1961.
37. Compounding of Metal and Ceramics, *Technica*, 10: 797–798 (June 9, 1961).
38. U. S. Bureau of Mines, Rolla Metallurgy Research Center, Vapor Deposition of Tungsten on Rocket Nozzle Inserts, Summary Report for Research Ending June 30, 1961.
39. W. Meier et al., Deposition of Pyrolytic Carbon on Graphite, British Report RAE-LIB/Trans-940; translated from *Schweiz. Arch. angew. Wiss. u. Tech.*, 26(1): 29–38 (1960).
40. J. D. Batchelor et al., Improvement of the Usefulness of Pyrolytic Graphite in Rocket Motor Applications, Quarterly Progress Report, June Through August 1961, Atlantic Research Corp., Sept. 15, 1961.
41. R. E. Viventi, Fabrication of Pyrolytic Graphite Rocket Nozzle Components, Progress Report for May 1961, General Electric Co., Flight Propulsion Laboratory Dept., June 1961.
42. D. J. Shipp, Fabrication of Pyrolytic Graphite Rocket Nozzle Components, Progress Report for April 1961, General Electric Co., Flight Propulsion Laboratory Dept., May 10, 1961.
43. High Temperature Materials, Inc., Pyrolytic Carbide Development Program, July 1961, 16th Monthly Progress Report, July 31, 1961.
44. G. R. Van Houten et al., Formation of Alumina Coatings on Beryllia by a Vapor Deposition Process, USAEC Report APEX-699, General Electric Co., Flight Propulsion Laboratory Dept., June 30, 1961.
45. L. Matteoli, Diffusion Processes of the Solid State, *Atti-Notizie*, 16: 99–103 (May–June 1961).
46. J. C. Withers, Protective Coatings for Refractory Metals, Preprint of Paper (presentation place not indicated), Aug. 19, 1961.
47. M. L. Rutkovskiy et al., Gaseous Bonding of Nickel, *Fiz. Metal. i Metalloved.*, 12(2): 217-222 (August 1961).
48. Powder Diffusion Coating, *Australasian Mfgr.*, 46: 52–55 (June 19, 1961).
49. I. Sprinz and R. L. Wachtell, Oxidation of Molybdenum, *Metal Ind.*, 98: 396 (May 19, 1961).
50. L. Matteoli, Siliconizing of Steel, *Atti-Notizie*, 16: 104–108 (May–June 1961).
51. A. L. Pranatis et al., High-Temperature Reactions and Protective Systems Involving Tungsten and Refractory Compounds, Paper Presented at 5th Meeting, Refractory Composities Group, Dallas, Texas, August 8–10, 1961.
52. The Pfaudler Co., Development of a Cementation Coating Process for High-Temperature Protection of Molybdenum, First Quarterly Progress Report for March 1–June 10, 1961, June 20, 1961.
53. Armour Research Foundation, High-Temperature Oxidation-Protective Coatings for Vanadium, Bimonthly Report No. 1, June 12–August 11, 1961, Sept. 8, 1961.
54. W. D. Klopp et al., Development of Protective Coatings for Tantalum-Base Alloys, 5th Quarterly

Progress Report, Battelle Memorial Institute, Aug. 1, 1961.

55. W. D. Klopp, Review of Recent Developments on Oxidation-Resistant Coatings for Refractory Metals, Report DMIC-Memo-120, Defense Metals Information Center, July 31, 1961.
56. Chromalloy Corp., Explosive Forming of Refractory Metals, Final Technical Report, June 30, 1959, to September 30, 1960, Report NP-10117, Dec. 31, 1960.
57. Chromalloy Corp., Propellex Chemical Div., A Study of Explosive Forming Selected Refractory Metals, Progress Report No. 1 Through June 30, 1961, Report NP-10491, July 15, 1961.
58. G. A. Reimann, High Energy Rate Extrusion, Interim Technical Progress Report No. 3, Phase II, April 1 to June 30, 1961, Report ASC-TR-7-882(III), Westinghouse Electric Corp., Materials Manufacturing Dept., July 1961.
59. Hanford Atomic Products Operation, Uranium Ceramic Fuels, U.S./U.K. Research Newsletter No. 11, April 1961.
60. S. W. Porembka, Development of Cold Bonding Processes for the CANDU Reactor Program, Third Quarterly Report, USAEC Report BMI-X-176, Battelle Memorial Institute, Sept. 12, 1961.
61. S. Beitscher, Mechanical Properties of Zircaloy-2 Weld Metal, USAEC Report KAPL-2111, Knolls Atomic Power Laboratory, Apr. 15, 1961.
62. R. A. Noland and D. E. Walker, Bonding Aluminum Metals, U. S. Patent 2,987,816 (to USAEC), June 13, 1961.
63. Aeroprojects, Inc., Applications of Ultrasonic Energy. Task 5: Development of Ultrasonic Roll-Bond Cladding for Plate Type Elements, Quarterly Report No. 2 Covering Period from February 1, 1961, to May 1, 1961, USAEC Report NYO-9589, June 1961.
64. C. W. Fox and R. G. Gilliland, Progress Report on Brazing of Columbium, USAEC Report CF-61-7-24, Oak Ridge National Laboratory, July 5, 1961.
65. Bureau of Mines, Albany Metallurgy Research Center, Quarterly Metallurgical Progress Report No. 11 for the Period of April 1, 1961, to June 30, 1961, USAEC Report USBM-U-839.
66. R. W. Keil et al., Metallurgical Evaluation of Tantalum Alloys. Part I. Tantalum Containing 0.1 or 3.0 Wt.% Tungsten, USAEC Report LAMS-2496, Los Alamos Scientific Laboratory, Dec. 1, 1960.
67. Argonne National Laboratory, Symposium on Physics and Nondestructive Testing Held at Argonne National Laboratory, October 4 and 5, 1960, USAEC Report ANL-6346.
68. J. J. Maguire, Determination of Flaw Geometry by Ultrasonic Pulse Contour and Spectrum Analysis, Report WAL-TR-830.5/2, Watertown Arsenal Laboratories, July 1961.
69. Oak Ridge National Laboratory, Proceedings of the Atomic Energy Commission Nondestructive Testing Conference Held at Gatlinburg, Tennessee, May 17–18, 1960, USAEC Report TID-7590. (Classified)
70. Hanford Atomic Products Operation, September 1961. (Unpublished)
71. W. J. McGonnagle et al., Argonne National Laboratory, Aug. 30, 1961. (Unpublished)
72. Argonne National Laboratory, Reactor Development Program Progress Report, July 1961, USAEC Report ANL-6399, Aug. 15, 1961.
73. Argonne National Laboratory, Reactor Development Program Progress Report, August 1961, USAEC Report ANL-6409, Sept. 15, 1961.
74. C. J. Renken, Argonne National Laboratory, August–September 1961. (Unpublished)
75. W. L. Pillinger, Savannah River Laboratory, February 1961. (Unpublished)
76. H. L. Libby, Hanford Atomic Products Operation, Jan. 5, 1961. (Unpublished)
77. H. L. Libby, Hanford Atomic Products Operation, July–September 1961. (Unpublished)
78. Argonne National Laboratory. (Unpublished)
79. Miniature Search Coil, *Elec. Eng.*, 80(10): 802 (October 1961).
80. R. I. Yanus and N. M. Rodigin (Eds.), Magnetic Methods of Flaw Detection (Nondestructive Testing), Analysis and Measurement, USAEC Translation AEC-tr-4512, from *Trudy Inst. Fiz. Metalloved., Akad. Nauk S.S.S.R., Ural.' Filial*, No. 21 (1959).

Section VI

Reactor Materials

General Materials Information

From a wide variety of sources, General Dynamics has compiled[1] data on the properties of pertinent materials for applications in nuclear systems. The information is divided into three main parts: (1) shielding materials, (2) reactor materials, and (3) materials at extreme temperatures. The materials characteristics required for each function are outlined, and specific materials are discussed in terms of properties, behavior, and fabrication techniques.

The objectives, status, cost, contract term, and reports issued on individual research projects of the Fuels and Materials Development Branch, Nuclear Technology, USAEC Division of Reactor Development, are presented in an April 1961 report.[2] Among the 125 listings are several of the contracts negotiated by the U. S.–Euratom Joint Research and Development Board. Although this document contains virtually no research results, it is a most valuable reference to who is doing what in the materials field. To simplify the finding of particular items of interest, contractors are listed alphabetically, and there is a detailed subject index.

A concentrated review of materials technology has been made by the United Nuclear Corporation. The presentation[3,4] is broken down according to fuels, moderators and reflectors, coolants, cladding and structural materials, shield materials, and control materials. The relative merits of candidate materials for each application are discussed, and recommendations are made for various types of compact reactors.

(E. M. Simons)

References

1. W. Q. Hullings, Materials Data for Nuclear Systems, Report NARF-61-24T(FZK-9-162), General Dynamics/Fort Worth, Div. of General Dynamics Corp., July 17, 1961.
2. Summaries of Fuels and Materials Development Programs, USAEC Report TID-6506(Suppl.), April 1961.
3. Nuclear Development Corp. of America and General Motors Corp., Survey of Technology for MCR Program, USAEC Report NDA-2143-2, May 22, 1961. (Classified)
4. United Nuclear Corp. and General Motors Corp., Military Compact Reactor Program Power Plant Concept Recommendation, USAEC Report NDA-2143-5(Vol. II), Aug. 15, 1961. (Classified)

LEGAL NOTICE

This document was prepared under the sponsorship of the U. S. Atomic Energy Commission. Neither the United States, nor the Commission, nor any person acting on behalf of the Commission:

A. Makes any warranty or representation, expressed or implied, with respect to the accuracy, completeness, or usefulness of the information contained in this report, or that the use of any information, apparatus, method, or process disclosed in this report may not infringe privately owned rights; or

B. Assumes any liabilities with respect to the use of, or for damages resulting from the use of any information, apparatus, method, or process disclosed in this report.

As used in the above, "person acting on behalf of the Commission" includes any employee or contractor of the Commission, or employee of such contractor, to the extent that such employee or contractor of the Commission, or employee of such contractor prepares, disseminates, or provides access to, any information pursuant to his employment or contract with the Commission, or his employment with such contractor.

NUCLEAR SCIENCE ABSTRACTS

The U. S. Atomic Energy Commission, Division of Technical Information, publishes *Nuclear Science Abstracts (NSA)*, a semimonthly journal containing abstracts of the literature of nuclear science and engineering.

NSA covers (1) research reports of the U. S. Atomic Energy Commission and its contractors; (2) research reports of government agencies, universities, and industrial research organizations on a world-wide basis; and (3) translations, patents, books, and articles appearing in technical and scientific journals.

Complete indexes covering subject, author, source, and report number are included in each issue. These are cumulated quarterly, semiannually, and annually providing a detailed and convenient key to the literature.

Availability of *NSA*

SALE *NSA* is available on subscription from the Superintendent of Documents, U. S. Government Printing Office, Washington 25, D. C., at $22.00 per year for the semimonthly abstract issues and $15.00 per year for the four cumulated-index issues. Subscriptions are postpaid within the United States, Canada, Mexico, and all Central and South American countries, except Argentina, Brazil, British and French Guiana, Surinam, and British Honduras. Subscribers in these Central and South American countries, and in all other countries throughout the world, should remit $27.50 per year for subscriptions to semimonthly abstract issues and $17.50 per year for the four cumulated-index issues.

EXCHANGE *NSA* is also available on an exchange basis to universities, research institutions, industrial firms, and publishers of scientific information. Inquiries should be directed to the Division of Technical Information Extension, U. S. Atomic Energy Commission, P. O. Box 62, Oak Ridge, Tennessee.